Degradation of (E)- and (Z)-Endoxifen: Kinetics, By-products Identification and Toxicity Assessment.

Miss Marina Arino Martin

A Thesis Submitted in Partial Fulfillment of the Requirements

for the Degree of Master of Science Program in Hazardous Substance and Environmental

Management

(Interdisciplinary Program)

Graduate School

Chulalongkorn University

Academic Year 2016

การย่อยสลายเอนด็อกซิเฟน(E) และ (Z): จลนศาสตร์ การระบุผลิตภัณฑ์พลอยได้จากการย่อย
และการประเมินความเป็นพิษ

นางสาวมารินา อาริโน มาร์ติน

Thesis Title	Degradation of (E)- and (Z)-Endoxifen: Kinetics, By-products Identification and Toxicity Assessment.
By	Miss Marina Arino Martin
Field of Study	Hazardous Substance and Environmental Management
Thesis Advisor	Professor Doctor Eakalak Khan
Thesis Co-Advisor	Doctor Prinpida Sonthiphand

Accepted by the Graduate School, Chulalongkorn University in Partial Fulfillment of the Requirements for the Master's Degree

┄┄┄┄┄┄┄┄┄┄┄┄┄┄┄┄┄┄┄┄ Dean of the Graduate School
(Associate Professor Sunait Chutintaranond)

THESIS COMMITTEE

┄┄┄┄┄┄┄┄┄┄┄┄┄┄┄┄┄┄┄┄ Chairman
(Associate Professor Doctor Tawan Limpiyakorn)

┄┄┄┄┄┄┄┄┄┄┄┄┄┄┄┄┄┄┄┄ Thesis Advisor
(Professor Doctor Eakalak Khan)

┄┄┄┄┄┄┄┄┄┄┄┄┄┄┄┄┄┄┄┄ Thesis Co-Advisor
(Doctor Prinpida Sonthiphand)

┄┄┄┄┄┄┄┄┄┄┄┄┄┄┄┄┄┄┄┄ Examiner
(Associate Professor Doctor Ekawan Luepromchai)

┄┄┄┄┄┄┄┄┄┄┄┄┄┄┄┄┄┄┄┄ External Examiner
(Associate Professor Doctor Duangrat Inthorn)

มารินา อาริโน มาร์ติน : การย่อยสลายเอนด็อกซิเฟน(E) และ (Z): จลนศาสตร์ การระบุ
ผลิตภัณฑ์พลอยได้จากการย่อย และการประเมินความเป็นพิษ (Degradation of (E)- and (Z)-
Endoxifen: Kinetics, By-products Identification and Toxicity Assessment.) อ.ที่ปรึกษา
วิทยานิพนธ์หลัก: เอกลักษณ์ คาน, อ.ที่ปรึกษาวิทยานิพนธ์ร่วม: พรินท์พิดา สนธิพันธ์, 117
หน้า.

เอนด็อกซิเฟนเป็นเมแทบอไลต์ของยาทาม็อกซิเฟนซึ่งใช้สำหรับเคมีบำบัดรักษามะเร็ง มีการ
ตรวจพบเอนด็อกซิเฟนในน้ำเสียที่ปล่อยจากโรงบำบัดน้ำเสีย ซึ่งการปล่อยเอนด็อกซิเฟนลงสู่แหล่งน้ำ
ตามธรรมชาติสามารถก่อให้เกิดผลเสียต่อสัตว์น้ำเพราะเอนด็อกซิเฟนมีฤทธิ์ต้านเอสโตรเจน งานวิจัยนี้มุ่ง
ศึกษาการใช้แบคทีเรียที่คัดแยกได้และแสงอัลตราไวโอเลต (253.7 นาโนเมตร) ในการย่อยสลายเอนด็อก
ซิเฟนในน้ำและอในน้ำเสีย รวมทั้งระบุผลิตภัณฑ์พลอยได้จากการย่อยเอนด็อกซิเฟนและประเมินความ
เป็นพิษของสารดังกล่าว ผลการทดลองแสดงให้เห็นว่าเอนด็อกซิเฟนไม่สามารถถูกย่อยได้อย่างมี
ประสิทธิภาพโดยใช้แบคทีเรียที่คัดแยกได้จากน้ำเสีย แต่เอนด็อกซิเฟนสามารถถูกย่อยโดยใช้แสง
อัลตราไวโอเลตได้อย่างน้อย 99.1% เมื่อใช้แสงที่ความเข้ม 598.5 มิลลิจูลต่อตารางเซนติเมตร เป็นเวลา
35 วินาที ความเข้มแสงและความข้มข้นเริ่มต้นของเอนด็อกซิเฟน(E) และ (Z) มีความสัมพันธ์เชิงบวกกับ
อัตราการย่อยเอนด็อกซิเฟนโดยใช้แสง ในขณะที่ pH ไม่มีผลต่ออัตราการย่อย การย่อยเอนด็อกซิเฟนที่
ละลายในน้ำโดยใช้แสงทำให้เกิดผลิตภัณฑ์พลอยได้สามชนิด (PBPs) การประเมินความเป็นพิษโดยใช้
แบบจำลองพบว่าผลิตภัณฑ์พลอยได้มีความเป็นพิษมากกว่าสารตั้งต้น การย่อยเอนด็อกซิเฟน(E) และ (Z)
ในน้ำเสียโดยใช้ความเข้มแสงเท่ากับที่ใช้ฆ่าเชื้อในโรงบำบัดน้ำเสียพบว่าเอนด็อกซิเฟน(E) และ (Z)
ลดลงอย่างน้อย 30 44 และ 71% ที่ความเข้มแสง 16 30 และ 97 มิลลิจูลต่อตารางเซนติเมตร ตามลำดับ
สองในสามของผลิตภัณฑ์พลอยได้จากการย่อยเอนด็อกซิเฟนในน้ำถูกตรวจพบในการย่อยเอนด็อกซิเฟน
ในน้ำเสีย ดังนั้นการใช้แสงอัลตราไวโอเลตเพื่อฆ่าเชื้อในโรงบำบัดน้ำเสียอาจก่อให้เกิดสารที่มีความเป็น
พิษมากได้ในกรณีที่น้ำเสียปนเปื้อนมีเอนด็อกซิเฟนผ่านการบำบัด

สาขาวิชา   การจัดการสารอันตรายและสิ่งแวดล้อม ลายมือชื่อนิสิต ---------------------------------------
ปีการศึกษา 2559   ลายมือชื่อ อ.ที่ปรึกษาหลัก ---------------------------------------
                                                                                            ลายมือชื่อ อ.ที่ปรึกษาร่วม ---------------------------------------

5787534220 : MAJOR HAZARDOUS SUBSTANCE AND ENVIRONMENTAL MANAGEMENT

KEYWORDS: ENDOXIFEN / PHOTODEGRADATION / BIODEGRADATION / BY-PRODUCTS / TOXICITY ASSESSMENT / KINETICS

MARINA ARINO MARTIN: Degradation of (E)- and (Z)-Endoxifen: Kinetics, By-products Identification and Toxicity Assessment.. ADVISOR: PROF. DR. EAKALAK KHAN, CO-ADVISOR: DR. PRINPIDA SONTHIPHAND, 117 pp.

Endoxifen is an effective metabolite of a commonly used chemotherapy agent, tamoxifen. Endoxifen has been detected in the final effluent of wastewater treatment plants. The release of endoxifen into the water environment could bring negative effect to aquatic lives due to its antiestrogenic activity. This research investigated the uses of isolated bacteria strains and ultraviolet (UV) radiation (253.7 nm) to degrade endoxifen in water and wastewater, and the generations of degradation by-products and their toxicity. Biodegradation of endoxifen by isolated bacteria strains from wastewater resulted in inefficient degradation of (E)- and (Z)-endoxifen. However, photodegradation with UV light eliminated endoxifen from water by at least 99.1% after 35 seconds of irradiation with a light dose of 598.5 mJ cm^{-2}. Light intensity and initial concentrations of (E)- and (Z)-endoxifen exhibited positive linear correlations with the photodegradation rates while pH had no effect. Photodegradation of (E)- and (Z)-endoxifen in water generated three photodegradation by-products (PBPs). Toxicity assessments through modeling of the identified PBPs suggest higher toxicity than the parent compounds. Photodegradation of (E)- and (Z)-endoxifen in wastewater at light doses used for disinfection in wastewater treatment plants (WWTPs) resulted in reduction of (E)- and (Z)-endoxifen by at least 30, 44, and 71% at the light doses of 16, 30, and 97 mJ cm^{-2}, respectively. Two of the three PBPs observed in the experiments with water were detected in the experiments in wastewater. Therefore, highly toxic compounds are potentially generated at WWTPs during UV disinfection process if (E)- and (Z)-endoxifen are present in the treated wastewater.

Field of Study:	Hazardous Substance and	Student's Signature	....
	Environmental Management	Advisor's Signature	....
Academic Year:	2016	Co-Advisor's Signature	....

ACKNOWLEDGEMENTS

CONTENTS

LIST OF FIGURES

LIST OF TABLE

CHAPTER 1: INTRODUCTION

1.1 Background

During the last decade, the presence of cytostatic drugs in the environment has been a growing concern worldwide. Cytostatic drugs are a group of chemotherapy drugs used to inhibit the proliferation of carcinogenic cells. The abundance of these chemotherapy drugs in the environment is related to their frequency of consumption (Johnson, Oldenkamp, Dumont, & Sumpter, 2013). According to the American Association Cancer Research (2015), breast cancer is the major cancer type among women globally. Among different types of breast cancer, positive endocrine (ER+) breast cancer accounts for 60-70% of all cases (Jager, Rosing, Linn, Schellens, & Beijnen, 2012). Patients with ER+ breast cancer commonly receive selective estrogen receptor modulators (SERMs) as chemotherapy treatment (Peng, Sengupta, & Jordan, 2009). SERMs block estrogen receptors in carcinogenic cells, inhibiting their proliferation (Negreira, Regueiro, Lopez de Alda, & Barceló, 2015). By definition, SERMs are chemotherapy treatments cataloged as cytostatic drugs.

In the last 40 years, tamoxifen has been the most widely used chemotherapy drug to treat and prevent ER+ breast cancer (Hoskins, Carey, & McLeod, 2009; M. D. Johnson et al., 2004; Negreira et al., 2015). Furthermore, it is used as a preventive treatment for women with high-risk of breast cancer (Fisher et al., 1998). The effectiveness of tamoxifen for patients diagnosed with breast cancer relies on an ability of the liver to actively metabolize the drug by cytochrme P450 enzymes to endoxifen (Zhang et al., 2015). The major metabolite resulting from tamoxifen conversion is the *trans* isomer Z-endoxifen, or commonly called endoxifen (Jaremko et al., 2010). However, (Z)-

endoxifen easily suffer *cis* isomerization to (E)-endoxifen (Elkins et al., 2014). Although both isomers present antiestrogenic activity, (Z)-endoxifen is considered the isomer responsible for the inhibition of breast cancer cell proliferation due to its higher antiestrogenic ability (Jaremko et al., 2010).

Despite the fact endoxifen is an effective treatment for breast cancer, it presents possible consequences on the environment (Goverment of Goverment of Canada, 2015). Endoxifen is not completely metabolized in human body and is actively excreted (Kisanga, Mellgren, & Lien, 2005). As a result, endoxifen is released to the water environment via wastewater treatment plants (WWTPs) (Negreira, Alda, & Barceló, 2014). Data on the actual concentrations of endoxifen in the environment is limited. Several studies reported the presence of tamoxifen in the level of ng L^{-1} to μg L^{-1} in surface water and wastewater (Ashton, Hilton, & Thomas, 2004; Coetsier, Spinelli, Lin, Roig, & Touraud, 2009; Goverment of Canada, 2015; Lara-Martín, González-Mazo, Petrovic, Barceló, & Brownawell, 2014; Roberts & Thomas, 2006; Thomas & Hilton, 2004). Studies reporting endoxifen concentration in water are even fewer than tamoxifen, probably due to the recent discovery of endoxifen pharmaceutical activity. However, tamoxifen and endoxifen present a similar chemical and molecular structure, which suggests a similar fate. Endoxifen has been detected in hospital effluents and wastewater, but there is no data on endoxifen concentration in the environment (Evgenidou, Konstantinou, & Lambropoulou, 2015).

Although the presence of endoxifen in water bodies could bring negative effects to the environment, there has been only one study on this issue (Borgatta, Decosterd, Waridel, Buclin, & Chèvre, 2015). Similar to other pharmaceutical compounds (PhCs), endoxifen is considered an environmental micropollutant (Evgenidou et al., 2015).

However, toxicology studies have been focused mainly on tamoxifen. The antiestrogenic activity of tamoxifen produces negative effects when it is present in the environment, affecting the fish reproduction and physiology (Maradonna, Batti, Marino, Mita, & Carnevali, 2009). Because endoxifen is 30-100 times more potent than tamoxifen (Jager et al., 2012) and presents antiestrogenic activity (Goverment of Canada, 2015; M. D. Johnson et al., 2004), its presence in the environment could result in a toxic effect on aquatic lives. Therefore, the elimination of endoxifen from wastewater is necessary to avoid these possible toxicological effects.

Several techniques can be applied in wastewater treatment plants to eliminate endoxifen. Among these techniques, a biological treatment scheme called bioaugmentation is a promising method to enhance the elimination of selected chemicals present in wastewater (Herrero and Stuckey, 2015). Bioaugmentation consists of the addition of selected microbial strains to wastewater treatment reactors in order to remove target compound(s). Bacteria are the main microorganism involved in the biodegradation of harmful chemicals during biological treatment in WWTPs. In an attempt to eliminate endoxifen from WWTPs, the identification and isolation of bacterial strains responsible for endoxifen biodegradation is the first key step in order to avoid the potential effects of endoxifen on the environment.

Another potential effective technique that has demonstrated to be a highly efficient method to eliminate pharmaceuticals from wastewater is photodegradation with UV light (253.7 nm) Previous laboratory bench-scale studies using low-pressure (LP) mercury lamps emitting UV light at 253.7 nm reported an efficient elimination of PhCs in water (Pereira, Linden, & Weinberg, 2007; Prados-Joya, Polo, Rivera-Utrilla, & Sanchez-Ferro-Garcia, 2010; Rivas, Gimeno, Borralho, & Carbajo, 2009). The

elimination of PhCs by UV light should produce photodegradation by-products (PBPs) that are less toxic than their parents compounds (Larson & Befenbaum, 1988). However, the identification and the toxicity assessment of potential PBPs need to be investigated before actual applications of the process. LP mercury lamps (253.7 nm) are also commonly used in UV disinfection process at WWTPs. However, the UV light doses applied at WWTPs are lower than those applied for photodegradation. Because the use of UV light as a disinfection process at WWTPs has gained more attention during the last decade (Guo, Hu, Bolton, & El-Din, 2009), it might be interesting to determine the photodegradability of endoxifen in wastewater at light doses similar to those applied at WWTPs.

1.2 Research objectives

The proposed research has the following objectives:

- To isolate and identify (E)- and (Z)-endoxifen bacterial degrader(s).

- To determine endoxifen biodegradation kinetics and its potential by-products.

- To investigate the suitability of LP mercury lamps emitting UV light at 253.7 nm to remove (E)- and (Z)-endoxifen from water

- To determine the effects of pH, light intensity and initial (E)- and (Z)-endoxifen concentrations on the photodegradation kinetics and efficiency

- To analyze the role of hydroxyl radicals on the photodegradation of (E)- and (Z)-endoxifen

- To identify the main PBPs of (E)- and (Z)-endoxifen

- To assess the toxicity of PBPs in the aquatic environment

- To determine the photodegradability of (E)- and (Z)-endoxifen at light doses similar to those applied at WWTPs.

1.3 Hypotheses

The proposed research has the following hypotheses:

- Endoxifen is biodegradable by bacteria isolated from wastewater.

- (E)- and (Z)-endoxifen are photodegradable by UV light at 253.7 nm.

- Photodegradation kinetics and efficiency of (E)- and (Z)-endoxifen are affected by pH, light intensity and initial concentrations of (E)- and (Z)-endoxifen.

- Photodegradation of (E)- and (Z)-endoxifen by UV light at 253.7nm results in PBPs that are less toxic than the parent compounds.

- (E)- and (Z)-endoxifen are not or minimally photodegraded by UV light at doses commonly used for disinfection in WWTPs.

1.4 Scope of study

Biodegradation of (E)- and (Z)-endoxifen by bacteria present in wastewater is investigated. Photodegradability of (E)- and (Z)-endoxifen by UV light (253.7 nm) in water is determined. The effects of pH between 5 to 9, light intensity between 28 to 224 W s^{-1} cm^{-2}, and initial concentrations of (E)- and (Z)-endoxifen between 0.5 to 2 µg mL^{-1} on photodegradation kinetics are examined. The role of hydroxyl radical during photodegradation reaction is determined by the addition of isopropyl alcohol (1%) as hydroxyl radical quencher. The formations of PBPs of (E)- and (Z)-endoxifen are identified by ultra high performance-tandem mass spectrometry (UHPLC-MS/MS). The potential toxicity of PBPs in the aquatic environment is assessed by modeling using the Toxicity Estimator Software Tool (TEST) developed by USEPA (2016).

Photodegradation of (E)- and (Z)-endoxifen by UV light (253.7 nm) is investigated at light doses used for disinfection in WWTPs such as 16, 30 and 97 mJ cm^{-2}.

1.5 Anticipated results and benefits

The research results will elucidate the ability of isolated bacteria strains and UV light (253.7 nm) to degrade (E)- and (Z)-endoxifen. Identification of potential (E)- and (Z)-endoxifen by-products and the estimation of their toxicity in the aquatic environment will demonstrate the suitability of biodegradation and UV light (253.7 nm) technologies as (E)- and (Z)-endoxifen treatments processes. An effective treatment technique for (E)- and (Z)-endoxifen would be useful in reducing their release to the aquatic environment and in turn potential toxicological effects on aquatic lives or even humans. Identification of (E)- and (Z)-endoxifen bacteria degraders will lead to a better understanding of the biological techniques needed in order to remove endoxifen in wastewater. Identifying the fate of (E)- and (Z)-endoxifen in WWTPs particularly UV disinfection process will lead to a better understanding on a potential source of the compounds and their PBPs in the aquatic environment.

CHAPTER 2: LITERATURE REVIEW

2.1 General background

Tamoxifen is the most widely used chemotherapy drug to treat and prevent ER+ breast cancer (Hoskins et al., 2009; Johnson et al., 2004; Negreira et al., 2015). Tamoxifen inhibits the tumor growth through its affinity to bind to estrogen receptor in cells, inhibiting cancer cells proliferation (Helland et al., 2015; Negreira et al., 2015). In addition, the ability of tamoxifen to mimic the endocrine system has also shown effective results for infertility treatment, gynecomastia, and bipolar disorder (Steiner, Terplan, & Paulson, 2005). However, in order to be effective, tamoxifen needs to be metabolized by cytochrome P450 enzymes (CYP2D6 and CYP3A4/5) present in the human liver (Fauq, Maharvi, & Sinha, 2010). There are two routes for the generation of the active metabolite, endoxifen; tamoxifen undergoes demethylation to form N-desmethyl tamoxifen and followed by hydroxylation, or hydroxylation to 4-hydroxy-tamoxifen and then demethylation (Figure 1) (Ahmad, Ali, Ahmad, Sheikh, & Ahmad, 2010; Zhang et al., 2015). Endoxifen is mainly formed through hydroxylation of N-desmethyl-tamoxifen and to a lesser extent by through demethylation of 4-hydroxy-tamoxifen (Figure 1).
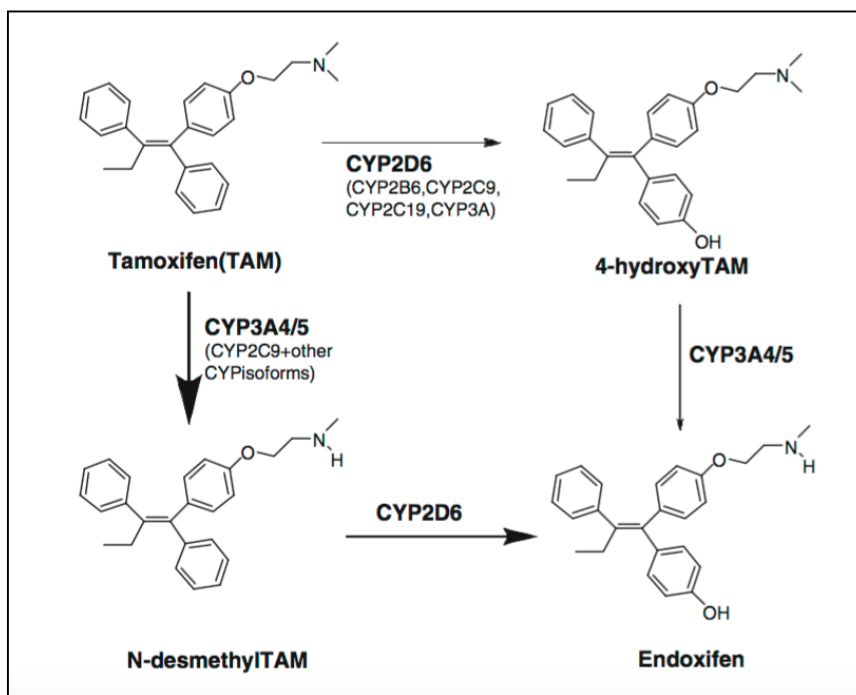
Figure 1.Metabolism of tamoxifen to the active metabolite endoxifen through
cytochrome P450 enzymes (Ahmad et al., 2010).

Endoxifen is the metabolite responsible for treatment effectiveness (Goverment of
Goverment of Canada, 2015). Besse, Latour, & Garric (2012) stated that endoxifen is
30 to100 times more potent and active than the parent compound. Accordingly, the anti-
estrogenic ability of endoxifen is 30 to 100 folds greater than tamoxifen, but its anti-
estrogenic activity relies on its ability to target and degrade estrogen receptor (Wu et
al., 2009). The enzymatic transformation of tamoxifen to endoxifen is crucial for
effective results (Helland et al., 2015), but a significant number of women present
genetic polymorphism of CYP2D6 (Ahmad et al., 2010), resulting in the inability to
metabolize tamoxifen to endoxifen. In addition, the concomitant administration of
serotonin reuptake inhibitor, a complementary treatment to avoid hot flushes as a side

effect of tamoxifen in 45% of patients, inhibits the activity of CYP2D6 (Ahmad et al., 2010; Binkhorst et al., 2011). As a consequence, several patients under tamoxifen treatment are not able to obtain optimal results (Ahmad et al., 2010). Because endoxifen shows independence from CYP2D6 action, it has been administered directly to patients and has shown promising results (Ahmad et al., 2010). According to the Mayo Foundation for Medical Education and Research (2014), a clinical trial in phase I has shown that endoxifen presents an anti-tumor activity and is safe for patients. A clinical trial phase II is being conducted by the National Cancer Institute with an estimated completion date in May 2017 (National Institute of National Institute of Health, 2015). Based on these clinical trials, endoxifen is a promising therapeutic agent to treat ER+ breast cancer (Ahmad et al., 2010).

Endoxifen, directly administered or as tamoxifen metabolite, does not suffer posterior metabolization in the human body (Negreira et al., 2014). As a result, endoxifen and unmetabolized tamoxifen are both actively excreted by patients (Negreira et al., 2014). A study by Kisanga et al. (2005) showed that patients under oral chemotherapy treatment of radio-labeled tamoxifen excreted 63% of the drug to municipal sewage during the following 10 days. The excreted tamoxifen was exclusively detected in feces while endoxifen was excreted via urine (Kisanga et al., 2005).

The excreted tamoxifen and endoxifen end up in WWTPs and consequently in surface waters receiving the WWTP effluent discharge (Borgatta et al., 2015). Several studies have detected tamoxifen in wastewater influent and effluent and surface water at a concentration range from 4 ng L^{-1} to 369 ng L^{-1} (Ashton et al., 2004; Coetsier et al., 2009; Goverment of Canada, 2015; Lara-Martín et al., 2014; Roberts & Thomas, 2006; Thomas & Hilton, 2004). However, the actual concentration of endoxifen in wastewater

and natural water bodies has been poorly documented (Borgatta et al., 2015). The lack of technology and the know-how to measure endoxifen in laboratories are handicaps in order to determine its concentration in wastewater and surface water (Heath et al., 2016; Kovalova, Siegrist, Singer, Wittmer, & McArdell, 2012). Ferrando-Climent, Rodriguez-Mozaz, & Barceló (2013) detected but did not quantify endoxifen in two hospital wastewater samples, while a study by Negreira et al. (2014) reported a concentration of 96 ng L^{-1} of endoxifen in a wastewater effluent sample.

2.2 Endoxifen detection methods

Micellar liquid chromatographic procedure, liquid chromatography-mass spectrometry (LC-MS), and ultra-high performance liquid chromatography tandem mass spectrometry (UHPLC-MS/MS) have been commonly used to detect and quantify tamoxifen and endoxifen in human plasma, blood, and scalp hair (Antunes et al., 2015; Aranda, Esteve-Romero, Rambla-Alegre, Peris-Vicente, & Bose, 2011; Binkhorst et al., 2011; Drooger et al., 2015; Heath et al., 2016). However, these methods require expensive equipment limiting routine analyses (Binkhorst et al., 2011). A more economical method used to identify and quantify endoxifen in human blood samples was liquid chromatography with a fluorescence detector (LC-FLD) (Aranda et al., 2011). The ability of tamoxifen to form a fluorescence phenanthrene nucleo within its structure after UV irradiation suggest a similar behavior for endoxifen (Mendenhall et al., 1978). The potential formation of a phenanthrene nucleo after irradiation of endoxifen with UV light makes LC-diode array detector (DAD) a suitable method to detect and quantify endoxifen in blood (Aranda et al., 2011). However, samples needed irradiation for 20 minutes with UV light, making it a lengthy process (Aranda et al., 2011).

Negreira et al. (2014) quantified endoxifen for the first time in wastewater samples. An automated on line solid-phase extraction-liquid chromatography-tandem mass spectrometry (SPE-LC-MS/MS) was used to determine several cytostatic drugs in wastewater samples. Endoxifen was detected only in one water sample at a concentration of 96 ng L^{-1} while tamoxifen was the most frequently detected drug in all samples with values ranging from 102-181 ng L^{-1}. These concentrations mimic the concentrations present in blood of administered patients. The concentration ratio of tamoxifen and endoxifen in blood of patients under tamoxifen treatment is about 2:1 (Helland et al., 2015). Therefore, the concentration of endoxifen obtained by Negreira et al., (2014) was close to the expected concentration (96 ng L^{-1} is approximately half of 181 ng L^{-1}). However, endoxifen was found in only one sample which does not allow a statistical analysis. This single detection can be explained because the method was developed to detect a large number of drugs instead of focusing exclusively on endoxifen. Therefore, the method by Negreira et al. (2014) must be refined in order to obtain better results for endoxifen detection.

A cost-effective method able to detect and quantify analytes in the presence of other compounds is high performance liquid chromatography coupled with DAD (HPLC-DAD) (Teunissen, Rosing, Schinkel, Schellens, & Beijnen, 2010). This method allows the identification of peak purity by spectra comparison (Pragst, Herzler, & Erxleben, 2004). Therefore, HPLC-DAD is a potential method to identify endoxifen in wastewater and natural water samples where other compounds are present. Furthermore, the identification and separation of endoxifen isomers through HPLC-DAD were previously reported by Elkins et al. (2014). Successful separation and resolution of (E)- and (Z)-endoxifen were observed during isomer characterization

using a phenyl-hexyl column. Therefore, HPLC-DAD could be a technology to determine the concentrations of endoxifen isomers in wastewater and receiving water bodies which are required to develop proper environmental risk assessments (Ferrando-Climent et al., 2013).

2.3 Toxicity of endoxifen

The available information to develop an environmental risk assessment of endoxifen is very limited. Potential effects of endoxifen in aquatic organisms have been poorly studied (Borgatta et al., 2015). However, several studies have focused on the ecological effect of tamoxifen (Government of Canada, 2015). Tamoxifen, as other endocrine disruptor compounds, has shown significant alteration in the sex ratio of exposed zebrafish (*Danio rerio*) at a low critical toxicity value (CTV) of 510 ng L^{-1} (Knacker et al., 2010; Liu, Zhang, & Wang, 2010; Singh, 2013; Van der Ven, Brandhof, Vos, & Wester, 2007) and modifications of gonadotropin expression in frogs at a concentration of 3.2 μg L^{-1} (Urbatzka et al., 2007). A study by Borgatta et al., (2015) showed a reproductive decline and mortality of *Daphnia pulex* exposed to tamoxifen metabolites, including endoxifen. The study showed an increase of sensitivity during the second generation, resulting in a significant decline of the population growth. Further long-term studies are needed in order to determine the chronic toxicity of endoxifen to aquatic organisms. Furthermore, the actual aquatic Predicted No Effect Concentration (PNEC) of tamoxifen is 51 pg mL^{-1}, and it is considered applicable to endoxifen due to the lack of toxicology studies focused on endoxifen (Government of Canada, 2015). This suggested same PNEC is questionable because endoxifen is a 100-fold more potent antiestrogen than tamoxifen. Similar chemical and physical properties of endoxifen and tamoxifen suggest a similar fate (Borgatta et al., 2015) and therefore

the potential release of endoxifen into the water environment presents a potential harm to aquatic lives (Government of Canada, 2015).

2.4 Chemical and physical properties of endoxifen

Endoxifen (Phenol, 4-(1-(4-(2-(methylamino)ethoxy)phenyl)-2-phenyl-1-butenyl)) is a relatively new polyaromatic hydrocarbon with registered CAS number 110025-28-0, crystalline solid with an off-white to pink solid color (TRC, 2016). The molecular weight is 373.48738 g/mol with a molecular formula $C_{25}H_{27}NO_2$. Three different isomers have been identified for endoxifen: (E)-endoxifen, (Z)-endoxifen (endoxifen) and (Z´)-endoxifen (Figure 2) (Jaremko et al., 2010). The major metabolite resulting from tamoxifen conversion is (Z)-endoxifen, or commonly called endoxifen, which presents 30 to 100-fold greater activity than tamoxifen. In the event of N-desmethyl-tamoxifen (Z-ND-Tam) hydroxylation at the para-benzene ring, the resulting metabolite is (Z')-endoxifen without anti-estrogenic activity reported (Jaremko et al., 2010). (E)-endoxifen (*cis*-isomer) is formed by non-enzymatic conversion of Z-endoxifen due to protonation and further deprotonation of the ethylene core by the electro-donating phenolic group (Jaremko et al., 2010). The (E)-isomer presents less estrogenic activity than (Z)-endoxifen and its concentration in human plasma is lower (Jaremko et al., 2010). However, the presence of (E)-endoxifen in the environment could also bring detrimental effects due to its estrogenic activity.
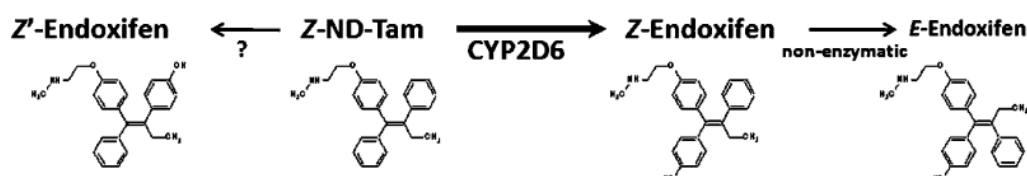
Figure 2. Isomerization of endoxifen (Jaremko et al., 2010).

The modeled physical and chemical properties of endoxifen that are relevant to its environmental fate are presented in Table 1 (Government of Canada, 2015). Briefly, the modeled vapor pressure is very low while its Henry's law constant is high (Government of Canada, 2015). These values suggest a minimal volatilization when endoxifen is released to water. The high modeled octanol-water partition coefficient of endoxifen suggests that it is potentially bioacumulate in aquatic life. However, further experimental analyses are needed in order to corroborate the values obtained by modeling. According to Government of Canada (2015), modeled data for degradation of endoxifen in water showed a half-life value greater or equal to 182 days. This value suggests that endoxifen is potentially a persistent organic pollutant in water. Therefore, these physical and chemical properties of endoxifen together with its potential toxicity in the aquatic environment, bring an urgent need to find effective techniques to eliminate endoxifen from water.

Table 1. Physical and chemical properties of endoxifen.

Property	Type	Value	Temperature (°C)
Melting point (ºC)	Model	212.4	
Boiling point (ºC)	Model	501.85	
Vapor pressure (Pa)	Model	4.32×10^{-9}	25
Henry's law constant (Pa·m^3/mol)	Model	2.16×10^{-9}	25
Log K_{ow} (dimensionless)	Model	5.61	
Log K_{oc} (dimensionless)	Model	6.56	
Water solubility (mg L^{-1})	Model (estimated from K_{ow})	2.79	25
Water solubility (mg L^{-1})	Model (estimated from fragments)	2.19	25
pKa (dimensionless)	Model	10.36 (acid) 9.4 (base)	
Log D (dimensionless)	Model	3.74	

*Source: Government of Canada, 2015

Abbreviations:

K_{ow}: Octanol-water partition coefficient

K_{oc}: Organic carbon-water partition coefficient

pKa: Acid dissociation constant

D: Distribution coefficient taking into account the presence of ionic species; represents a net amount of the neutral and ionic forms expected to partition into the lipid or organic carbon phases at a given pH

2.5 Potential treatment methods for endoxifen in water

Several studies report advanced treatment processes to eliminate PhCs from water (Heberer, 2002; Heberer, Reddersen, & Mechlinski, 2002; Hu, Bao, Hu, Liu, & Yin, 2017). However, information about removal of cytostatic drugs is limited and there are no studies on treatment of endoxifen in water (Franquet-Griell, Medina, Sans, & Lacorte, 2017).

2.5.1 Biodegradation of endoxifen

Bioaugmentation is a promising technique to enhance removal efficiency of PhCs

(Herrero and Stuckey, 2014). A common process to perform bioaugmentation is the addition of pre-adapted pure bacterial strains with ability to degrade a specific contaminant into wastewater bioreactors. However, the survival of introduced exogenous bacteria strains is a common problem faced by bioaugmentation in WWTPs (Herrero and Stuckey, 2014). Therefore, the introduction of these selected bacteria strains in a membrane bioreactor is also a growing technology that overcomes this problem and potentially enhance the removal efficiency of contaminants (El Fantroussi and Agathos, 2005). The isolation and identification of bacteria strain capable of degrading or biotransforming endoxifen into a less hazardous compound are the initial steps to determine a specialized inoculum to potentially be introduced for bioaugmentation (Der Gast, Knowles, Starkey, & Thompson, 2002). However, bacteria responsible for endoxifen biodegradation have not been reported.

2.5.2 Photodegradation of endoxifen

The use of direct UV photolysis to remove xenobiotic compounds from water is a cost-effective method that does not require the addition of hazardous chemicals making it an environmental friendly process (Zhang et al., 2017). Although UV photolysis is an effective treatment method, it may not be enough to eliminate certain xenobiotic compounds. For treatment of these compounds, a combination of advanced oxidants (sometimes with a catalyst) such as UV + hydrogen peroxide, UV + ozone, and UV + persulfate (Shemer, Kunukcu, & Linden, 2006). However, the elimination of xenobiotic compounds by direct photolysis is a chemical-free technology that does not influence the aesthetical quality of the treated water (Zhang et al., 2017). Compared with other oxidation processes, the use of UV light is expected to produce less toxic by-products

(Fatta-Kassinos et al., 2010; Zhang et al., 2017). Photodegradation with UV light has shown to be an effective treatment method to remove PhCs from water (Challis, Hanson, Friesen, & Wong, 2014). The presence of aromatic rings and conjugated π bonds in the molecule structure of some PhCs results in a great absorption of UV-C light (100-280 nm). The absorption of UV-C light by the molecule itself led to the degradation of PhCs (Challis et al., 2014). Endoxifen has three aromatic rings and a conjugated π bond, its photodegradation by UV light irradiation is a potential effective treatment method.

The direct photolysis of PhCs depends on the absorption spectra of the molecule (Trawiński & Skibiński, 2017b). PhCs usually have a maximum absorbance of light at wavelengths below 280 nm (Mathon, Choubert, Miege, & Coquery, 2016). Likewise, endoxifen has a light absorbance region between 220 and 340 nm with a maximum absorption around 240 nm (Teunissen et al., 2010). This maximum absorption wavelength suggests that UV-C (100-280 nm) light is potentially an effective light source to photodegrade endoxifen through direct photolysis. The wavelength produced by UV lamps is directly related to the mercury vapor pressure present inside the lamp (USEPA, 2003). Low pressure (LP) and medium pressure (MP) mercury UV lamps are the most common types of UV lamps used for UV photodegradation in water (Pereira et al., 2007). As shown in Figure 3, LP lamps emit a mono-chromatic wavelength at 253.7 nm while MP lamps emit a broad spectrum of UV light in a wavelength range of 205 to above 500 nm (USEPA, 2003).
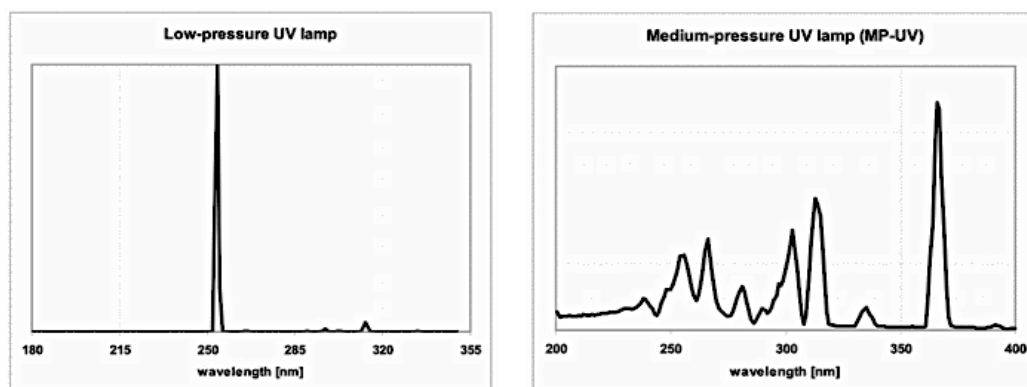
Figure 3. Wavelength spectrum for LP lamps and MP (BestUV, 2011).

In addition to the light energy source, several factors could influence the photodegradation of endoxifen in water. The pH of solution, the emission light intensity, the initial concentration, and quantum yield are important parameters to consider for photodegradation (Pereira et al., 2007; Udom et al., 2014). Quantum yield is the ratio of photodegraded molecules per photon absorbed (Trawiński & Skibiński, 2017b). If quantum yield is constant, photolysis rate of endoxifen will depend only on the number of photons absorbed by the molecule (Tønnesen, 2004). However, the presence of organic and inorganic molecules in water such as those in wastewater samples could vary the photolysis rate of endoxifen (Trawiński & Skibiński, 2017b).

WWTPs with UV light as a disinfection process commonly use LP lamps as UV light source. LP lamps have demonstrated their ability to degrade PhCs efficiently in wastewater samples through direct photolysis using a light dose of 100 mJ cm^{-2} (Oppenländer, 2003; Pereira et al., 2007). However, light doses used during WWTPs disinfection process are lower than those used to photodegrade a specific target compound. Little is known about the fate of endoxifen in WWTPs with UV light as a disinfection process.

2.6 Fate of endoxifen in WWTPs

The detection of endoxifen in wastewater effluents questions the treatment efficiency of WWTPs. There has been only one study on endoxifen removal process in WWTPs. Negreira et al. (2015) showed how chlorination process in ultrapure water and wastewater results in an ineffective degradation of endoxifen. Thirteen chlorinated by-products of endoxifen were formed after two minutes of reaction (Negreira et al., 2015). The toxicity assessment of the resultant disinfection by-products (DBPs) showed a low concentration for the predicted LC50 value for crustacean and fish categorizing them as hazardous to the aquatic environment. Therefore, the inefficient degradation of endoxifen and the production of hazardous DBPs during wastewater disinfection process bring an urgent need for further research particularly on endoxifen removal.

The use of UV light as a disinfection process at WWTPs has gained more traction (Guo et al., 2009). It should produce less toxic DPBs than disinfection through chlorination process (Larson & Befenbaum, 1988). However, the light doses used at WWTPs are low compare to those applied for photodegradation. According to EPA (2002), small WWTPs (3.8 to 76 m^3 day^{-1}) that use UV light (253.7 nm) for disinfection need a minimum UV light dose of 16 mJ cm^{-2} in order to meet the standard fecal coliform for secondary effluent (200 CFU per 100 mL). WWTPs with filtered nitrified secondary effluents use a minimal UV light dose of 30 mJ cm^{-2} (Shin, Linden, Arrowood, & Sobsey, 2001) while conventional WWTPs with activated sludge process use a minimal UV light dose of 97 mJ cm^{-2} (Darby, Snider, & Tchobanoglous, 1993). Although these light intensities are low, it might be interesting to determine if endoxifen photodegradation by UV disinfection takes place in WWTPs. Identifying the fate of

endoxifen in WWTPs will led to a better understanding of endoxifen removal and release to receiving waters.

CHAPTER 3: MATERIALS AND METHODS

3.1 Materials

3.1.1 Chemicals

A mixture of (E/Z)-endoxifen (1:1, w/w) was purchased from AdooQ Bioscience (Irvine, CA, USA). (Z)-endoxifen isomer was purchased from MedChem Express (Monmouth Junction, NJ, USA). Water, dymethyl sulfoxide (DMSO), acetonitrile, methanol, and isopropyl alcohol, all of them HPLC-grade, and sulfuric acid, hexane, ammonium chloride, sodium nitrate, choline chloride, D-biotin, D-Ca-pantothenate hemicalcium, p-aminobenzoic acid, potassium phosphate, sodium bicarbonate, monopotassium phosphate, calcium chloride, magnesium sulfate, potassium chloride, and sodium chloride, and tris(hydroxymethyl)-aminomethane, all of them reagent grade, were supplied by VWR (Chicago, IL, USA). Iron(III) sulfate, potassium oxalate monohydrate, folic acid, niacinamide, pyridoxine hydrochloride, riboflavin, thiamine hydrochloride, vitamin B12, i-inositol, sodium acetate trihydrate, hydroxylamine hydrochloride and 1,10-phenanthroline, all of them analytical grade, and HPLC-grade ammonium formate (>99.99%) were purchased from Sigma-Aldrich (St Louis, MO, USA).

3.2. Methods

3.2.1 Experimental framework

Experimental framework is shown in Figure 4.
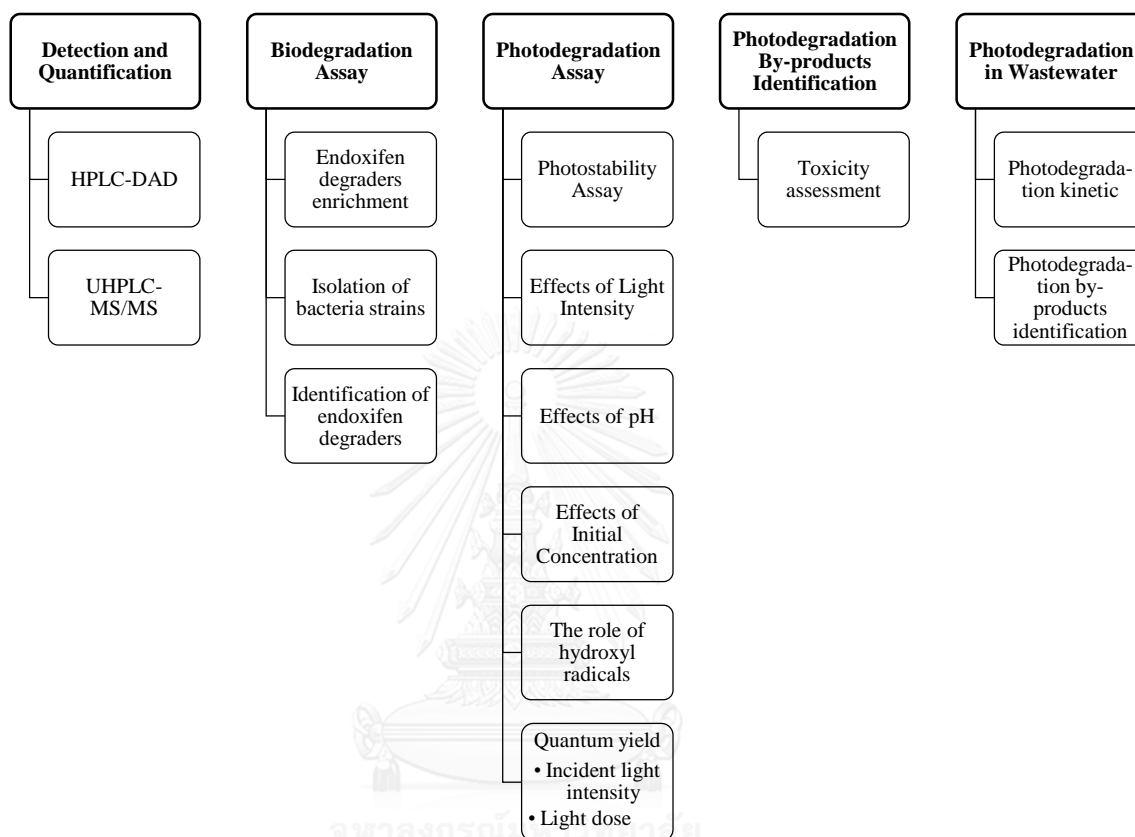
Figure 4. Experimental framework.

3.2.2 Preparations of (E)- and (Z)-endoxifen stock solutions

Stock solutions of (E)- and (Z)-endoxifen were prepared in a mixture of water and methanol (10:1, v/v) at 1 mg mL^{-1} and kept at -20°C. Standard samples for analytical calibration were obtained by diluting the stock solution in HPLC water to desired concentrations. For biodegradation, stock solutions of (E)- and (Z)-endoxifen were prepared by diluting five milligrams of (E)- and (Z)-endoxifen in 0.5 mL DMSO followed by 4.5 mL deionized water and stored at 4°C. Prior to the addition of endoxifen into the culture media, the stock solution was filter sterilized through a 1.2

µm pore size glass fiber filter (Sigma-Aldrich, St Louis, MO, USA). For photodegradation, water samples directly spiked with (E)- and (Z)-endoxifen were prepared daily.

3.2.3 Detection and quantification of endoxifen by HPLC-DAD

The concentrations of (E)- and (Z)-endoxifen in the water samples were analyzed using a HPLC (AGILENT® 1620 Poroshell 120 Phenyl-Hexyl Column 2.7 µm, 4.6 mm × 100 mm, 60±0.8°C) with a DAD. The isocratic mobile phase was a mixture of HPLC-grade acetonitrile and ultrapure water (50:50 v/v) containing 5 mM ammonium formate (pH 3.4). The isocratic mobile flow was 0.3 mL min^{-1} with a constant injection volume of 50 µL. An absorbance 3D plot analysis showed the optimum absorbance wavelength of (E)- and (Z)-endoxifen at a wavelength of 244 nm (Appendix A, Figure A.1). The described HPLC-DAD method was validated according to the International Council of Harmonization (ICH) guidelines for selectivity, linearity, sensitivity, accuracy, and precision (ICH, 2005) (Results in Appendix A). The data was processed by LC Chemstation software.

3.2.3.1 Selectivity

Blank water and wastewater samples and spiked with (E)- and (Z)-endoxifen at 2 µg mL^{-1} were analyzed for peak detection by HPLC-DAD. The absence of co-elution impurities was determined by comparing the resultant chromatograms (Appendix A, Figure A.2). Selectivity was confirmed by successfully separating the analytes from possible impurities found in water and wastewater samples.

3.2.3.2. (E)- and (Z)-endoxifen retention times

The identifications of (E)- and (Z)-endoxifen isomers retention times were determined by spiking water samples with only (Z)-endoxifen isomer at 1 μg mL^{-1} and analyzed for retention time by HPLC-DAD. According to (Elkins et al., 2014), the major observed peak at the resultant chromatogram was (Z)-endoxifen while the minor peak was (E)-endoxifen (Appendix A, Figure A.3). Eighteen water samples spiked with a mixture of (E)- and (Z)-endoxifen at 1 μg mL^{-1} were analyzed in triplicate by HPLC-DAD. Chromatogram peaks with retention times of 9.24±0.3 minutes and 10.03±0.4 minutes corresponded to (E)- and (Z)-endoxifen, respectively.

3.2.3.3 Linearity and sensitivity

Nine standard samples for analytical calibration were prepared by combining aliquots of the stock solution with the proper volume of water to obtain standard samples with (E)- and (Z)-endoxifen (1:1, w/w) concentrations in the range of 25 to 500 ng/ml per isomer. The calibration was performed in triplicate. The resultant chromatograph peak areas were correlated with the known concentration using a linear regression analysis (significance level p = 0.95) (Appendix A, Figure A.4). Coefficient of determination (R^2) was calculated for (E)- and (Z)-endoxifen isomers and was greater than 0.997 for both isomers (Appendix A, Table A.1). The limit of detection (LOD) and limit of quantification (LOQ) were calculated based on the slopes and the standard deviation of the response using the following equations (ICH, 2005):

$$LOD = \frac{3.3\sigma}{S} \qquad\qquad (1)$$

$$LOQ = \frac{10\sigma}{S} \qquad\qquad (2)$$

Where: σ = standard deviation of the response; and S= slope of the calibration curve.

3.2.3.4 Accuracy and precision

Quality control (QC) samples were prepared for within-day and inter-day assays by combining aliquots of the stock solution with the proper volume of water to obtain three standard samples with the following concentrations of (E)- and (Z)-endoxifen: 100 ng mL^{-1} for the quality control low (QCL), 350 ng mL^{-1} for the quality control medium (QCM), and 700 ng mL^{-1} for quality control high (QCH). Five replicates of each QC sample were prepared individually to analyze the precision and accuracy of the HPLC-DAD method. Within-day assay was calculated by injecting five times each QC sample during the same day and inter-day assay was calculated by injecting each QC sample for five consecutive days. The accuracy was presented as percent coefficient of variation (CV, %) while precision was calculated as percent deviation of the sample consistency (RSD) (Appendix A, Table A.2). The method was considered accurate and precise when CV and RSD values were below 15%.

3.2.4 Biodegradation experimental setup and procedure

3.2.4.1 Sample collection and preparation

Wastewater samples were collected from the Moorhead WWTP, Moorhead, MN, USA. The samples were collected in amber glass bottles and transported to a laboratory in cold boxes.

3.2.4.2 Inoculum source

Mixed liquor suspended solids (MLSS) obtained from the Moorhead WWTP (Moorhead, MN, USA) prior to secondary sedimentation tanks were used as an inoculum for endoxifen degrader enrichment. The sample (1 L) was aerated and mixed (100 rpm) during storage (less than 3 hours) (Zhou, Lutovsky, Andaker, Gough, &

Ferguson, 2013), and used within the collection day.

3.2.4.3 Liquid media

Two liquid media, mineral media (MM) and mineral media vitamin (MMV), without nutrient were used as culture media for enrichment. A mineral solution as described by (Tanner, 2007), was used as MM with the nitrogen source reduction ($NH_4Cl = 50$ mg L^{-1}) and the addition of sodium nitrate (5 mg L^{-1}). MMV was MM added with vitamins (choline chloride (0.3 g L^{-1}), D-biotin (0.02 g L^{-1}), D-Ca-pantothenate hemicalcium (0.025 g L^{-1}), folic acid (0.1 g L^{-1}), niacinamide (0.1 g L^{-1}), pyridoxine hydrochloride (0.1 g L^{-1}), riboflavin (0.02 g L^{-1}), thiamine hydrochloride (0.1 g L^{-1}), vitamin B12 (0.05 mg L^{-1}), i-inositol (3.5 g L^{-1}), *p*-aminobenzoic acid (0.02 g L^{-1})). MM and MMV were buffered by potassium phosphate (1 M) and sodium bicarbonate (1 M). MM, MMV, and sodium bicarbonate were filter sterilized through a 1.2 μm pore size glass fiber filter (Sigma-Aldrich, St Louis, MO, USA) and potassium phosphate was autoclaved. MM and basal salt media (BSM) were used to identify endoxifen degraders in biodegradation assays. BSM contained monopotassium phosphate (0.1 g L^{-1}), calcium chloride (0.4 g L^{-1}), magnesium sulfate (0.2 g L^{-1}), potassium chloride (0.1 g L^{-1}), and sodium chloride (0.8 g L^{-1}) (Siripattanakul, Wirojanagud, McEvoy, Limpiyakorn, & Khan, 2009) and was filter sterilized through a 1.2 μm pore size glass fiber filter (Sigma-Aldrich, St Louis, MO, USA). For all media, stock solutions were prepared in 100× concentration and stored at 4°C.

3.2.4.4 (E)- and (Z)-endoxifen degrader enrichment

To enhance the presence of endoxifen degraders in the sample, the following enrichment method was performed. Half milliliter of the (E)- and (Z)-endoxifen stock

solutions and 50 mL MLSS inoculum were added to 1,000 mL flasks containing 449.5 mL MM and MMV, respectively (MM1 and MMV1). Two control media were used to ensure that endoxifen degradation was through microbial activity: mineral media vitamin control (MMVC1) to ensure that endoxifen does not react with the components in MM and MMV, and deionized water control (IWC1) to ensure that endoxifen was not hydrolyzed and/or subject to other losses (such as volatilization and adsorption to glassware). For MMVC1, 1,000 mL flasks containing 449 mL MMV and 50 mL MLSS inoculum were autoclaved and (E)- and (Z)-endoxifen were added as the flask cooled down to 25ºC. For IWC1, (E)- and (Z)-endoxifen (1 mg L^{-1}) were incubated in 499.5 mL deionized water previously autoclaved. All batches (MM1, MMV1, MMVC1, and IWC1) were incubated in the dark, at $23.5\pm1.5°C$, and 150 rpm in a rotary shaker for 40 days.

In order to reduce the initial concentration of MLSS due the presence of organic compounds that can serve as carbon and nitrogen sources for bacteria, dilutions on the initial batches (MM1, MMV1, MMVC1, and IWC1) were performed in 1,000 mL flasks containing fresh media until a dilution factor of 10^{-4} was reached. In order to achieve this dilution factor, after 4 days incubation, 50 mL from each batch (MM1, MMV1, MMVC1, and IWC1) were transferred to 450 mL fresh media reaching a MLSS dilution factor of 10^{-2}. The new batches (MM2, MMV2, MMVC2, and IWC2) were incubated along with the initial batches (MM1, MMV1, MMVC1, and IWC1) in the same rotary shaker under the same conditions. After 18 days incubation of MM2, MMV2, MMVC2, and IWC2, 5 mL from these batches were transferred to 450 mL fresh media reaching the target dilution factor of 10^{-4}. The new batches (MM4, MMV4, MMVC4, and IWC4) were incubated along with the initial batches (MM1, MMV1,

MMVC1, and IWC1) in the same rotary shaker under the same conditions for 18 days. For all batches, (E)- and (Z)-endoxifen (1 mg L^{-1}) were added every 10 days of incubation and two methods were used to monitor microbial growth: The plate count in R2A agar and volatile suspended solids concentration(APHA, AWWA, & WEF, 1998) (Appendix B, Figure B7-B12). Temperature and pH were also monitored daily (Appendix B, Figure B1-B6).

3.2.4.5 (E)- and (Z)-endoxifen degrader isolation

Isolated colonies after the enrichment process obtained from the mixed cultures during plate counting were subcultured for further endoxifen biodegradation assay. The colonies were picked with a sterilized loop and resuspended in 1 mL sterile buffer phosphate saline (PBS) enriched with (E)- and (Z)-endoxifen (1 mg L^{-1}). One hundred microliter aliquots were incubated on R2A agar plates through the streak plate method. The agar plates were incubated in the dark at 23.5°C for 3 days. The resultant isolated colonies were individually incubated in two different sterilized glass test tubes containing 10 mL of MM and BSM respectively, both enriched with sterilized (E)- and (Z)-endoxifen (1 mg L^{-1}). The tubes were capped, mixed and incubated for 6 days in the dark, at 23.5±1.5°C, and 150 rpm in a rotary shaker. Optical density (OD) were used to monitor bacterial growth in MM and BSM (Zhou et al., 2013). OD were measured by using a spectrophotometer at 600 nm wavelength and a semi-micro acrylic cuvette (VWR, Chicago, IL, USA) with a 1 cm path length. OD were measured at days 0, 3 and 6. Test tubes containing the growing media (MM or BSM) that have shown positive results for bacteria growth were analyzed for endoxifen concentration at days 0, 3, and 6. Control samples with the bacteria strain previously autoclaved were run in parallel

under the same conditions. (E)- and (Z)-endoxifen in the growing media samples were subjected to extraction prior to their quantification analysis.

3.2.4.6 Extraction and quantification of (E)- and (Z)-endoxifen

The extraction method developed by (Antunes et al., 2013) to extract tamoxifen and its metabolites from human plasma was slightly modified in order to extract (E)- and (Z)-endoxifen from BSM and MM. Briefly, two milliliters of the sample, 0.7 mL Tris buffer (tris(hydroxymethyl)-aminomethane 23.4 g L^{-1}) and 5.2 mL hexane with propanol (95:5, v/v) were added into a glass tube and were mixed for 10 minutes followed by a 10-minute centrifugation at 2000 *g*. The upper layer was transferred into a clean tube and dried with nitrogen until no liquid was observed. The remaining residue was resuspended in a mixture of HPLC-water and HPLC-grade methanol (9:1, v/v) and directly injected to HPLC-DAD to determine (E)- and (Z)-endoxifen concentrations by the previously describe method in subsection 3.2.3.

3.2.5 Photodegradation experimental setup and procedure

Laboratory-scale photodegradation experiments were performed in a RPR-200 Rayonet™ photoreactor (Southern New England Ultraviolet Company, Brandfort, UK), equipped with a cooling fan to keep the photoreactor temperature at 23-25°C (Figure 5). The photoreactor was equipped with sixteen 14W low-pressure mercury lamps emitting UV light at 253.7 nm. The emitted light intensity (14 W/lamp) was determined by the lamp manufacturer (Southern New England Ultraviolet Company, n.d.). The light intensity was regulated by controlling the number of lamps in the photoreactor. Photodegradation experiments were performed using 10 mL quartz test tubes (ACE Glass incorporate, Vineland, NJ, USA) filled with 5 mL of the sample. The

pH was adjusted with either 1 M HCl or 1 M NaOH. The quartz tubes were placed vertically at a fixed distance of 3.5 inches from the lamp in a rotary merry-go-round at 5 rpm. Sample aliquots were collected in 2 mL HPLC amber vial (VWR, Chicago, IL, USA) with time and analyzed for endoxifen and PBPs using HPLC-DAD and/or UHPLC-MS/MS.

According to (Elkins et al., 2014), (Z)-endoxifen isomer suffer *trans* isomerization to (E)-endoxifen isomer under certain conditions. In this study, the direct dilution of (Z)-endoxifen in water results in an immediate *trans* isomerization to (E)-endoxifen. Likewise, (E)-endoxifen in aqueous solution suffered an immediate *cis* isomerization to (Z)-endoxifen. (E)- and (Z)-endoxifen present estrogenic activity in water but the third isomer (Z')-endoxifen has no estrogenic activity reported and is not a potential risk to the environment (Jaremko et al., 2010). Therefore, photodegradation experiments were conducted using a mixture of (E)- and (Z)-endoxifen (1:1, w/w).

Figure 5. RPR-200 Rayonet™ photoreactor (Source: Southern New England Ultraviolet Company, Brandfort, UK).

3.2.6. Optimization of photodegradation kinetics and efficiency

3.2.6.2 Effect of UV light intensity

Photodegradation kinetics and efficiency of (E)- and (Z)-endoxifen were tested at the following UV light intensities in triplicate: 28 W s^{-1} cm^{-2} (2 lamps), 56 W s^{-1} cm^{-2} (4 lamps), 112 W s^{-1} cm^{-2} (8 lamps), 168 W s^{-1} cm^{-2} (12 lamps), and 224 W s^{-1} cm^{-2} (16 lamps). Water samples directly spiked with a mixture of (E)- and (Z)-endoxifen (1:1, w/w) at 2 μg mL^{-1} were exposed to UV light (253.7 nm). The water samples were irradiated for 80 seconds at 28 W s^{-1} cm^{-2}, 60 seconds at 56 W s^{-1} cm^{-2}, 45 seconds at 112 W s^{-1} cm^{-2}, and 30 seconds at 168 and 224 W s^{-1} cm^{-2}. At certain time intervals, 1 mL aliquots were collected and analyzed for endoxifen concentration by HPLC-DAD. Controls in dark condition ran in parallel for 80 seconds.

3.2.6.3 Effect of initial pH

Water samples directly spiked with a mixture of (E)- and (Z)-endoxifen (1:1, w/w) at 2 μg mL^{-1} were irradiated in triplicate at a constant UV light intensity of 28 W s^{-1} cm^{-2} for 80 seconds. Initial pH of the samples was varied at 5, 6, 7, 8, and 9. The pH adjustment was performed by using 1 M HCl or 1 M NaOH. One milliliter aliquots were collected every 10 seconds and analyzed for (E)- and (Z)-endoxifen concentrations by HPLC-DAD. The first order rate constant (k) was calculated for each isomer. The pH after the irradiation was also recorded.

3.2.6.4 Effect of initial concentration

Effect of initial concentrations of (E)- and (Z)-endoxifen (0.5, 1, and 2 μg mL^{-1}) on the photodegradation kinetic and efficiency was tested in triplicate. Water samples directly spiked with the desired concentrations of (E)- and (Z)-endoxifen were irradiated at a

constant UV light intensity of 224 W s^{-1} cm^{-2} for 30 seconds. One milliliter aliquots were collected every 5 seconds and analyzed for (E)- and (Z)-concentration by HPLC-DAD.

3.2.6.5 Effect of light source

Photodegradation of (E)- and (Z)-endoxifen was tested under three different light sources in triplicate: sun light (May 31, 2017, 1:00 PM, Fargo, ND, USA, GPS coordinate: 46.895128, -96.801131), indoor light (F15T8/CW 15 W T8 cool white fluorescent bulb), and UV light (253.7 nm and emission light intensity of 224 W s^{-1} cm^{-2}). Ten milliliter quartz test tubes filled with 5 mL of water directly spiked with (E)- and (Z)-endoxifen at 2 µg mL^{-1} and pH 7 were irradiated for 1 minute. Controls were run in the dark in parallel. One milliliter aliquots of water samples exposed to UV light were collected every 5 seconds while aliquots of water samples exposed to sunlight and indoor lamp were collected every 15 seconds. The collected samples were analyzed for (E)- and (Z)-endoxifen using HPLC-DAD.

3.2.7 The role of hydroxyl radicals

The oxidation of (E)- and (Z)-endoxifen by hydroxyl radicals generated during UV photodegradation was investigated. Isopropyl alcohol (IPA) was added to water samples to quench hydroxyl radical generated by UV light (253.7 nm) (Jo et al., 2016). Water samples with IPA (1%, v/v) and without IPA, both directly spiked with (E)- and (Z)-endoxifen at 2 µg mL^{-1} were irradiated by UV light (253.7 nm) at a constant light intensity of 224 W s^{-1} cm^{-2} for 30 seconds. The experiment was conducted in triplicate. Controls (dark condition) were included. One milliliter aliquots were collected with time and analyzed for (E)- and (Z)-endoxifen concentrations by HPLC-DAD.

3.2.8 Molar extinction coefficient of (E/Z)-endoxifen

The molar extinction coefficient (ε) of (E/Z)-endoxifen was determined at a wavelenght of 253.7 nm using a UV-Vis spectophotometer (Cari 7000, Agilent, Santa clara, CA, USA.) Aborbance (253.7 nm) was measured in triplicate for water samples directly spiked with (E/Z)-endoxifen at the following concentrations: 0.375, 0.7, 1.4, 2.8 an 5 μg mL^{-1}. The observed absorbance values were plotted versus (E/Z)-endoxifen concentrations and the resultant slope (0.1097 mM^{-1} cm^{-1}) revealed the molar extinction coefficient of (E/Z)-endoxifen (Appendix C, Figure C.1). The molar extintion coefficient is a indispensable parameter to calculate quantum yield (Φ) in order to determine the photolysis efficiency (Jin et al., 2017).

3.2.9 Quantum yield, incident light intensity and light dose

Quantum yield (Φ) was calculated by the ferroxilate actinometer method (Bolton, Stefan, Shaw, & Lykke, 2011). Briefly, iron(III) sulfate solution (0.2 M) was prepared in H$_2$SO$_4$ solution (2 N) and storage in the dark. Ferroxilate solution (6 mM) for the determination of quantum yield was prepared in a 1,000-mL volumetric flask containing 800 mL deionized water added with 15.2 mL of potassium oxalate solution (1.2 M) and 35 mL of H$_2$SO$_4$ solution (2 N). The solution was mixed well and 15.23 mL of the previously prepared iron(III) sulfate solution was added. Ferroxilate samples were prepared in the dark to avoid photolysis of the ferroxilate.The iron(III) percentage for the ferroxilate solution (21.72%) was calculated using the Beer-Lambert law equation:

$$A = C \, \varepsilon \, l \qquad\qquad (3)$$

Where: A = absorbance of the iron (III) sulfate solution at 302 nm; C = concentration of iron (III) (M); ε = molar extintion coefficient of iron (III) (2,196 M^{-1} cm^{-1} at 25°C); and l = path lenght (cm^{-1}).

Photoreaction of the ferroxilate solution was performed exactly as the photodegradation experiemnts of (E)- and (Z)-endoxifen. The ferroxilate solutions were irradiated in triplicate at four emission light intensities (56, 112, 168, and 224 W s^{-1} cm^{-2}) for 60 seconds. After that, one mililiter aliquots were adeed to 10-mL volumetric flasks containing 164 mg of sodium acetate trihydrate and 0.4 mg of 1,10-phenantroline. Dionized water was adeed to the 10 mL mark and the flasks were kept in the dark for 1 hour. The solution was then transfered into a quartz cuvette and the absorbance at 502 nm was read (Appendix C, Figure C.2). Unirradiated samples (controls in the dark) were included). The mole of Fe^{2+} formed in the ferroxilate solutions was determined spectrophophotometrically by using the following equation:

$$\text{moles of } Fe^{2+} = \frac{[A_{510}(\text{sample})-A_{510}(\text{blank})] \times V_1 \times V_2}{\varepsilon \ Fe^{2+}\text{-o-phenantroline} \times 1{,}000 \times V_3} \tag{4}$$

Where: A = absorbance (510 nm); V_1 = volume of the complexation solution (10 mL); V_2 = volume collected from the irradiated sample (1 mL); ε Fe^{2+}-o-phenantroline = molar extintion coefficient of Fe^{2+}-o-phenantroline complex (11,110 M^{-1} cm^{-1}); and V_3 = volume of the irradiated sample (5 mL)

Photon irradiance (E_p) (Einstein^{-1} cm^{-2} min^{-1}) at each emission light intensity was calculated using the following equation:

$$E_p = \frac{\text{moles Fe}^{2+}}{\Phi Fe^{2+}_{(254nm)} \times Area \times t} \qquad (5)$$

Where: $\Phi Fe^{2+}_{(254\,nm)} = 1.25$ (mol Einstein^{-1}); Area = quartz test tube area (2.54 cm^2); and t = irradiation time (1 min).

Photon irradiance gave information about the number of photons reaching the water sample in mol Einstein^{-1}. The application of the appropriated conversions units (1 Einstein $_{(254\,nm)}$ = 47,0954.74 W s^{-1}) allowed the calculation of the incident light intensity (mW s^{-1} cm^{-2}), and light dose (mJ cm^{-2}) was calculated using the following formula:

Light dose = Incident light intensity × Irradiation time

Quantum yield (Φ) (mole Einstein^{-1}) at each emission light intensity was calculated using the following formula:

$$\Phi = \frac{k}{2.303 E_p \times \varepsilon_{(253.7nm)}} \qquad (6)$$

Where: k = first order reaction of (E)- and (Z)-endoxifen (M min^{-1}); E_p = photon irradiance (Einstein^{-1} cm^{-2} min^{-1}); and $\varepsilon_{(254nm)}$ = molar extinction coefficient of (E)- and (Z)-endoxifen at 257.3 nm (0.1097 mM^{-1} cm^{-1}).

3.2.10 Photodegradation by-products identification by UHPLC-MS/MS

The molecular structure of PBPs were identified using UHPLC-MS/MS (ACQUITY UPLC® BEH C18 column 17 μm, 100 mm × 2.1 mm, 25°C) with a mixture of acetonitrile and 10 mM ammonium formate solution (1:1, v/v), both HPLC-grade, as a mobile phase. The isocratic flow rate was 0.26 mL min^{-1} and the sample injection

volume was 5 μL. The mass range analyzed was between 50 and 1000 Da. The assessment of mass measurement error (Δm) in ppm was performed for detected compounds. Total analytical run was 5 minutes with retention times of 1.67±0.04 minutes and 1.79±0.05 minutes for (E)- and (Z)-endoxifen, respectively (Appendix C, Figure C.2). (E)- and (Z)-endoxifen were observed at the ion-m/z = 374.21 with Δm within less than 3.74 ppm (Appendix C, Figure C.3). Chromatography peaks showing different ion-*m/z* values and retention times than (E)- and (Z)-endoxifen were determined as potential PBPs. These PBPs were analyzed with Tandem Quadrupole Mass spectrometry (MS/MS) with an electrospray ionization (ESI) source and operated at a positive mode (Collison energy = 27 V). Data and potential molecular composition were analyzed through MassLynk V4.1 SCN627 software.

3.2.11 Toxicity assessment

The toxicity of (E)-endoxifen, (Z)-endoxifen, and the potential PBPs were assessed using the Toxicity Estimator Software Tool (TEST) developed by (USEPA, 2016). TEST is a mathematical model that predicts the biological activity of analytes based on their molecular structures through Quantitative Structure Activity Relationships (QSAR) analyses (USEPA, 2016). The consensus method was selected because it provides the average of five QSAR methodologies giving the best toxicology approach. Among the different toxicology analysis offered by TEST, the calculation of the 50 % Lethal Concentration (LC$_{50}$) acute end-points of the crustacean *Daphnia magna* (48 h) and the fish fathead minnow (96 h) were selected as recommended by Negreira et al. (2015) as suitable species for an aquatic toxicity assessment.

3.2.12 Photodegradation experiments in wastewater

Photodegradation experiments of (E)- and (Z)-endoxifen were performed in secondary treated (high purity oxygen activated sludge and moving bed bioreactor) wastewater samples collected from the Moorhead WWTP, MN, USA. The wastewater sample was filtered through a 0.45 μm pore-size cellulose acetate membrane filter (Whatman, Pittsburgh, PA, USA). Total organic carbon (TOC) of the wastewater was determined using a UV/persulfate oxidation TOC analyzer (Phoenix 8000, Tekmar Dohrmann, OH, USA). Nitrite and nitrate concentrations were analyzed using the nitrite TNT840 plus vial test and nitrate TNT835 plus vial test, respectively (HACH, Loveland, CO, USA). Two experiments were conducted with wastewater samples, one to determine the photodegradation kinetics of (E)- and (Z)-endoxifen in wastewater and the other to simulate photodegradation of (E)- and (Z)-endoxifen at light doses used in WWTPs disinfection process. For both experiments, wastewater was directly spiked with (E)- and (Z)-endoxifen isomers at 1 μg mL^{-1} and control samples were run parallel in the dark to determine the presence of side reactions that could reduce the concentration of (E)- and (Z)-endoxifen in the sample. To determine the photodegradation kinetics of (E)- and (Z)-endoxifen, wastewater samples were irradiated in triplicate with an emission light intensity of 56 W s^{-1} cm^{-2} for 45 seconds. One milliliter aliquots were collected with time and analyzed for (E)- and (Z)-endoxifen concentrations by HPLC-DAD.

For the second experiment, wastewater samples were irradiated at a UV light intensity of 56 W s^{-1} cm^{-2} (Incident light intensity = 2.77 mW s^{-1} cm^{-2}) for 6, 11, and 35 seconds in order to simulate the minimal UV light doses applied at WWTPs of 16, 30 and 97 mJ cm^{-2} respectively. One milliliter aliquots were collected at the specified time points

and analyzed for (E)- and (Z)-endoxifen concentrations by HPLC-DAD. The potential molecular structures of observed PBPs at 35 seconds were identified by UHPLC-MS/MS following the previously described method.

3.2.13 Statistical analysis

Statistical analysis of data was performed by the analysis of variance (ANOVA) using Minitab 1.7. The significance of the independent variables (light intensity, pH, initial endoxifen concentration, and IPA addition) was evaluated for (E)- and (Z)-photodegradation rate in water with a 95% level of confidence using the Tukey test. The significance criterion is $p < 0.05$.
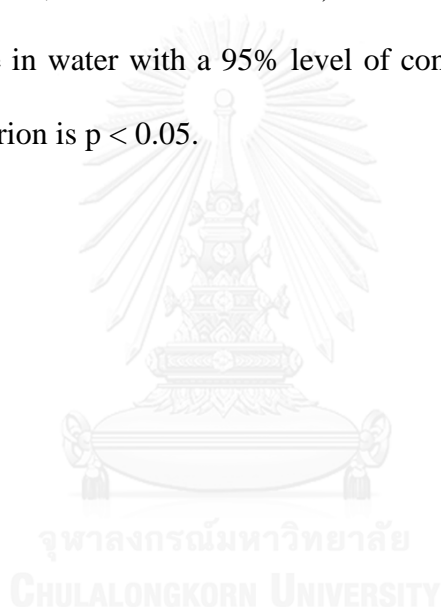
CHAPTER 4: RESULTS AND DISCUSSION

4.1 Biodegradation

Eleven colonies were isolated after the enrichment process. The isolated colonies were incubated individually on MM and BSM both enriched with (E)- and (Z)-endoxifen at $1\mu g$ mL^{-1} for 6 days. OD analyses revealed that only one colony (colony 6) showed positive result for bacteria growth (Figures 6 and 7). Therefore, the concentrations of (E)- and (Z)-endoxifen were only analyzed for colony 6 at days 0, 3, and 6. As observed in Figure 8, (E)- and (Z)-endoxifen concentrations were not reduced after 6 days of incubation. This result suggests that the bacteria strain (isolated colony 6) was not able to use (E)- and (Z)-endoxifen as carbon and or nitrogen source. The observed growth of colony 6 in BSM could be explained by the presence of trace concentration of DMSO from (E)- and (Z)-endoxifen stock solution used to enrich the growing media. The presence of two methyl groups in the molecular structure of DMSO could serve as a carbon source for bacteria. However, the concentration of DMSO in the growing media was lower than 1% (v/v) which could also explain the limited growth (based on OD). Biodegradation of DMSO by a bacteria strain from activated sludge was previously reported by Sz-Chwun et al. (2007). Colony 6 could use the residual DMSO as a carbon source for growth instead of using (E)- and (Z)-endoxifen. This suggests that colony 6 will not degrade (E)- and (Z)-endoxifen if DMSO is present in the media. However, DMSO is commonly found in wastewater at concentration raging from mg L^{-1} to g L^{-1} due to it widespread use in industries (Cheng, Wodarczyk, Lendzinski, Peterkin, & Burlingame, 2009; Glindemann, 2005). Any further work on colony 6 as a potential (E)- and (Z)-endoxifen degrader in wastewater is not fruitful because DMSO is

expected to be present in WWTPs at higher concentrations than (E)- and (Z)-endoxifen.

Therefore, the research focus was shifted to photodegradation of (E)- and (Z)-endoxifen
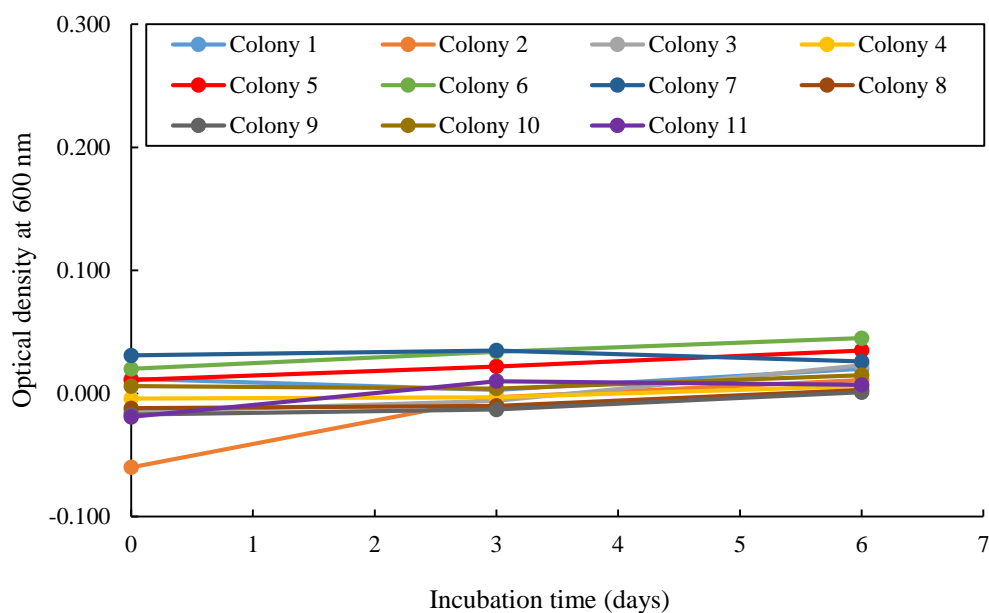
by UV light.

Figure 6. Optical density results of eleven isolated bacteria incubated in MSM for 6

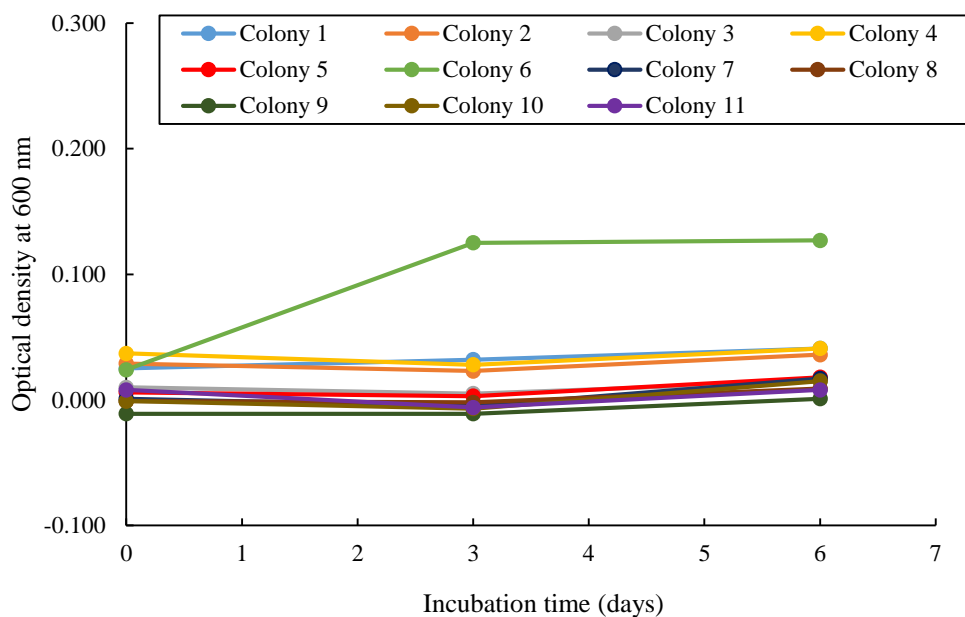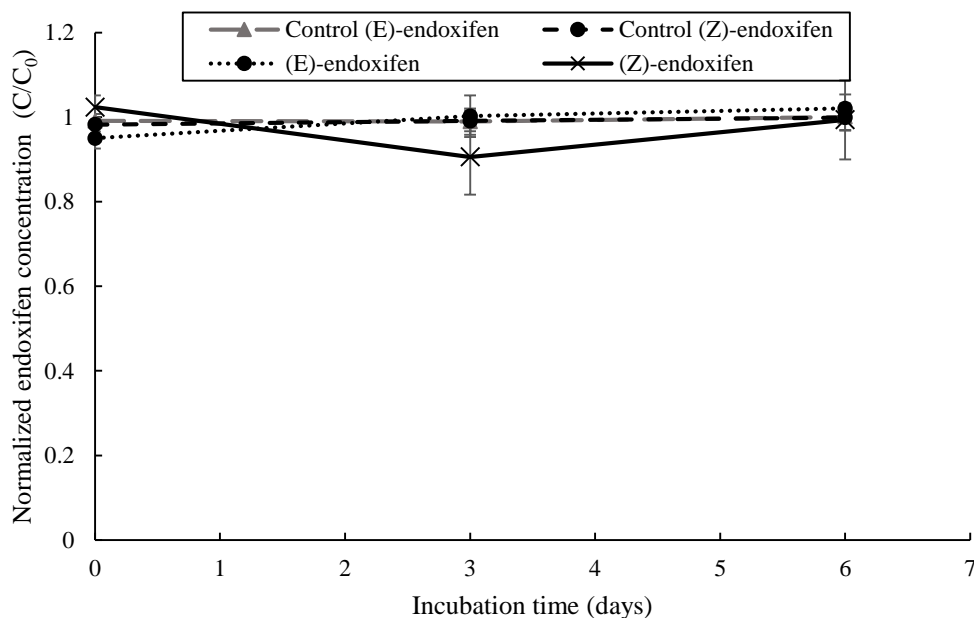days in the dark, at 23.5±1.5°C, and 150 rpm on a rotary shaker.

Figure 7. Optical density results of eleven isolated bacteria incubated in BSM for 6 days in the dark, at 23.5±1.5°C, and 150 rpm on a rotary shaker.

Figure 8. Normalized (E)- and (Z)-endoxifen concentrations in BSM during the incubation of Colony 6 in the dark, at 23.5±1.5°C, and 150 rpm in a rotary shaker for 6 days.

4.2 Photodegradation

4.2.1 Optimization of photodegradation kinetics and efficiency

4.2.1.1 Effect of light intensity on endoxifen photodegradation

Linear regression analyses of (E)- and (Z)-endoxifen photodegradation data at five different light intensities (28, 56, 112, 168, and 224 W s^{-1} cm^{-2}) revealed that both endoxifen isomers followed a first order kinetic model (Figures 9 and 10). The determination coefficient values (R^2) of the fitness of the model were greater than 0.97 at all light intensities for first order reaction while zero and second order fits had the same or lower R^2 (Appendix C, Table C.1). The photodegradation rate constants (k) of (E)- and (Z)-endoxifen isomers for the first order kinetic model and the emission light intensities were linearly related ($R^2 > 0.949$ and 0.935 for (E)- and (Z)-endoxifen, respectively) (Appendix C, Figure C.1). ANOVA results also indicated that the effect of light intensity on the photodegradation rate was significant (p = 0.0001 for (E)- and (Z)-endoxifen). The maximun emission light intensity of 224 W s^{-1} cm^{-2} provided the highest photodegradation rates of (E)- and (Z)-endoxifen isomers with k values of 77.1±5.4 µM s^{-1} and 82.5± 5.6 µM s^{-1}, respectively. Previous studies focused on phenol photodegradation reported that the greater the UV light intensity, the greater the number of photons present in the water sample to carry on first order photodegradation reactions (Chiou & Juang, 2007; Udom et al., 2014). Likewise, the photodegradation rates of (E)- and (Z)-endoxifen were greater as the emission light intensity increased.
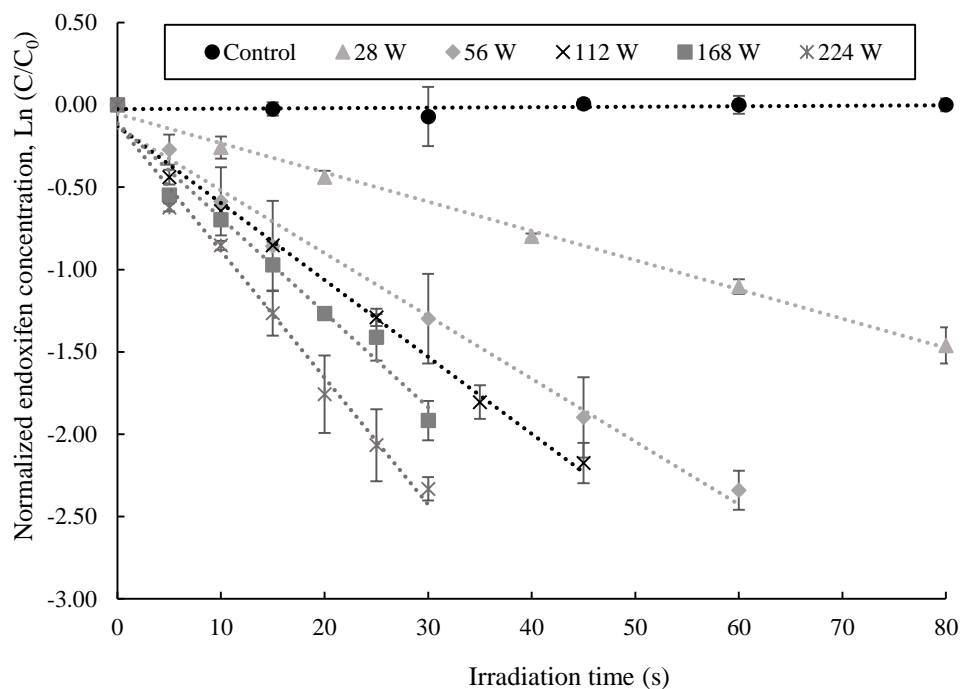
Figure 9. Kinetics of photodegradation (E)-endoxifen in aqueous solution at 2 µg ml^{-1} (pH 7 and 22.4 °C) and at five different emission light intensities (28, 56, 112, 168, and 224 W s^{-1} cm^{-2}) and first-order fit.
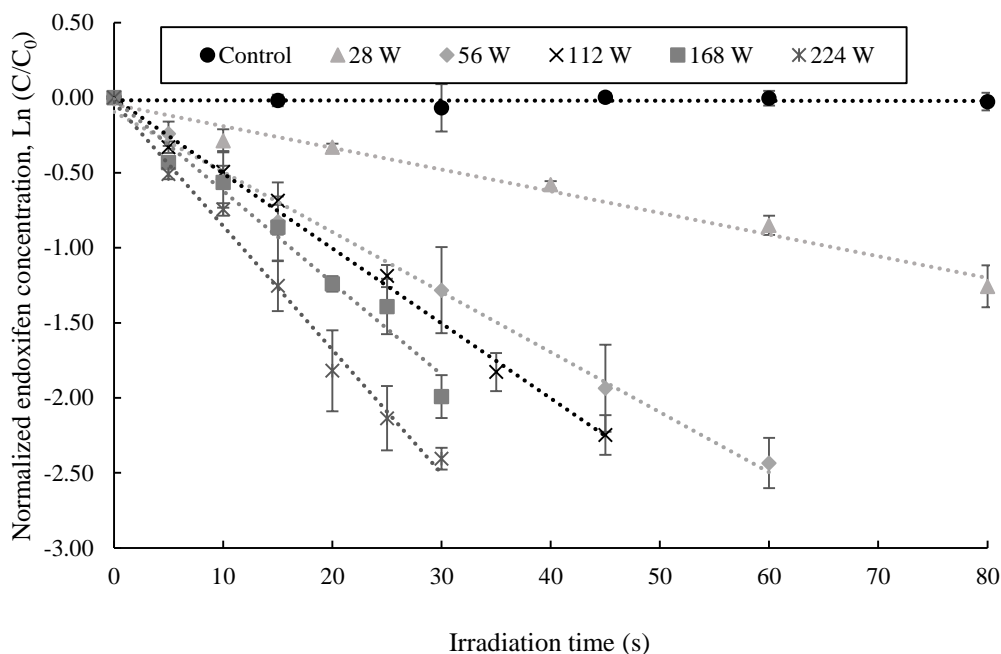
Figure 10. Kinetics of photodegradation (Z)-endoxifen in aqueous solution at 2 µg ml^{-1} (pH 7 and 22.4 °C) and at five different emission light intensities (28, 56, 112, 168, and 224 W s^{-1} cm^{-2}) and first-order fit.

4.2.1.2 Effects of pH on endoxifen photodegradation

The influence of pH on the photodegradation rate constant (k) was investigated in a pH range of 5-9 and at a constant emission light intensity of 28 W s^{-1} cm^{-2}. The results are summarized in Figure 11 where the calculated k value for each tested pH was plotted against its corresponding pH value. The maximum k value for (E)- and (Z)-endoxifen isomers were 16.61 and 15.36 μM s^{-1} at pH 7 and 9, respectively. The differences between the maximum and minimum k values for (E)- and (Z)-endoxifen isomers were 2.06 and 2.39 μM s^{-1}, respectively. These results suggest that the photodegradation of (E)- and (Z)-endoxifen isomers in water is not pH dependent. A statistical analysis

(ANOVA) confirms that the photodegradation rate is independent of the pH tested (p = 0.950 for (E)-endoxifen and p = 0.884 for (Z)-endoxifen). The neutral pH of 7 was selected as the working pH because it presents the maximum k value for (E)-endoxifen and the k value that is slightly lower the maximum value for (Z)-endoxifen (0.83 μM s^{-1} difference).
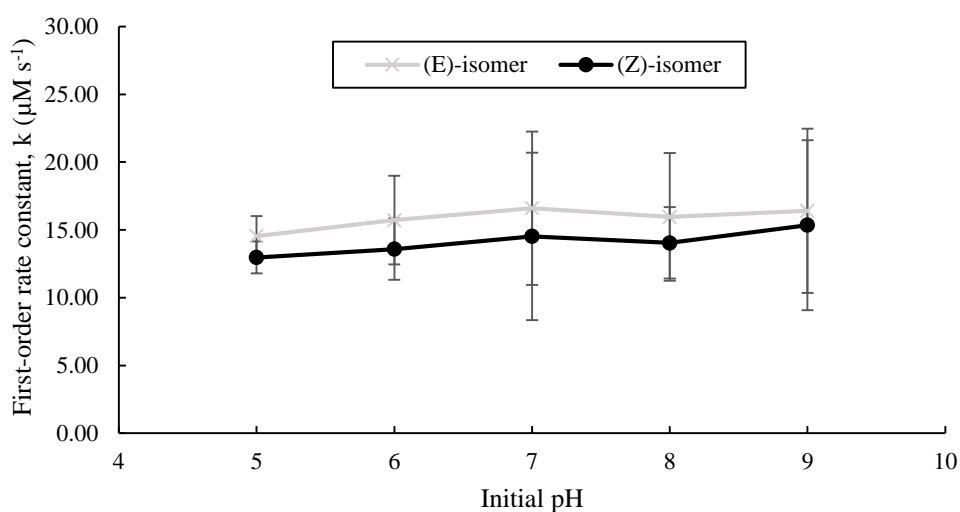

Figure 11. Effect of pH on photodegradation first-order rate constant (k) for aqueous solution with 2 μg mL^{-1} of (E)- and (Z)-endoxifen isomers at an emission light intensity of 28 W s^{-1} cm^{-2}. (22.4°C).

Changes in pH before and after 80 seconds of photodegradation reaction (with an emission light intensity of 28 W s^{-1} cm^{-2}) were calculated in the water samples (Appendix C, Figure C.2). pH decreased in all the cases except for the initial pH of 5. This acidification could be due to the presence of a hydroxyaromatic group in the molecular structure of endoxifen. It is well known that hydroxyaromatic compounds present a different pK$_a$ value during the lowest excitation state due to their acid-based

property (Jin et al., 2017; Lawrence, Marzzacco, Morton, Schwab, & Halpern, 1991). Greater pK_a values during the lowest excited state result in a deprotonation of the hydroxyl group. Therefore, the acidification of the low acidic (pH 6), neutral (pH 7), and alkaline (pH 8 and 9) solutions could be explained by the deprotonation of (E)- and (Z)-endoxifen isomers during the lowest excited state due to the presence of a phenol group in their molecular structures. Further analyses need to be conducted in order to determine the pK_a of (E)- and (Z)-endoxifen at their lower excitation state during photodegradation.

4.2.1.3 Effect of initial endoxifen concentration on endoxifen photodegradation

The role of the initial concentrations of (E)- and (Z)-endoxifen (500, 1,000, and 2,000 ng mL^{-1}) on the photodegradation reaction was investigated at a constant light intensity of 224 W s^{-1} cm^{-2}. The higher concentration tested in this study was selected based on the solubility of (E)- and (Z)-endoxifen in water (maximum of 2,000 ng mL^{-1}). The photodegradation rate constants (k) were calculated for each isomer. The reaction rate constants (k) for (E)- and (Z)-endoxifen exhibit positive linear relationships with their initial concentrations ($R^2 > 0.99$) (Appendix C, Figure C.3). The photodegradation rate was dependent on initial concentrations of (E)- and (Z)-endoxifen ($p < 0.0001$ for (E)- and (Z)-endoxifen). The percentage photodegradation of (E)- and (Z)-endoxifen notably decreased by 59 and 57% respectively when the concentration was reduced from 2 to 0.5 mg L^{-1}. Previous studies reported a similar correlation between k (pseudo first order) and the initial concentration of an aromatic compound (oxytetracycline, chrysene, benzo[a]pyrene, phenanthrene, and acenaphthene) during photodegradation (Jin et al., 2017; Miller & Olejnik, 2001). Weller (1961) used the molecular

photosensitization of aromatic compounds to explain the positive linear relationship between k and initial concentration of target compound. However, the fluorescence emission of (E)- and (Z)-endoxifen (Appendix A, Figure A.5) is not in the same range as their absorption spectra (Appendix A, Figure A.1). Therefore, photosensitization is not a possible explanation for these results. Another theory is that thermodynamic collision occurs along with photolysis (Jin et al., 2017). In this study, two photo-excited endoxifen molecules collided, triggering the thermodynamic collision reaction. Therefore, the number of excited molecules is directly proportional to the concentration of endoxifen in the ground state. Hence, the photolysis of (E)- and (Z)-endoxifen is not only due to the light energy, but molecular collision could also play an important role.

4.2.1.4 Effect of light source on endoxifen photodegradation

As shown in Figures 12 and 13, the concentrations of (E)- and (Z)-endoxifen isomers remained constant with time after 60 seconds of indoor and sunlight irradiation. Effective photodegradation of (E)- and (Z)-endoxifen isomers was observed when the water samples were exposed to UV light (253.7 nm). After 35 seconds of UV light exposure, the concentrations of (E) and (Z)-endoxifen isomers were below the lower limit of detection ($LOD_{(E)\text{-endoxifen}}$ = 12.66 ng mL^{-1}; $LOD_{(Z)\text{-endoxifen}}$=12.12 ng mL^{-1}). Therefore, the concentrations of both isomers, (E)- and (Z)-endoxifen, were reduced by at least 99.1% after 35 seconds of UV light exposure at 224 W s^{-1} cm^{-2}. These results showed the suitability of UV light to effectively photodegrade (E)- and (Z)-endoxifen isomers in HPLC water.

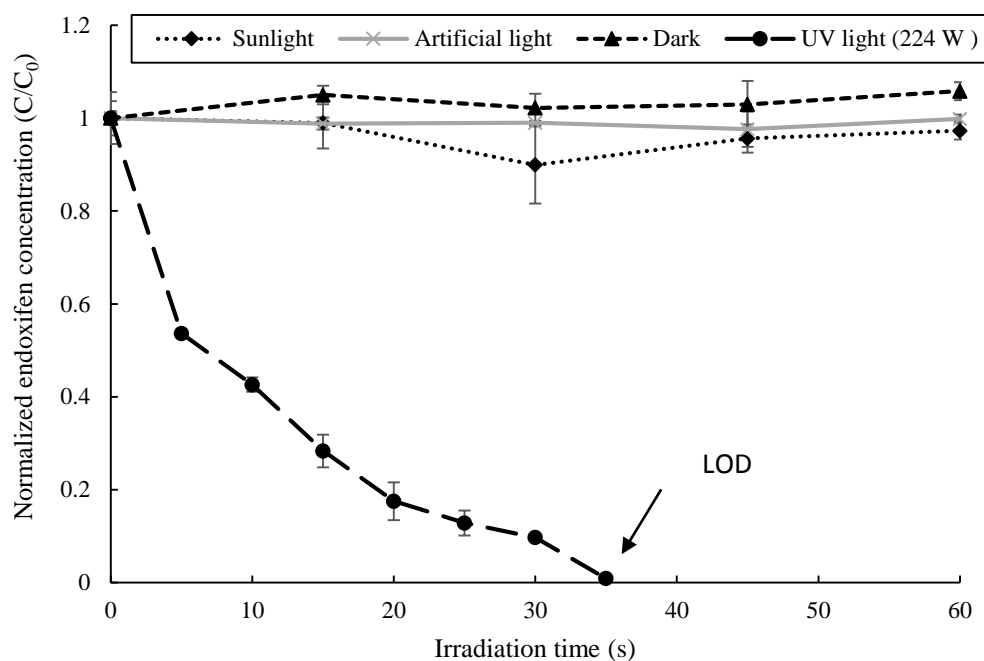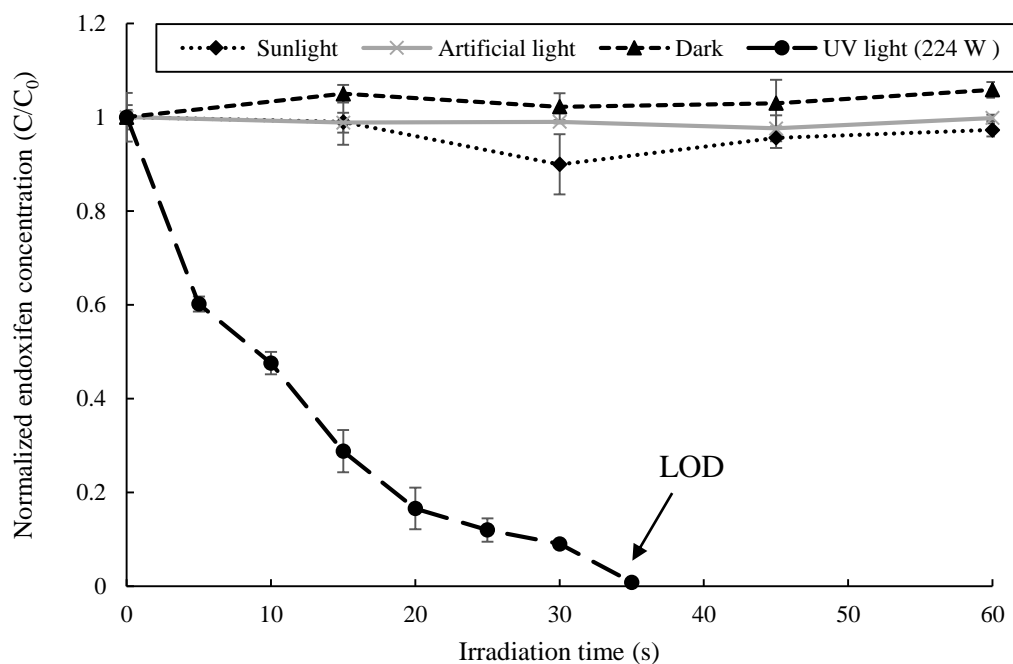Figure 12. Effect of light source on photodegradation of (E)-endoxifen in aqueous solution at 2 μg mL^{-1}. (E)-endoxifen was undetectable at 35 seconds of irradiation with UV light (224 W s^{-1} cm^{-2}, pH 7, and 22.4°C) (LOD$_{\text{(E)-endoxifen}}$ = 12.66 ng mL^{-1}).

Figure 13. Effect of light source on photodegradation of (Z)-endoxifen in aqueous solution at 2 µg mL^{-1}. (Z)-endoxifen was undetectable at 35 seconds of irradiation with UV light (224 W s^{-1} cm^{-2}, pH 7, and 22.4°C) (LOD$_{(Z)\text{-endoxifen}}$ = 12.12 ng mL^{-1}).

4.2.2 The role of hydroxyl radicals

HPLC water was used as solvent for (E)- and (Z)-endoxifen isomers during UV photodegradation reactions at 254 nm. According to Dobrovic, Juretić , & Ružinski (2017), vacuum ultraviolet (VUV) process with UV light at 185 nm in water generates $^{\bullet}$OH free radicals which can oxidize organic molecules. The formation of $^{\bullet}$OH from water irradiated with UV light at 254 nm was unlikely. To confirm that, the contribution of $^{\bullet}$OH to photodegradation of (E)- and (Z)-endoxifen was examined. IPA (1%) was used as an $^{\bullet}$OH scavenger during the photodegradation. The samples with and without IPA spike showed similar reaction courses (Figures 14 and 15) but ANOVA results

showed that (E)- and (Z)-endoxifen photodegradation is dependent on the addition of IPA (p = 0.003 for both (E)- and (Z)-endoxifen). The samples with IPA had k values of 60.1±0.6 and 65.3±1.3 μM s^{-1} while the samples without IPA (1%) resulted in k values of 84.6±6.5 and 89.9±6.6 μM s^{-1} for (E)- and (Z)-endoxifen, respectively. A previous study focused on the photodegradation of low-brominated diphenyl ether in water reported similar results and attributed to the effect of IPA addition (dual solvent of IPA and HPLC water versus single solvent of HPLC water) rather than ˙OH contribution (Wang et al., 2015). That is also likely the case for the observed (E)- and (Z)-endoxifen photodegradation results.
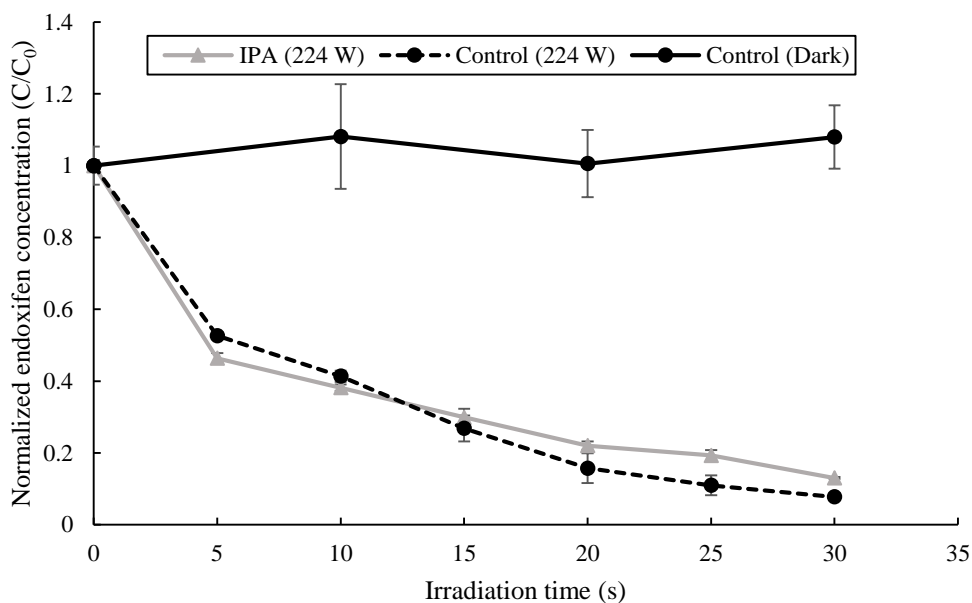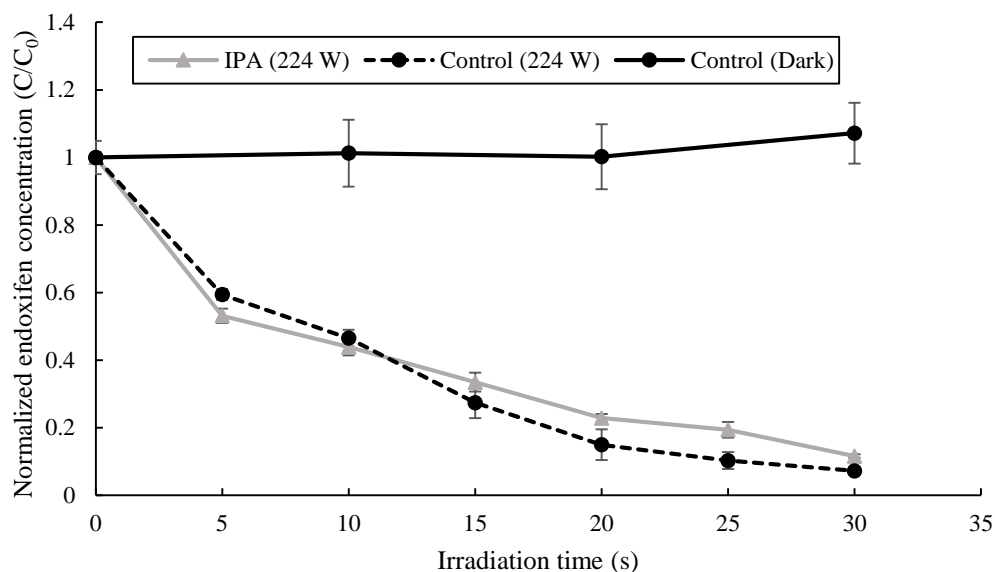

Figure 14. Effect of IPA (1%) on normalized (E)-endoxifen concentration (C/C$_0$) in aqueous solution at 2 μg mL^{-1} during photodegradation reaction at a UV light intensity of 224 W s^{-1} cm^{-2} (pH 7 and 22.4°C).

Figure 15. Effect of IPA (1%) on normalized (Z)-endoxifen concentration (C/C$_0$) in aqueous solution at 2 µg mL^{-1} during photodegradation reaction at a UV light intensity of 224 W s^{-1} cm^{-2} (pH 7 and 22.4°C).

4.2.3 Quantum yield and emission light intensity

Quantum yield (Φ) of endoxifen photoreaction was calculated at four emission light intensities (56, 112, 168, and 224 W s^{-1} cm^{-2}). Photon irradiance (E$_p$) (Einstein cm^{-2} min^{-1}), moles of Fe^{2+} formed in the iron (III) sulfate solution, and the k values of (E)- and (Z)-endoxifen were previously calculated for each emission light intensity (Table 2). In order to determine the quantum yield for the first order kinetic photodegradation reaction of (E/Z)-endoxifen, the molar extinction coefficient (ε) of (E/Z)-endoxifen at 253.7 nm was calculated (Appendix D, Figure D.1). Equation 6 in subsection 3.2.9 was then used to calculate the quantum yield.

The quantum yield values decreased as the emission light intensity increased (Figure 16). These results suggest that photon absorbance by (E)- and (Z)-endoxifen was more

efficient at lower light intensities. This inverse relationship between emission light intensity and quantum yield was previously observed in photoreaction studies (Chowdhury, Athapaththu, Elkamel, & Ray, 2017; Fujishima, Rao, & Tryk, 2000). (E)- and (Z)-endoxifen were photodegraded more efficiently at low emission light intensities.

There is a need to calculate the incident light intensity in the sample as the emission light intensity is attenuated by several factors such as lamp aging, lamp bulb wall temperature, lamp operating frequency, quartz sleeve absorption, and distance between sample and light source. As expected, the emission light intensities were at least three orders of magnitude higher than the incident light intensities (Table 3). The information provided by the manufacturer of the lamps specified an incident light intensity of 16 mWs^{-1} cm^{-2} in samples placed 2 inches from the brand new lamps using an emission light intensity of 35 W s^{-1} cm^{-2} (Southern New England Ultraviolet Company, n.d.). Therefore, the calculated light intensities in this study at the four-selected emission light intensities were reasonable values compared to the information from the manufacturer. The incident light intensities allow the calculation of light doses applied to the water samples by multiplying by the irradiation time (s). The light doses during the photodegradation of (E)- and (Z)-endoxifen are shown in Table 3. As expected, lower irradiation intensities need longer irradiation time to achieve a targeted light dose. However, the incident light intensity at the lower emission intensity (56 W s^{-1} cm^{-2}) was remarkably low. This result suggests that light energy dissipation was even higher when lower emission energies were applied to the water samples in the photoreactor.

Table 2. Moles of Fe^{2+} formed in Iron (III) sulfate solution after one minute of UV light irradiation, photon irradiance (Einstein min^{-1} cm^{-2}), and the first order reaction rate constants (k) of (E)- and (Z)-endoxifen isomers at four emission light intensities (56, 112, 168, and 224 W s^{-1} cm^{-2}).

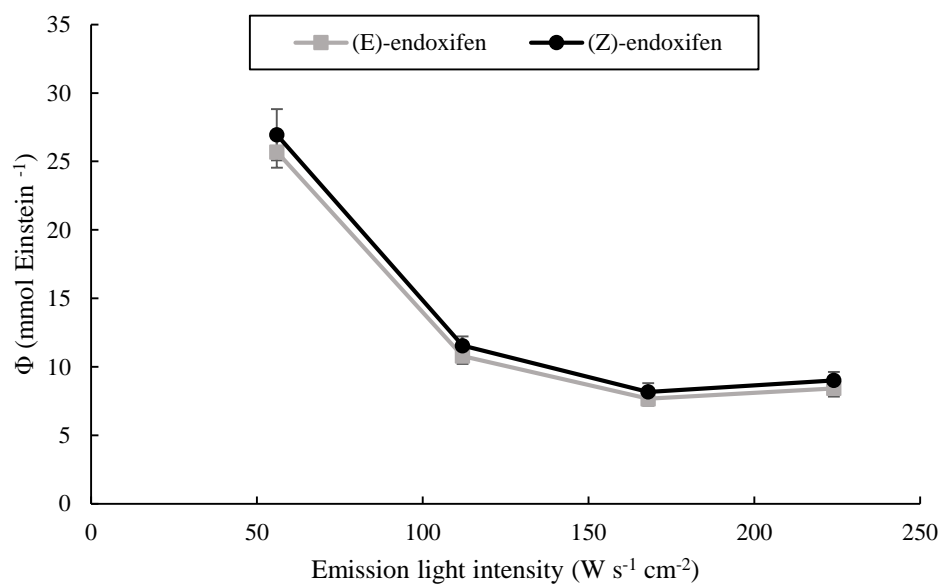| Emission Light Intensity (W s^{-1} cm^{-2})	Fe^{2+} (μM)	E_p (Einstein min^{-1} cm^{-2})	k (mM m^{-1})	
			(E)-endoxifen	(Z)-endoxifen
56	1.12	0.35×10^{-6}	2.29±0.10	2.40±0.17
112	3.26	1.03×10^{-6}	2.80±0.15	3.00±0.17
168	5.65	1.78×10^{-6}	3.45±0.22	3.67±0.29
224	6.90	2.17×10^{-6}	4.62 ±0.33	4.95±0.33

Figure 16. The effect of the emission light intensity (W s^{-1} cm^{-2}) on the quantum yield value (mmol $Einstein^{-1}$) for (E)- and (Z)-endoxifen isomers.

Table 3. Incident light intensity (mW s^{-1} cm^{-2}), exposure time (s), and light doses (mJ cm^{-2}) at four emission light intensities (56, 112, 168, and 224 W s^{-1} cm^{-2}).

Emission light intensity (W s^{-1} cm^{-2})	Incident light intensity (mW s^{-1} cm^{-2})	Irradiation time (s)	Light dose (mJ cm^{-2})
56	2.77	60	166.2
112	8.07	45	363.15
168	14	30	420
224	17.1	30	513

4.2.4 Detection and identification of photodegradation by-products

4.2.4.1 Detection of photodegradation by-products by HPLC-DAD

The chromatogram peak areas corresponding to (E)- and (Z)- endoxifen isomers decreased with time until they became undetectable (LOD$_{(E)\text{-endoxifen}}$ = 12.66 ng mL^{-1}; LOD$_{(Z)\text{-endoxifen}}$=12.12 ng mL^{-1}) after 35 seconds of UV light exposure at 224 W s^{-1} cm^{-2} (Appendix E, Figure E.1). However, a new chromatogram peak with a retention time of 11.43 minutes was observed as (E)- and (Z)-endoxifen isomers were degraded. After 30 seconds of photodegradation, the new peak presented a total chromatogram percentage area of 82%. The presence of this new peak suggested the formation of at least one photodegradation by-product.

4.2.4.2 Identification of photodegradation by-products by UHPLC-MS/MS

A water sample containing (E)- and (Z)-endoxifen isomers was exposed to UV light (253.7 nm) for 35 seconds to reproduce the photodegradation by-product previously observed by HPLC-DAD. The irradiated water sample was then injected to UPLC-MS/MS in order to identify the molecular weight of the photodegradation by-product. However, instead of only one peak, three new peaks were observed (Figure 17). The

first peak (PB1a) and the second peak (PB1b) had the same ion-*m/z* value (372.19)
(Appendix E, Figure E.4). This ion-*m/z* value indicated an aromatization of (E) and (Z)-
endoxifen isomers forming a phenanthrene nucleo (by the elimination of two hydrogen
(H^+) and the formation of one molecular bond between two benzene rings) (Table 4).
The elimination of two hydrogens (H^+) through endoxifen aromatization could explain
the recorded ion-*m/z* value of PB1a and PB1b. A previous study on the detection of
endoxifen by HPLC with a fluorescence detector reported the formation of a
photocycled derivate with a phenanthrene nucleo after the irradiation of endoxifen by
UV light (Aranda et al., 2011). According to Miller & Olejnik (2001), irradiated
polyaromatic hydrocarbons (PAHs) undergo chemical changes during their excited
state after photon absorption. The most probable way for these PAHs to return to their
ground state is through energy dissipation by proton transfer. Likewise, deprotonation
of (E)- and (Z)-endoxifen forming a phenanthrene nucleo by molecular changes during
their excited state is the most probable explanation for the observed ion-*m/z* values.
Furthermore, the minimal difference in ppm (<10) between the expected ion-*m/z* mass
and the theoretical ion-*m/z* mass of the proposed molecular structure for PB1a and PB1b
support the suggested aromatization of (E)- and (Z)-endoxifen after 35 seconds of UV
irradiation. This aromatization of endoxifen was also proposed by Negreira et al. (2015)
during chlorination analyses by the addition of two chlorine (Cl^-) to the phenol group
followed by an oxidative carbon-carbon coupling that results in a chlorinated
phenanthrene nucleo (Figure 19).

The third peak (3) observed with a retention time of 2.03 minutes (PB2) showed an ion-
m/z value of 314.21 (Appendix E, Figure E.4). This ion-*m/z* value observed at 35
seconds was similar to the observed ion-*m/z* value of (E)- and (Z)-endoxifen isomers at

time 0 chromatogram (Appendix E, Figure E.3). However, the retention time of PB2 was different than the retention times observed for (E)- and (Z)- endoxifen isomers at time 0 (Appendix E, Figure E.1). Therefore, the presence of this new peak (PB2) with the same ion-*m/z* value as (E)- and (Z)-endoxifen isomers but different retention time suggests the presence of a new photodegradation by-product with the same molecular weight as (E)- and (Z)-endoxifen isomers. The hydrogenation by the addition of two H^+ to the phenanthrene nucleo formed during the aromatization of endoxifen could explain the obtained ion-*m/z* value of PB2. However, the determination of the molecular structure of PB2 was challenging due the presence of only one peak instead of two peaks.

PB1 showed two peaks corresponding to the aromatization of (E)- and (Z)-endoxifen isomers resulting in two well differentiated photodegradation by-products. The observation of only one peak for PB2 suggests that either only one of the two endoxifen isomers underwent hydrogenation to PB2 or the two peaks overlapped. However, PB2 was not considered as the main photodegradation by-product due to a small percentage of the chromatogram peak area.

Table 4 shows the two possible molecular structures of PB2 depending on whether the hydrogenation occurred in the (E)-endoxifen isomer or the (Z)-endoxifen isomer. The proposed molecular structures of PB1(a, b) and PB2 were analyzed through UPLC-MS/MS. In order to identify the formed product ions after the fragmentation of (E/Z)-endoxifen and PB2 through MS/MS, the ion-*m/z* value of 374.21 was selected and fragmented with a cone voltage of 27 eV.

(E)- and (Z)-endoxifen present similar formed product ions as PB2 but the ion-*m/z* = 223.1140 and the ion-*m/z* = 194.0757 were not observed in the PB2 MS/MS spectrum

(Appendix E, Figure E.5). The proposed molecular structure of PB2 contain a phenanthrene nucleo that could hinder the cleavage of PB2 to generate the fragment ion-*m/z* values of 223.1140 and 194.0757. The proposed molecular structures of PB1(a, b), also present a phenanthrene nucleo as a molecular core. MS/MS spectra for PB1(a, b) showed no fragmentation within the phenanthrene nucleo (Appendix E, Figure E.6). Finally, two more peaks (3 and 4) were observed in the chromatogram (Figure 17). These two peaks had the same retention times and ion-*m/z* values as the peaks observed in the initial chromatogram before the photodegradation reaction (Appendix E, Figures E.2 and E.3). Therefore, these two peaks represented remaining (E)- and (Z)-endoxifen isomers present in the water sample after 35 seconds of photodegradation reaction that were undetectable by HPLC-DAD. The observation of (E)- and (Z)-endoxifen isomers after 35 seconds of photodegradation using UPLC-MS/MS could be explained by the higher sensitivity of MS/MS than DAD techniques. Kopec, Schweiggert, Riedl, Carle, & Schwartz (2013) compared MS and DAD detector during a quantitative analysis and showed that MS detector was 37 times more sensitive than DAD detector.
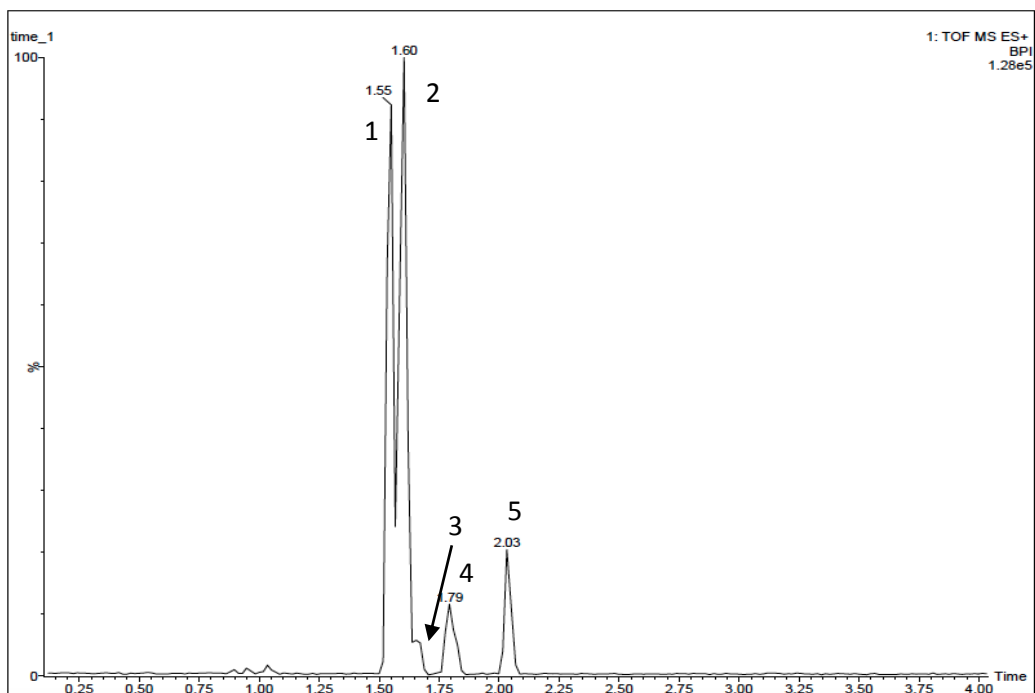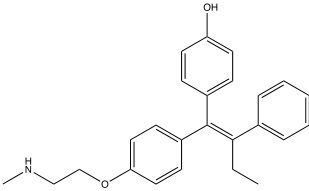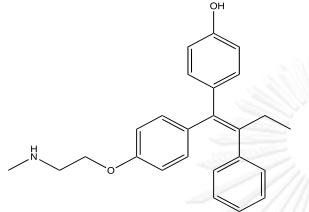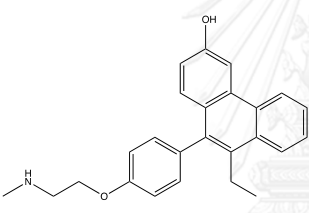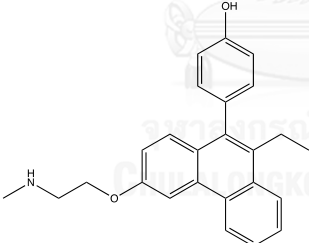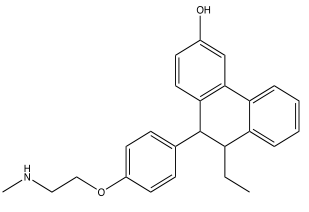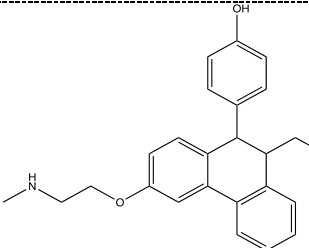
Figure 17. UHPLC-MS chromatogram of aqueous solution of (E)- and (Z)-endoxifen (1 µg ml^{-1} each, pH 7, and 22.4°C) after 35 seconds of irradiation with a UV light intensity of 224 W s^{-1} cm^{-2}: PB1a and PB1b (1 and 2); (E)-endoxifen (3); (Z)-endoxifen (4); and PB2 (5).

Table 4. Molecular mass and proposed molecular structures of (E)- and (Z)-endoxifen photodegradation by-products.

Compound	Predicted Molecular Structure	Rt	Molecular Formula (M+H$^+$)	Expected ion-m/z	Theoretical ion-m/z	|ppm|
(E)-endoxifen		1.65	$C_{25}H_{27}NO_2$	374.2120	374.2106	3.74
(Z)-endoxifen		1.78	$C_{25}H_{27}NO_2$	374.2120	374.2107	3.47
PB1a		1.55	$C_{25}H_{25}NO_2$	372.1919	372.1949	8.06
PB1b		1.60	$C_{25}H_{25}NO_2$	372.1919	372.1949	8.06
PB2		2.03	$C_{25}H_{27}NO_2$	374.2120	374.2109	2.94

4.2.5 Toxicity assessment

There has been only one study by Borgatta et al. (2015) that examined the aquatic toxicity of endoxifen. There are no toxicity assessments on the potential effects of endoxifen in the aquatic environment (Borgatta et al., 2015). This lack of information on the toxicity of endoxifen has led to a proposal to use the same PNEC as tamoxifen (Government of Canada, 2015). Endoxifen is 100-folds more potent than tamoxifen (Borgatta et al., 2015). Therefore, the toxicity of (E)- and (Z)-endoxifen and their photodegradation by-products (PBs) should be assessed.

The toxicity of (E)-endoxifen, (Z)-endoxifen, PB1a, PB1b and PB2 were assessed using TEST (USEPA, 2016). Among different options offered by TEST, the bioaccumulation factor (BAF) and 50% Lethal Concentration (LC_{50}) acute end-points of a crustacean *Daphnia magna* (48h) and a fish fathead minnow (96 h) were selected because they are more suitable for aquatic toxicity assessments (Negreira et al., 2014). Furthermore, LC_{50} predictions for *D. magna* and fathead minnow for endoxifen PBPs were based on coefficients of similarities greater than 0.5 between the molecular structures of PBPs and those of analytes used by the software confirming the reliability of the modeling results. It should be noted that predictions by TEST rely on experimental toxicity results of compounds/analytes (available through database) that have molecular structures similar to compounds of interest. The more molecular structure similarity, the more reliable the prediction. TEST also offers the calculation of the 50% impairment growth concentration (IGC_{50}) of the protozoa *Tetrahymena pyriformis* which is widely used for aquatic toxicology (Suavant et al., 1999). However, for this study, predicted *T. pyriformis* IGC_{50} was unreliable due to low similarity between the molecular structures of endoxifen PBPs and those of the analytes used by

TEST (the observed similarity coefficients were < 0.5 suggesting unreliable modeling results). The rest of the indicators and conditions offered by TEST is not relevant to aquatic toxicology.

Based on the acute toxicity (48-h) for *D. magna*, LC_{50} for (E)- and (Z)-endoxifen is 1.45 μg mL^{-1} compared to 0.28 μg mL^{-1} for PB1a and PB1b (Figure 18). These modeling results suggest that PB1a and PB1b are more toxic than (E)- and (Z)-endoxifen. Further photodegradation of PB1a or PB1b led to the formation of PB2 which has even higher toxicity (LC_{50} for *D. magna* of 0.21 μg mL^{-1}). The results for fathead minnow showed the same trend as those for *D. magna*. Therefore, the photodegradation of (E)- and (Z)-endoxifen provided more toxic photodegradation by-products. According to the European Commission Regulation (EC) No 1272 (2008), substances with acute toxicity LC_{50} for *D. magna* and fathead minnow ≤ 1 μg mL^{-1} are considered hazardous to the aquatic environment. However, further experimental work is needed to confirm the modeling results although QSAR predictions are known to reliable if the molecular structures of the compounds used for the analyses are sufficiently similar to the analyte of interest (He & Jurs, 2005).
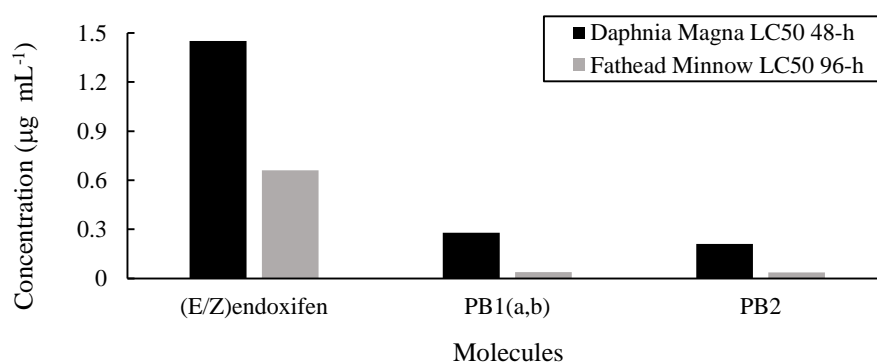

Figure 18. Toxicity data obtained through TEST QSAR assessment.

Photolysis of (E)- and (Z)-endoxifen resulted in PBPs that are less toxic than products generated from chlorination of endoxifen observed by Negreira et al. (2015). Chlorination of endoxifen potentially generated five DBPs through hydroxilation, chlorination and aromatization (Figure 19). The toxicity assessment of these DBPs by TEST (US EPA, 2016) showed acute toxicity LC50 values for *D. magna* from 0.008 to 0.130 µg mL^{-1} (Negreira et al., 2015). According to Larson (1988), UV light disinfection process in WWTPs should produce less toxic DPBs than chlorination process. Likewise, photolysis of (E)- and (Z)-endoxifen by UV light in this study resulted in products that are less toxic than DBPs from chlorination of endoxifen. However, both processes provided more toxic by-products than the parent compounds.
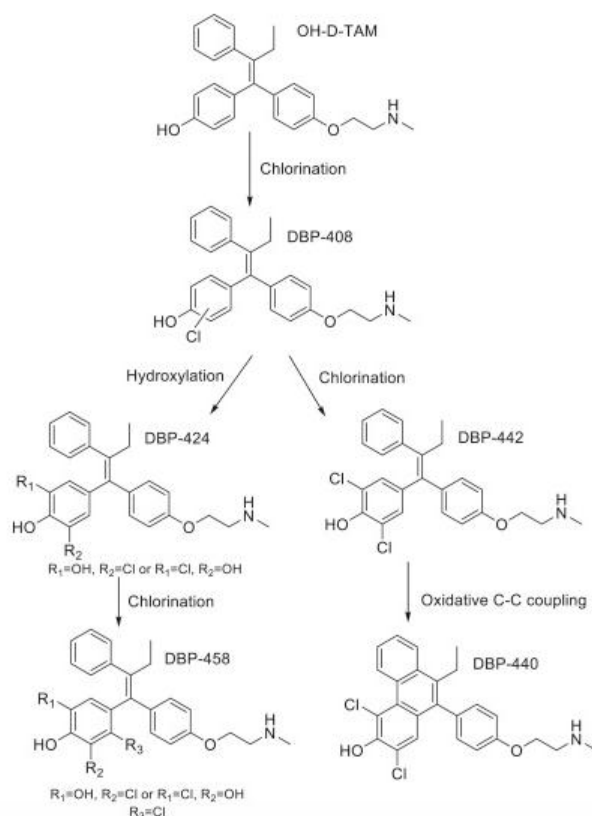

Figure 19. By-products generated from chlorination of endoxifen (Negreira et al., 2015).

4.2.6 Photodegradation of (E)- and (Z)-endoxifen in wastewater

Photodegradation of (E)- and (Z)-endoxifen was tested in wastewater samples collected from the secondary effluent of a WWTP spiked with (E)- and (Z)-endoxifen at 1 µg mL^{-1}. The photodegradation reaction of (E)- and (Z)-endoxifen in wastewater followed a second order model with $R^2 > 0.99$ and reaction rate constants (k) of 72.9 and 75.9 µM s^{-1}, respectively (Appendix F, Figure F.2). Based on R^2 of the fittings, second order model is a more suitable choice than zero and first order models (Appendix F, Table F.1). Using the same emission light intensity (56 W s^{-1} cm^{-2}), the photodegradation reaction rate constants (k) of (E)- and (Z)-endoxifen in the wastewater samples were almost twice greater than the reaction rate constants in the HPLC water samples. This large difference in k values could be explained by different photochemical processes in wastewater and HPLC water.

The photodegradation of (E)- and (Z)-endoxifen in water samples occurred through direct photolysis by the direct absorption of UV light that resulted in a chemical transformation of the molecular structures of (E)- and (Z)-endoxifen. However, the presence of other molecules in the wastewater sample that also absorbed UV light could induce the chemical transformation of (E)- and (Z)-endoxifen through indirect or sensitized photolysis. Therefore, photodegradation of (E)- and (Z)-endoxifen in wastewater occurred likely through two different mechanisms (direct and indirect photolysis) resulting in higher k values. The indirect photolysis of (E)- and (Z)-endoxifen in wastewater samples also explains the difference in the photodrgadation kinetics (first order in water and second order in wastewater).

In order to determine if (E)- and (Z)-endoxifen photodegradation would take place during UV light disinfection at WWTPs, wastewater samples spiked with (E)- and (Z)-

endoxifen were irradiated with light doses similar to those applied at WWTPs (Figure 20). The initial concentrations of (E)- and (Z)-endoxifen in wastewater were reduced by 30 and 31% after receiving the minimal UV light dose for disinfection established by the USEPA (2016) of 16 mJ cm^{-2}. WWTPs with filtered nitrified secondary effluents normally apply a minimal UV light dose of 30 mJ cm^{-2} (Shin et al., 2001). The irradiation of (E)- and (Z)-endoxifen in wastewater with a light dose of 30 mJ cm^{-2} resulted in a reduction of the concentrations by 44.3 and 45.7%, respectively. Moreover, the use of higher light dose of 97 mJ cm^{-2} which is not uncommon for conventional WWTPs (Darby et al., 1993) reduced (E)- and (Z)-endoxifen by 71.2 and 72.4%, respectively. Therefore, (E)- and (Z)-endoxifen if present in secondary treated wastewater would be photodegraded by UV disinfection process. As in HPLC water, this photodegradation reaction could form PB1(a, b) and PB2 which are more toxic than the parent compounds.

In order to determine the presence of PB1(a, b) and PB2 in the wastewater sample after the photodegradation of (E)- and (Z)-endoxifen isomers, UPLC-MS/MS analyses were performed before and 35 seconds after irradiation at a light intensity of 56 W s^{-1} cm^{-2} (Figure 21). The chromatogram of the wastewater sample before irradiation with UV light (Figure 21.b) has two main peaks (Rt = 1.71 and 1.83 minutes) with the same ion-m/z values as endoxifen (ion-m/z = 374.21) (Appendix F, Figure F.1). The absence of these two peaks in the initial chromatogram (Figure 21.a) before (E)- and (Z)-endoxifen were spiked suggests that these two peaks were (E)- and (Z)-endoxifen isomers. The chromatogram after 35 seconds of irradiation has four main peaks (Figure 21.c). Two of the peaks (Rt = 1.57 and 1.64 minutes) had the same ion-m/z value as PB1(a, b) (ion-m/z = 372.19) (Figure 22). Further MS/MS analyses revealed that these two peaks

represented PB1(a, b) (Appendix F, Figure F.3).

The other two peaks in the chromatogram after 35 seconds of irradiation showed similar retention times (Rt = 1.71 and 1.84 minutes) and the same ion-m/z values (ion-m/z = 374.21) as the peaks observed in the initial chromatogram before the photodegradation reaction (Appendix F, Figure F.1). These two peaks were from undegraded (E)- and (Z)-endoxifen isomers in the wastewater sample. Therefore, the photodegradation of (E)- and (Z)-endoxifen in WWTPs potentially led to the generation of the toxic PB1(a, b). However, the initial concentration of (E)- and (Z)-endoxifen used in this study (1 µg mL^{-1}) was higher than the expected concentration in wastewater (ppb). The positive correlation observed between initial endoxifen concentration and the first-order photodegradation rate suggests that lower concentrations of (E)- and (Z)- endoxifen in wastewater could lead to lower photodegradation rates. However, photodegradation of (E)- and (Z)-endoxifen in the wastewater samples followed a second order model possibly due to photosensitization by inorganic and other organic compounds in wastewater. This photosensitization led to greater photodegradation rates suggesting that (E)- and (Z)-endoxifen could be photodegraded in wastewater even at low concentrations. Further work on the development of precise quantification methods for endoxifen with LOD and LOQ below the expected concentrations in wastewater (ppb level) is needed. With better quantification methods, the photodegradability of (E)- and (Z)- endoxifen at concentrations similar to those expected in wastewater can be elucidated.
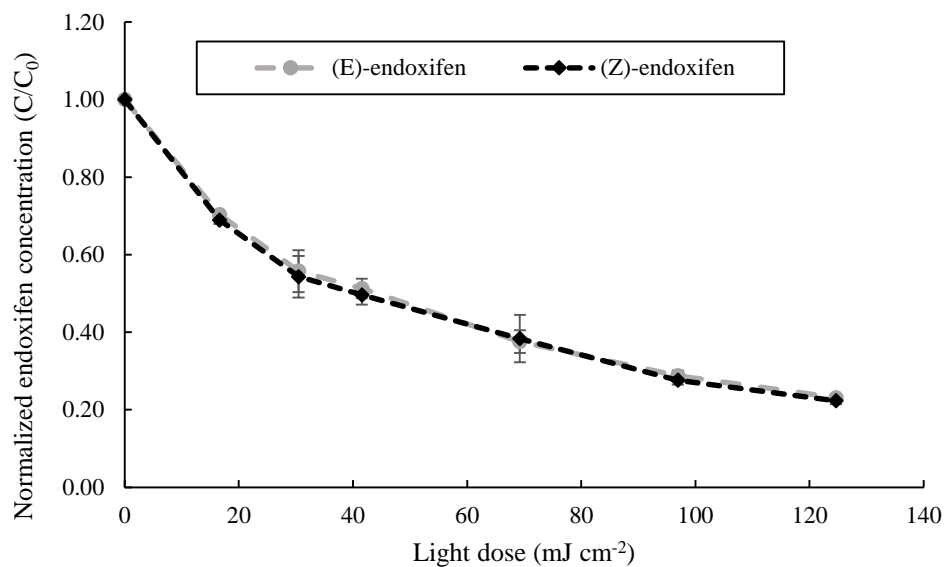
Figure 20. Effect of light dose (mJ cm^{-2}) on (E)- and (Z)-endoxifen concentrations in a wastewater sample (pH 7.59, $NO_2^- = 0.032$ mg L^{-1}, $NO_3^- = 0.010$ mg L^{-1}, TOC = 19.17 mg L^{-1}, and 22.4°C) irradiated with an emission light intensity of 56 W s^{-1} cm^{-2}.
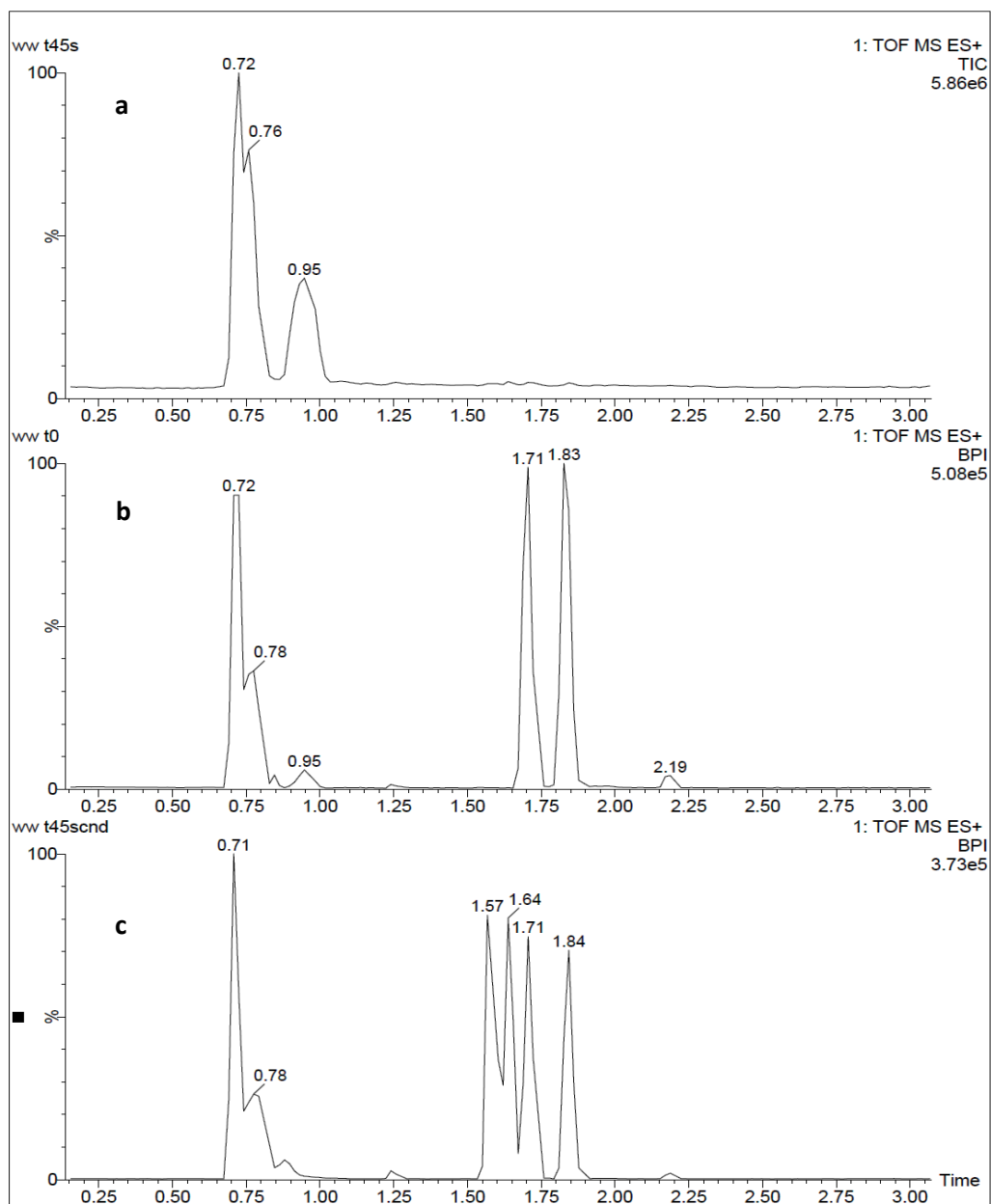
Figure 21. UHPLC-MS/MS chromatogram of (E)- and (Z)-endoxifen in wastewater (1 μg ml^{-1}) and PBPs (Photodegradation conditions: pH 7.59, NO$_2^-$ = 0.032 mg L^{-1}, NO$_3^-$ = 0.010 mg L^{-1}, TOC = 19.17 mg L^{-1}, 22.4°C, and UV light intensity of 56 W s^{-1} cm^{-2}): (a) wastewater sample with no (E)- and (Z)-endoxifen; (b) wastewater sample spiked with (E)- and (Z)-endoxifen before irradiation; (c) wastewater sample spiked with (E)- and (Z)-endoxifen and irradiated for 35 seconds.
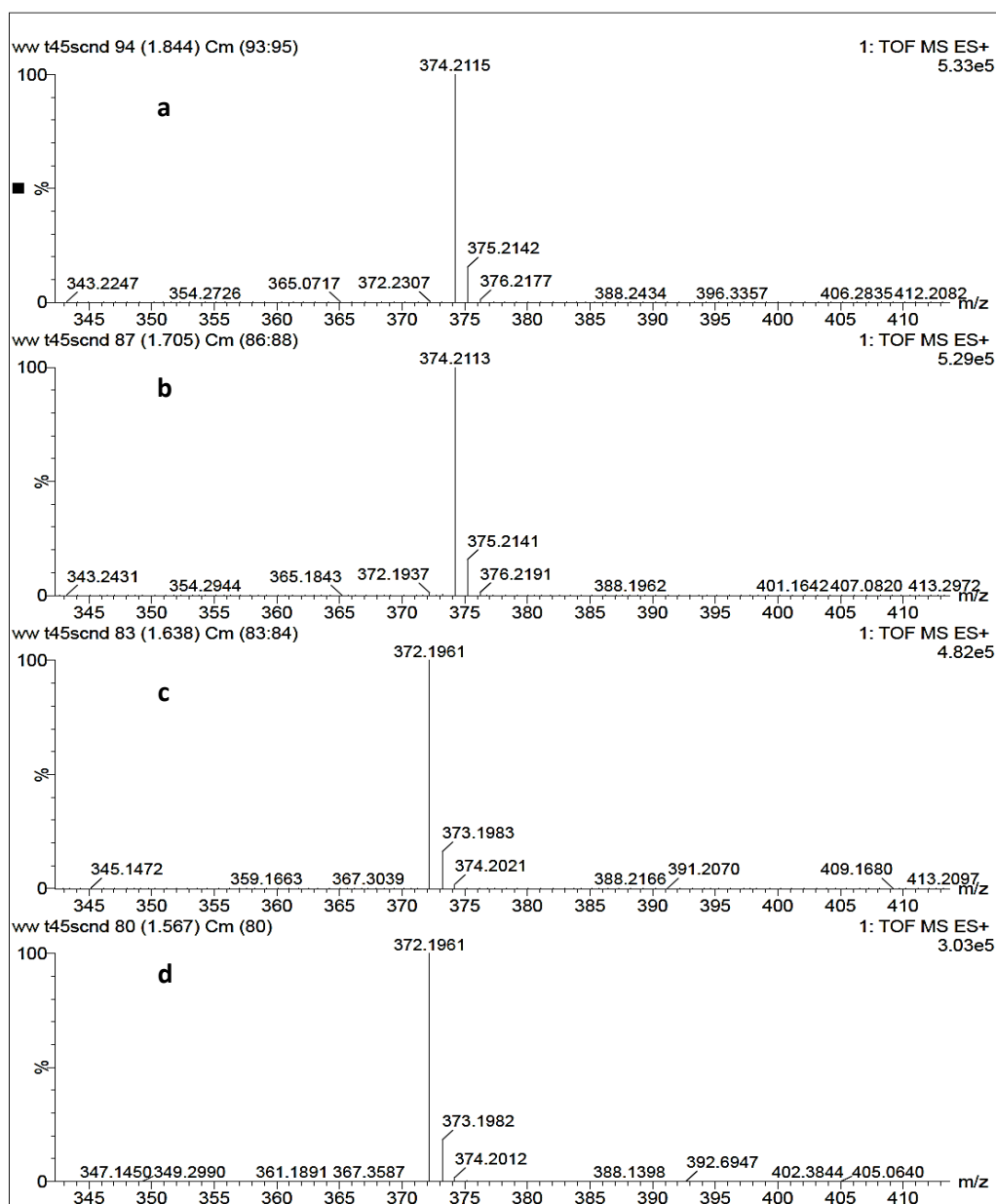
Figure 22. Mass spectrometry of the wastewater sample spiked with (E)- and (Z)-endoxifen (1 μg ml^{-1}) after 35 seconds of irradiation with UV light (pH 7.59, NO$_2^-$ = 0.032 mg L^{-1}, NO$_3^-$ = 0.010 mg L^{-1}, TOC = 19.17 mg L^{-1}, 22.4°C, light intensity = 56 W s^{-1} cm^{-2}): (a) (Z)-endoxifen (Rt = 1.84 minutes, ion-m/z = 374.2115); (b) (E)-endoxifen (Rt = 1.71 minutes, ion-m/z = 374.2113); (c) PB1b (Rt = 1.64 minutes, ion-m/z = 372.1961); (d) PB1a (Rt = 1.57 minutes, ion-m/z = 372.1961).

CHAPTER 5: CONCLUSIONS AND RECOMMENDATIONS FOR FUTURE WORK

5.1 Conclusions

An attempt on biodegradation of (E)- and (Z)-endoxifen by isolated bacteria strains from wastewater was not successful questioning the biodegradability of the compounds. Photodegradation process based on monocromatic UV light irradiation at 253.7 nm is an efficient process for removing (E)- and (Z)-endoxifen from water. The irradiation resulted in $\geq$ 99.1% elimination of (E)- and (Z)-endoxifen at a light dose of 513 mJ/cm^2. The use of higher emission light intensities provided greater photodegradation rates. The initial concentrations of (E)- and (Z)-endoxifen impacted the photodegradation rates. A linear relationship was observed between the initial concentration and the photodegradation rates of (E)- and (Z)-endoxifen. This observation suggests that collisions of E)- and (Z)-endoxifen molecules during the excited state could play an important role in the photodegradation. On the contrary, the solution pH (5 to 9) was not a meaningful parameter for the photodegradation. Limited pH reduction after the photodegradation in alkaline, neutral and slightly acidic solutions indicates that (E)- and (Z)-endoxifen become more acidic during the lowest excitation state due to their acid-base property.

Although UV photodegradation is a promising process for degrading (E)- and (Z)-endoxifen in water, PBPs potentially more toxic than (E)- and (Z)-endoxifen were observed along the photodegradation time course. Two PBPs from aromatization of (E)- and (Z)-endoxifen (PB1a and PB1b) were identified. Further hydrogenation of PB1a and PB1b provided the third PBP which by modeling is a highly toxic compound.

PB1a and PB1b were also observed during the photodegradation of (E)- and (Z)-endoxifen in wastewater with UV light doses similar to those applied at WWTPs. Therefore, highly toxic compounds are potentially generated at WWTPs during UV disinfection process if (E)- and (Z)-endoxifen are present in the treated wastewater. Furthermore, endoxifen photodegradation followed first order kinetics in water and second order kinetics in wastewater. The presence of organic and inorganic molecules in wastewater that absorb UV light could lead to sensitized photodegradation of (E)- and (Z)-endoxifen resulting in higher photodegradation rates and consequently greater generation of PBPs. The presence of these PBPs in the water environment could bring negative effects to aquatic lives.

5.2 Recommendations for future works

Endoxifen is a relatively new contaminant. More studies on their fate and transport, treatment, and toxicology are needed and therefore recommended as follows.

- Modelled physical and chemical properties of endoxifen should be confirmed experimentally to better understand the fate of endoxifen in the environment.

- Limits of detection and quantification of HPLC methods should be improved to identify actual and exact concentrations of endoxifen in engineered and natural systems and to determine photodegradability of (E)- and (Z)-endoxifen in WWTPs at ppb concentrations.

- Environmental risk assessments and toxicity studies of endoxifen and its PBPs in the aquatic environment are needed.

- Advanced oxidation processes using UV and other oxidants such as ozone and peroxide should be evaluated as methods to drive the endoxifen degradation

pathway completely beyond its toxic DPBs.

REFERENCES

Ahmad, A., Ali, S. M., Ahmad, M. U., Sheikh, S., Ahmad, I. (2010). Orally administered endoxifen is a new therapeutic agent for breast cancer. Breast cancer Research Treatment, 122(2), 579-584.

American Association Cancer Research. (2015). National Cancer Institute- cancer statistics. Retrieved 11.24.15 http://www.cancer.gov/about-cancer/what-is-cancer/statistics1

Antunes, M. V., Raymundo, S., de Oliveira, V., Staudt, D. E., Gössling, G., Peteffi, G. P., Linden, R. (2015). Ultra-high performance liquid chromatography tandem mass spectrometric method for the determination of tamoxifen, N-desmethyltamoxifen, 4-hydroxytamoxifen and endoxifen in dried blood spots--development, validation and clinical application during breast cancer adjuvant therapy. Talanta, 132, 775-784.

Antunes, M. V., Rosa, D. D., Viana, T. O. S., Andreolla, H., Fontanive, T. O., Linden, R. (2013). Sensitive HPLC-PDA determination of tamoxifen and its metabolites N-desmethyltamoxifen, 4-hydroxytamoxifen and endoxifen in human plasma. Journal of Pharmaceutical and Biomedical Analysis, 76, 13-20.

APHA, AWWA, WEF. (1998). Standard methods for the examination of water and wastewater (20th Edition ed.). Washinton, DC: APHA.

Aranda, E. O., Esteve-Romero, J., Rambla-Alegre, M., Peris-Vicente, J., Bose, D. (2011). Development of a methodology to quantify tamoxifen and endoxifen in breast cancer patients by micellar liquid chromatography and validation according to the ICH guidelines. Talanta, 84(2), 314-318.

Ashton, D., Hilton, M., Thomas, K. V. (2004). Investigating the environmental transport of human pharmaceuticals to streams in the United Kingdom. Science of the Total Environment, 333(1-3), 167-184.

Besse, J. P., Latour, J. F., Garric, J. (2012). Anticancer drugs in surface waters: what can we say about the occurrence and environmental significance of cytotoxic, cytostatic and endocrine therapy drugs? Environmental International, 39(1), 73-86.

BestUV. (2011). bestUV.   Retrieved 06.20.17. http://www.bestUV.com.

Binkhorst, L., Mathijssen, R. H., Ghobadi Moghaddam-Helmantel, I. M., de Bruijn, P., van Gelder, T., Wiemer, E. A., Loos, W. J. (2011). Quantification of tamoxifen and three of its phase-I metabolites in human plasma by liquid chromatography/triple-quadrupole mass spectrometry. Journal of Pharmaceutical Biomedical Analalysis, 56(5), 1016-1023.

Bolton, J. R., Stefan, M. I., Shaw, P.S., Lykke, K. R. (2011). Determination of the quantum yields of the potassium ferrioxalate and potassium iodide-iodate actinometers and a method for the calibration of the radiometer detectors. Journal of Photochemistry and Photobiology A: Chemistry, 222, 166-169.

Borgatta, M., Decosterd, L. A., Waridel, P., Buclin, T., Chèvre, N. (2015). The anticancer drug metabolites endoxifen and 4-hydroxy-tamoxifen induce toxic effects on Daphnia pulex in a two-generation study. Science of the Total Environment, 520, 232-240.

Challis, J. K., Hanson, M. L., Friesen, K. J., Wong, C. S. (2014). A critical assessment of the photodegradation of pharmaceuticals in aquatic environments: defining

our current understanding and identifying knowledge gaps. Environmental Science Process Impacts, 16(4), 672-696.

Cheng, X., Wodarczyk, M., Lendzinski, R., Peterkin, E., Burlingame, G. A. (2009). Control of DMSO in wastewater to prevent DMS nuisance odors. Water Research, 43(12), 2989-2998.

Chiou, C. H., Juang, R. S. (2007). Photocatalytic degradation of phenol in aqueous solutions by Pr-doped TiO2 nanoparticles. Journal of Hazardous Materials, 149(1), 1-7.

Chowdhury, P., Athapaththu, S., Elkamel, A., Ray, A. K. (2017). Visible-solar-light-driven photo-reduction and removal of cadmium ion with Eosin Y-sensitized TiO2 in aqueous solution of triethanolamine. Purifying Technology, 174, 109-115.

Coetsier, C. M., Spinelli, S., Lin, L., Roig, B., Touraud, E. (2009). Discharge of pharmaceutical products (PPs) through a conventional biological sewage treatment plant: MECs vs PECs? Environ International, 35(5), 787-792.

Darby, J. L., Snider, K. E., Tchobanoglous, G. (1993). Ultraviolet Disinfection for Wastewater Reclamation and Reuse Subject to Restrictive Standards. Water Environmental Research, 65, 169-180.

Der Gast, C., Knowles, C., Starkey, M., Thompson, I. (2002). Van Selection of microbial consortia for treating metal-working fluids. Journal of Industrial Microbiology and Biotechnology, 29(1), 20-27.

Dobrovic, S., Juretić , H., Ružinski, N. (2017). Separation Science and Technology Photodegradation of Natural Organic Matter in Water with at 185 and 254 nm: Importance of Hydrodynamic Conditions on the Decomposition Rate

Photodegradation of Natural Organic Matter in Water with UV Irradiation. Sciences and Technology, 42, 1421-1432.

Drooger, J. C., Jager, A., Lam, M. H., den Boer, M. D., Sleijfer, S., Mathijssen, R. H., de Bruijn, P. (2015). Development and validation of an UPLC-MS/MS method for the quantification of tamoxifen and its main metabolites in human scalp hair. Journal of Pharmaceutical and Biomedical Analysis, 114, 416-425.

Elkins, P., Coleman, D., Burgess, J., Gardner, M., Hines, J., Scott, B., Liu, P. (2014). Characterization of the isomeric configuration and impurities of (Z)-endoxifen by 2D NMR, high resolution LC-MS, and quantitative HPLC analysis. Journal Pharmaceutical Biomedical Analysis, 88, 174-179.

EPA. (2002). Wastewater Technology Fact Sheet-Disinfection for Small Systems.

Evgenidou, E. N., Konstantinou, I. K., Lambropoulou, D. A. (2015). Occurrence and removal of transformation products of PPCPs and illicit drugs in wastewaters: a review. Science of the Total Environment, 505, 905-926.

Fauq, A. H., Maharvi, G. M., Sinha, D. (2010). A convenient synthesis of (Z)-4-hydroxy-N-desmethyltamoxifen (endoxifen). Bioorganic & Medicinal Chemistry Letters, 20(10), 3036-3038.

Ferrando-Climent, L., Rodriguez-Mozaz, S., Barceló, D. (2013). Development of a UPLC-MS/MS method for the determination of ten anticancer drugs in hospital and urban wastewaters, and its application for the screening of human metabolites assisted by information-dependent acquisition tool (IDA) in sewage samples. Analytical and Bioanalytical Chemistry, 405(18), 5937-5952.

Fisher, B., Costantino, J. P., Wickerham, D. L., Redmond, C. K., Kavanah, M., Cronin, W. M.,Wolmark, N. (1998). Tamoxifen for prevention of breast cancer: report

of the National Surgical Adjuvant Breast and Bowel Project P-1 Study. Journal of the National Cancer Institute, 90(18), 1371-1388.

Franquet-Griell, H., Medina, A., Sans, C., Lacorte, S. (2017). Biological and photochemical degradation of cytostatic drugs under laboratory conditions. Journal of Hazardous Materials, 323, 319-328.

Fujishima, A., Rao, T. N., Tryk, D. (2000). TiO2 photocatalysts and diamond electrodes. Electrochimica Acta, 4686, 4683-4690.

Glindemann, D. (2005). Dimethyl Sulfoxide (DMSO) waste residues and municipal wastewater odor. Paper presented at the Water Environment Federation, WEFTEC.

Goverment of Canada. (2015). Screening Assessment Ethanamine, 2-[4-[(1Z)-1,2-diphenyl-1-butenyl]phenoxy]-N,N-dimethyl-(Tamoxifen).(978-1-100-25661-0).

Guo, M., Hu, H., Bolton, J. R., El-Din, M. G. (2009). Comparison of low-and medium-pressure ultraviolet lamps: Photoreactivation of Escherichia coli and total coliforms in secondary effluents of municipal wastewater treatment plants. Water Research, 43(3), 815-821.

He, L., Jurs, P. C. (2005). Assessing the reliability of a QSAR model's predictions. Journal of Molecular Graphics Modelling, 23, 503-523.

Heath, E., Česen, M., Negreira, N., de Alda, M. L., Ferrando-Climent, L., Blahova, L., Kosjek, T. (2016). First inter-laboratory comparison exercise for the determination of anticancer drugs in aqueous samples. Environmental Science and Pollution Research, 23(15), 14692-14704.

Heberer, T. (2002). Occurrence, fate, and removal of pharmaceutical residues in the aquatic environment: a review of recent research data. Toxicology letters, 131(1-2), 5-17.

Heberer, T., Reddersen, K., Mechlinski, A. (2002). From municipal sewage to drinking water: fate and removal of pharmaceutical residues in the aquatic environment in urban areas. Water Science Technology, 46(3), 81-88.

Helland, T., Gjerde, J., Dankel, S., Fenne, I. S., Skartveit, L., Drangevåg, A., Lien, E. A. (2015). The active tamoxifen metabolite endoxifen (4OHNDtam) strongly down-regulates cytokeratin 6 (CK6) in MCF-7 breast cancer cells. PLoS One, 10(4), 1-19.

Hoskins, J. M., Carey, L. A., McLeod, H. L. (2009). CYP2D6 and tamoxifen: DNA matters in breast cancer. Nature Review Cancer, 9(8), 576-586.

Hu, X., Bao, Y., Hu, J., Liu, Y., & Yin, D. (2017). Occurrence of 25 pharmaceuticals in Taihu Lake and their removal from two urban drinking water treatment plants and a constructed wetland. environmental Science Pollution, 24, 14889-14902.

ICH. (2005). Guideline on Validation of Analytical Procedures: Methodology developed to complement the Parent Guideline. ICH Harmonised tripartite guideline validation of analytical procedures: Text and methodology, Q2 (R1).

Jager, N., Rosing, H., Linn, S., Schellens, J., Beijnen, J. (2012). Highly selective LC-MS/MS analysis for the accurate quantification of tamoxifen and its metabolite: focus on endoxifen and 4-hydroxytamoxifen. Breast cancer Research Treatment, 133(2), 793-798.

Jaremko, M., Kasai, Y., Barginear, M. F., Raptis, G., Desnick, R. J., Yu, C. (2010). Tamoxifen metabolite isomer separation and quantification by liquid

chromatography-tandem mass spectrometry. Analytical Chemistry, 82(24), 10186-10193.

Jin, X., Xu, H., Qiu, S., Jia, M., Wang, F., Zhang, A. (2017). Direct photolysis of oxytetracycline: Influence of initial concentration, pH and temperature. Journal of Photochemestry and Photobiology, 332, 224-231.

Jo, W., Kumar, S., Isaacs, M. A., Lee, A. F., Karthikeyan, S. (2016). Cobalt promoted TiO2/GO for the photocatalytic degradation of oxytetracycline and Congo Red. Applied Catalysis, 201, 159-168. 2

Johnson, A. C., Oldenkamp, R., Dumont, E., Sumpter, J. P. (2013). Predicting concentrations of the cytostatic drugs cyclophosphamide, carboplatin, 5-fluorouracil, and capecitabine throughout the sewage effluents and surface waters of europe. Environmental toxicology and Chemistry, 32(9), 1954-1961.

Johnson, M. D., Zuo, H., Lee, K. H., Trebley, J. P., Rae, J. M., Weatherman, R. V., Skaar, T. C. (2004). Pharmacological characterization of 4-hydroxy-N-desmethyl tamoxifen, a novel active metabolite of tamoxifen. Breast cancer Research Treatment, 85(2), 151-159.

Kisanga, E. R., Mellgren, G., Lien, E. A. (2005). Excretion of hydroxylated metabolites of tamoxifen in human bile and urine. Anticancer Research, 25(6C), 4487-4492.

Knacker, T., Boettcher, M., Frische, T., Rufli, H., Stolzenberg, H. C., Teigeler, M., Schäfers, C. (2010). Environmental effect assessment for sexual endocrine-disrupting chemicals: Fish testing strategy. Integrated Environmental Assessment and Management, 6(4), 653-662.

Kopec, R. E., Schweiggert, R. M., Riedl, K. M., Carle, R., Schwartz, S. J. (2013). Comparison of high-performance liquid chromatography/tandem mass

spectrometry and high-performance liquid chromatography/photo-diode array detection for the quantitation of carotenoids, retinyl esters, α-tocopherol and phylloquinone in chylomicron-rich fractions of human plasma. Rapid Communication in Mass Spectrometry, 27, 1393-1402.

Kovalova, L., Siegrist, H., Singer, H., Wittmer, A., McArdell, C. S. (2012). Hospital wastewater treatment by membrane bioreactor: performance and efficiency for organic micropollutant elimination. Environment Science & Technology, 46(3), 1536-1545.

Lara-Martín, P. A., González-Mazo, E., Petrovic, M., Barceló, D., Brownawell, B. J. (2014). Occurrence, distribution and partitioning of nonionic surfactants and pharmaceuticals in the urbanized Long Island Sound Estuary (NY). Marine Pollution Bulletin, 85(2), 710-719.

Larson, R. A., Befenbaum, M. R. (1988). Environmental phototoxicity Solar ultraviolet radiation affects the toxicity of natural and man-made chemicals. Environmental Science Technology, 22(4), 354-360.

Lawrence, M., Marzzacco, C. J., Morton, C., Schwab, C., Halpern, A. M. (1991). Excited-state deprotonation of 2-naphthol by anions. Journal of Physical Chemistry, 95, 10294-10299.

Liu, Z. H., Zhang, Y. G., Wang, D. S. (2010). Studies on feminization, sex determination, and differentiation of the Southern catfish, Silurus meridionalis-a review. Fish Physiology Biochemistry, 36(2), 223-235.

Maradonna, F., Batti, S., Marino, M., Mita, D. G., Carnevali, O. (2009). Tamoxifen as an emerging endocrine disruptor. effects on fish reproduction and detoxification

target genes. Annuals of the New York Academy of Sciences, 1163(1), 457-459.

Mathon, B., Choubert, J. M., Miege, C., Coquery, M. (2016). A review of the photodegradability and transformation products of 13 pharmaceuticals and pesticides relevant to sewage polishing treatment. Science of Total Environment, 551-552, 712-724.

Mayo Foundation for Medical Education and Research. (2014). Endoxifen shows promise as breast cancer treatment.

Mendenhall, D. W., Kobayashi, A., Mel, F., Shih, L., Sternson, L. A., Fabian, C. (1978). ClinicalAnalysis of Tamoxifen, an Anti-NeoplasticAgent, in Plasma. Clinical Chemistry, 24, 1518-1524.

Miller, J. S., Olejnik, D. (2001). Photolysis of polycyclic aromatic hydrocarbons in water. Water Research, 1354, 233-243.

Oppenländer, T., 2003. Photochemical purification of water and air. Wiley-VCH, New York.

National Institute of Health. (2015). Tamoxifen citrate or Z-endoxifen hydrochloride in treating patients with locally advanced or metastatic, estrogen receptor-positive, HER2-negative breast.

Negreira, N., Alda, M., Barceló, D. (2014). Cytostatic drugs and metabolites in municipal and hospital wastewater in Spain: Filtration, occurrence, and environmental risk. Science of the Total Environment, 497-498, 68-77.

Negreira, N., Regueiro, J., Lopez de Alda, M., Barceló, D. (2015). Transformation of tamoxifen and its major metabolites during water chlorination: Identification

and in silico toxicity assessment of their disinfection byproducts. Water Research, 85, 199-207.

Oppenländer, T. (2003). Photochemical purification of water and air: Advance oxidation processes (AOPs)- Principles, reaction mechanisms, reactor concepts. New York: Wiley-VCH.

Peng, J., Sengupta, S., & Jordan, V. (2009). Potential of selective estrogen receptor modulators as treatments and preventives of breast cancer. AntiCancer Agents in Medicinal Chemistry, 9(5), 481-499.

Pereira, V. J., Linden, K. G., Weinberg, H. S. (2007). Evaluation of UV irradiation for photolytic and oxidative degradation of pharmaceutical compounds in water. Water Research, 41, 4413-4423.

Prados-Joya, G., Polo, M., Rivera-Utrilla, J., Sanchez-Ferro-Garcia, M. (2010). Photodegradation of the antibiotics nitroimidazoles in aqueous solution by ultraviolet radiation. Water Research, 45, 393-403.

Pragst, F., Herzler, M., Erxleben, B.-T. (2004). Systematic toxicological analysis by high-performance liquid chromatography with diode array detection (HPLC-DAD). Clinical Chemistry and Laboratory Medicine, 42(11), 1325-1340.

Rivas, J., Gimeno, O., Borralho, T., Carbajo, M. (2009). UV-C photolysis of endocrine disruptors. The influence of inorganic peroxides. Journal of Hazardous Materials, 174(1-3), 393-397.

Roberts, P. H., Thomas, K. V. (2006). The occurrence of selected pharmaceuticals in wastewater effluent and surface waters of the lower Tyne catchment. Science of the Total Environment, 356(1-3), 143-153.

Sauvant, M. P., Pepin, D., Piccinni, E. (1999). Tetrahymena pyriformis: a tool for toxicological studies. A review. Chemosphere, 38(7), 1631-1669.

Shemer, H., Kunukcu, Y. K., Linden, K. G. (2006). Degradation of the pharmaceutical metronidazole via UV, Fenton and photo-Fenton processes. Chemosphere, 63(2), 269-276.

Shin, G. A., Linden, K. G., Arrowood, M. J., Sobsey, M. D. (2001). Low-pressure, U. V. inactivation and DNA repair potential of Cryptosporidium parvum oocysts. Applied Environmental Microbiology, 67, 3029-3032.

Singh, A. (2013). Introduction of modern endocrine techniques for the production of monosex population of fishes. General and Comparative Endocrinology, 181, 146-155.

Siripattanakul, S., Wirojanagud, W., McEvoy, J., Limpiyakorn, T., Khan, E. (2009). Atrazine degradation by stable mixed cultures enriched from agricultural soil and their characterization. Journal of Applied Microbiology, 106(3), 986-992.

Steiner, A., Terplan, M., Paulson, R. (2005). Comparison of tamoxifen and clomiphene citrate for ovulation induction: a meta-analysis. Human Reproduction, 20(6), 1511-1515.

Sz-Chwun, H., Jane-Yii, W. (2007). Optimal dimethyl sulfoxide biodegradation using activated sludge from a chemical plant. Process Biochemistry, 42(10), 1398-1405

Tanner, R. (2007). Manual of Environmental Microbiology (Third ed.). Washinton, DC.: ASM Press.

Teunissen, S. F., Rosing, H., Schinkel, A. H., Schellens, J. H., Beijnen, J. H. (2010). Bioanalytical methods for determination of tamoxifen and its phase I metabolites: a review. Analitycal Chim Acta, 683(1), 21-37.

Thomas, K. V., Hilton, M. J. (2004). The occurrence of selected human pharmaceutical compounds in UK estuaries. Marine Pollution Bulletin, 49(5-6), 436-444.

Tønnesen, H. H. (2004). Photostability of drugs and drug formulation. Boca Raton, Florida: CRC-Press.

Trawiński, J., & Skibiński, R. (2017). Photolytic and photocatalytic degradation of tandospirone: Determination of kinetics, identification of transformation products and in silico estimation of toxicity. Science of Total Environment, 590, 775-798.

TRC. (2016). Trc-canada.   Retrieved 05.18.16.http://www.trc-canada.com

Udom, I., Myers, P. D., Ram, M. K., Hepp, A. F., Archibong, E., Stefanakos, E. K., Yogi Goswami, D. (2014). Optimization of Photocatalytic Degradation of Phenol Using Simple Photocatalytic Reactor. American Journal of Analytical Chemistry, 5, 743-750.

Urbatzka, R., Bottero, S., Mandich, A., Lutz, I., Kloas, W., Part, C. (2007). Endocrine disrupters with (anti) estrogenic and (anti) androgenic modes of action affecting reproductive biology of xenopus laevis: I. Effects on sex steroid levels and biomarker expression. Comparative Biochemistry and Physiology Toxicology Pharmacology, 144(4), 310-318.

USEPA. (2003). Ultraviolet Disinfection Guiadance.

USEPA. (2016). User's guide for T.E.S.T. (version 4.2)(Toxicity estimation Software Tool):A program to estimate toxicity from molecular structure.

Van der Ven, L., Brandhof, E., Vos, J., Wester, P. (2007). Effects of the estrogen agonist 17β-estradiol and agonist tamoxifen in a partial life-cycle assay with zebrafish (Danio rerio). Environmental toxicology and Chemistry, 26(1), 92-99.

Wang, M., Wang, H., Zhang, R., Ma, M., Mei, K., Fang, F., Wang, X. (2015). Photolysis of Low-Brominated Diphenyl Ethers and Their Reactive Oxygen Species-Related Reaction Mechanisms in an Aqueous System. PLoSOne, 10, 1-14.

Weller, A. (1961). Fast reaction of excited molecules. Progress in Reaction Kinetics, 1(187), 189-214.

Wu, X., Hawse, J. R., Subramaniam, M., Goetz, M. P., Ingle, J. N., Spelsberg, T. C. (2009). The tamoxifen metabolite, endoxifen, is a potent antiestrogen that targets estrogen receptor alpha for degradation in breast cancer cells. Cancer Research, 69(5), 1722-1727.

Zhang, C., Zhong, Q., Zhang, Q., Zheng, S., Miele, L., Wang, G. (2015). Boronic prodrug of endoxifen as an effective hormone therapy for breast cancer. Breast Cancer Research and Treatment, 152(2), 283-291.

Zhou, N., Lutovsky, A., Andaker, G., Gough, H., Ferguson, J. (2013). Cultivation and characterization of bacterial isolates capable of degrading pharmaceuticals and personal care products for improved removal in activated sludge wastewater treatment. Biodegradation, 24(6), 813-827.

APPENDIX A

HPLC-DAD METHOD OPTIMIZATION AND VALIDATION

A.1 Chromatography parameters optimization

A.1.1 Absorbance wavelength selection
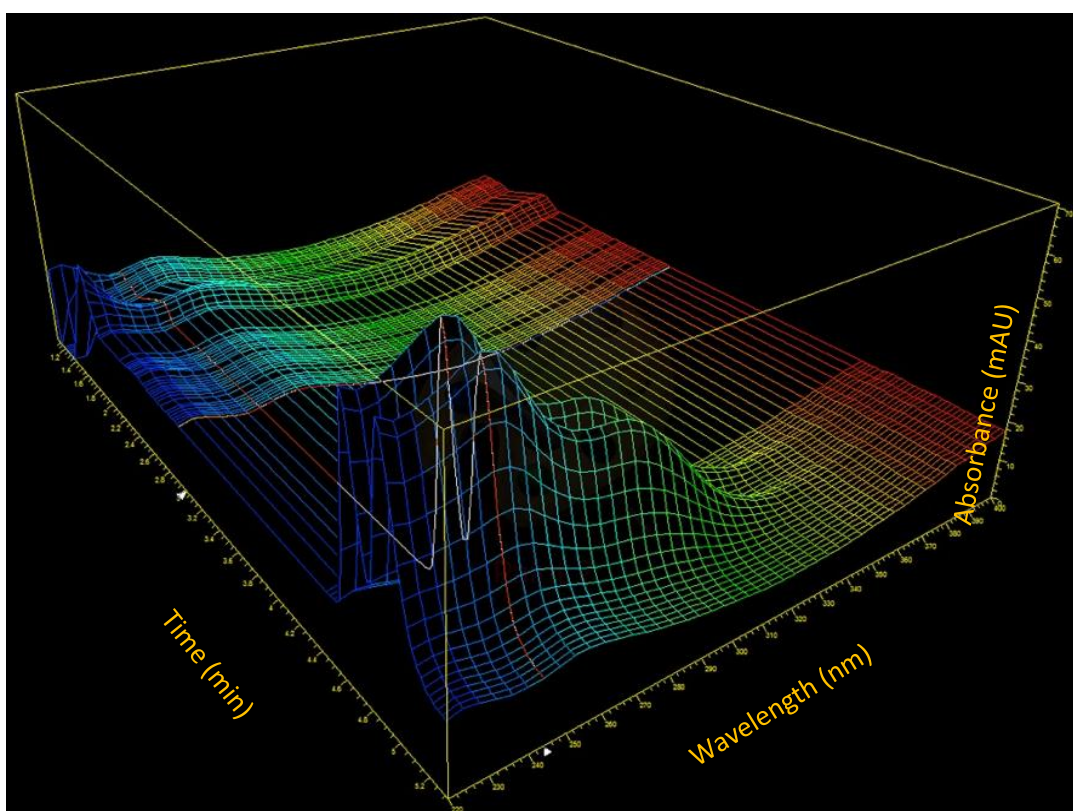
Figure A.1. Absorbance 3D plot for (E)- and (Z)-endoxifen in the wavelength range of 190 to 390 nm. The maximum absorbance is indicated with a red line crossing the spectrum. (E)- and (Z)-endoxifen isomers showed a maximum isoabsorbance at 244 nm. Spectral coloring indicates an increase in the length of the wavelength starting with blue color for the shorter wavelengths (220 nm) and red color for the longer wavelengths (400 nm).

A.2 HPLC-DAD method validation

A.2.1 Selectivity
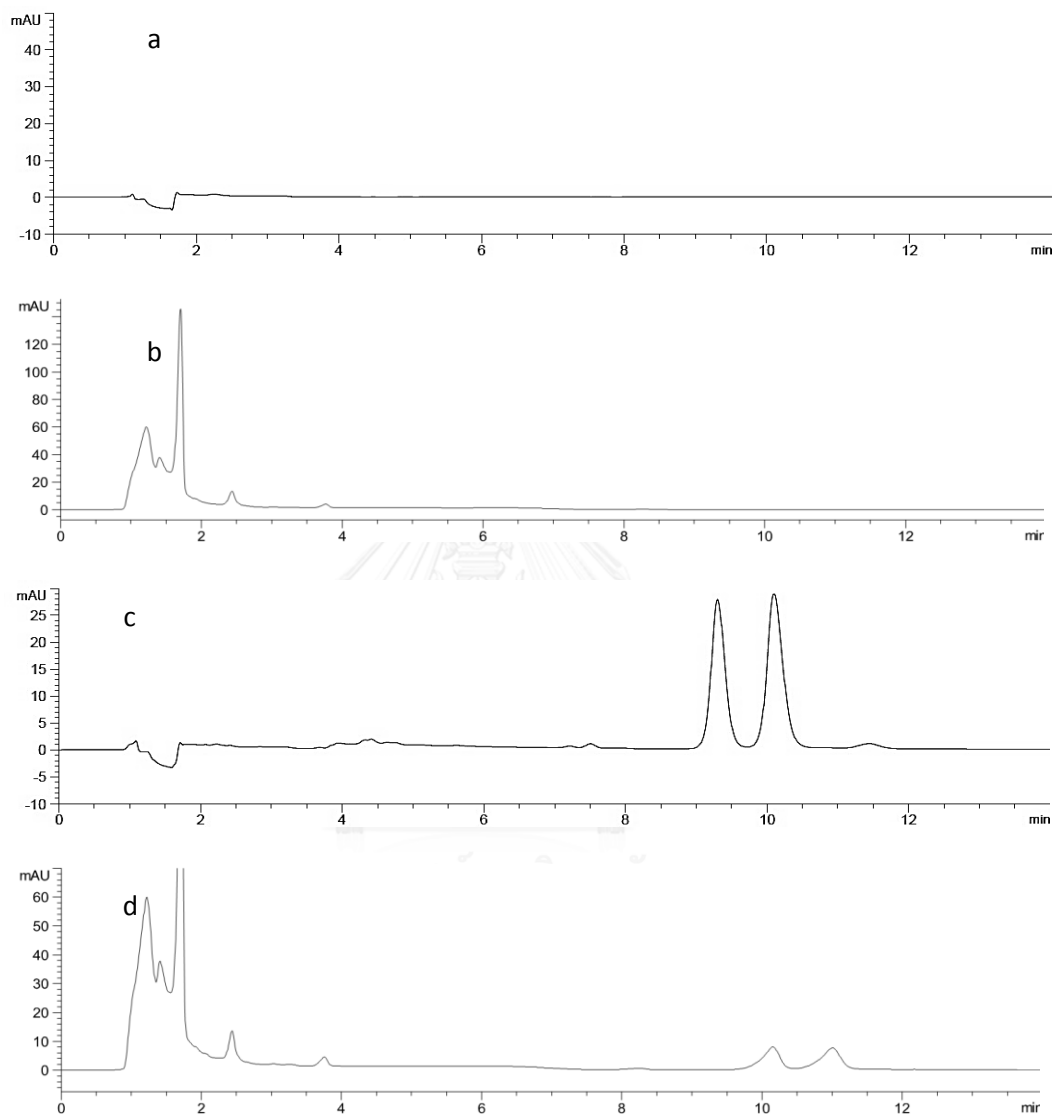
Figure A.2. HPLC-DAD chromatograms obtained by the proposed method: (a) blank water sample, (b) blank wastewater; (c) water sample spiked with 1μg mL^{-1} of (E)-endoxifen and 1μg mL^{-1} of (Z)-endoxifen; (d) wastewater sample spiked with 1μg mL^{-1} of (E)-endoxifen and 1μg mL^{-1} of (Z)-endoxifen

A.2.2 Isomer Identification
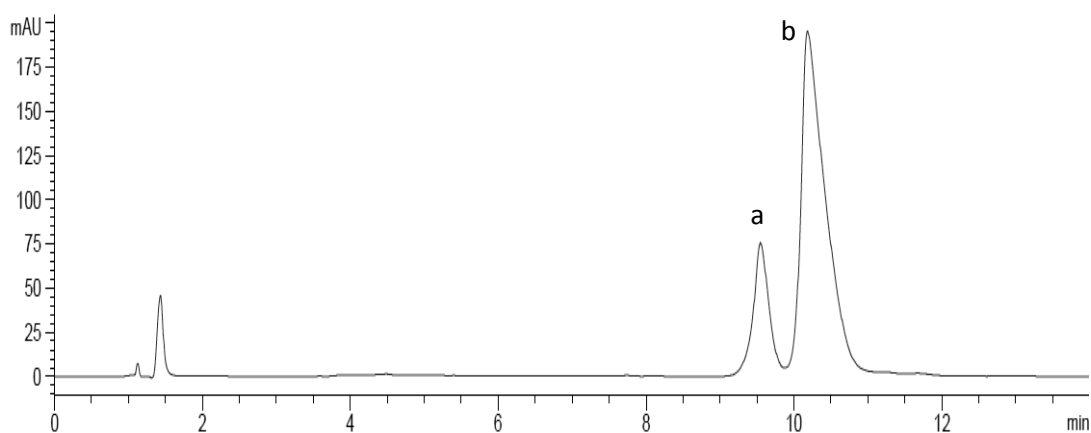
Figure A.3. HPLC-DAD chromatogram monitored at 244 nm of (Z)-endoxifen isomer in aqueous solution (0.5 mg mL^{-1}): (1) (E)-endoxifen impurity with a chromatograph area percentage of 19.2% of the total chromatogram area and a retention time of 9.55 minutes, (2) (Z)-endoxifen with a chromatogram area percentage of 75.5 % of the total chromatogram area and a retention time of 10.12 minutes.

A.2.3 Linearity and Sensitivity
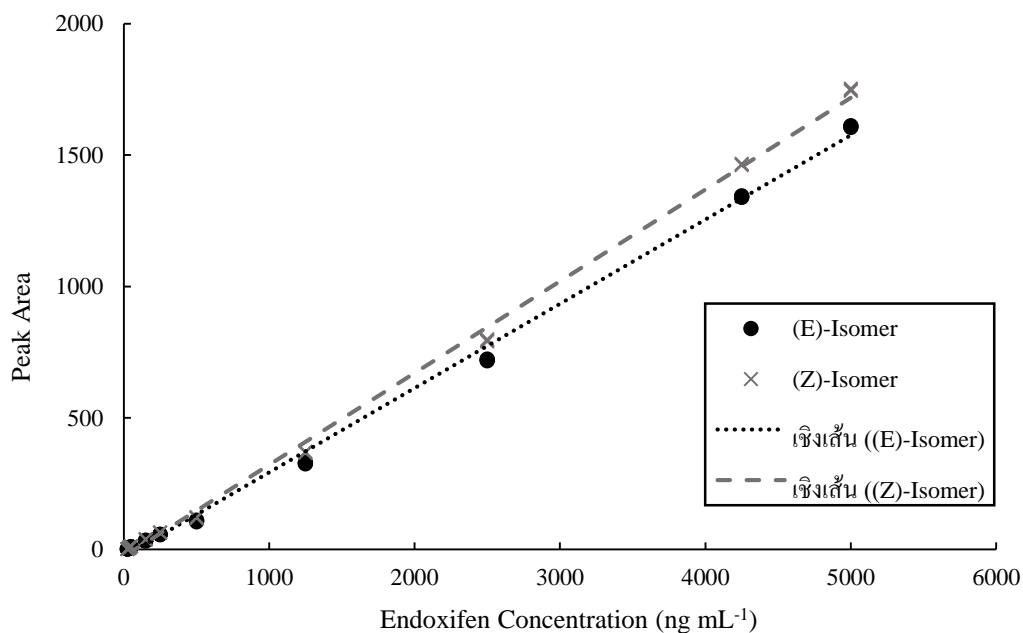
Figure A.4. Linear calibration curve with the response peak areas as a function of (E)-
and (Z)-endoxifen conentration.

Table A.1. Coefficient of correlation (R^2), linear equation, LOD and LOQ of (E)- and
(Z)-endoxifen by the proposed HPLC-DAD method.

Analyte	R^2	Linear Equation	LOD (ng mL^{-1})	LOQ (ng mL^{-1})
(E)-endoxifen	0.9975	y=0.3493x-27.931	12.66	38.35
(Z)-endoxifen	0.9981	y=0.3208x-28.440	12.12	36.74

A.2.4 Accuracy and Precision

Table A.2. Method validation for accuracy and precision in intra-day assay; QCL: Quality control low (n=5); QCM: quality control medium (n=5); QCH: Quality control High (n=5).

Analyte	Standard Quality Control	Nominal Concentration (ng mL^{-1})	Theoretical Concentration (ng mL^{-1})	Accuracy (%)	Precision RSD (%)
(E)-endoxifen	QCL	100	95.5±1.32	4.5±1.32	1.38
	QCM	350	354.1±10.50	2.8±0.98	2.97
	QCH	700	685.1±14.76	2.6±1.62	2.15
(Z)-endoxifen	QCL	100	87.2±1.31	12.8±1.31	1.51
	QCM	350	367.1±11.15	4.9±3.19	3.04
	QCH	700	717.0±15.08	2.5±2.04	2.10

Table A.3. Method validation for accuracy and precision in intra-day assay; QCL: Quality control low (n=5); QCM: quality control medium (n=5); QCH: Quality control High (n=5).

Analyte	Standard Quality Control	Nominal Concentration (ng mL^{-1})	Theoretical Concentration (ng mL^{-1})	Accuracy (%)	Precision RSD (%)
(E)-endoxifen	QCL	100	93.2±1.06	6.8±1.06	1.14
	QCM	350	349.1±11.06	1.7±4.17	4.60
	QCH	700	640.3±34.67	8.5±4.22	5.41
(Z)-endoxifen	QCL	100	84.8±0.80	15.2±0.80	0.95
	QCM	350	358.4±13.34	3.3±2.81	3.72
	QCH	700	666.2±45.93	5.8±5.52	6.90

A.3 3D-Plot Fluorescence emission of (E)- and (Z)-endoxifen
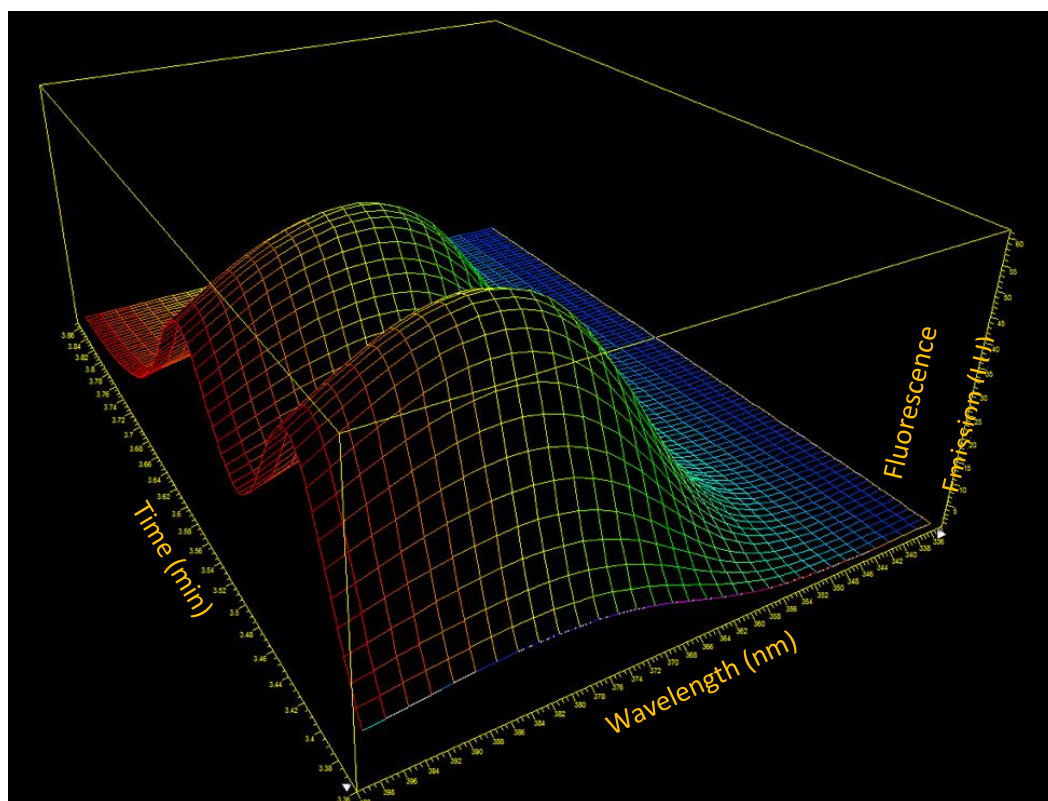
Figure A.5. Fluorescence emission 3D plot for (E)- and (Z)-endoxifen in a wavelength range of 335 to 400 nm. (E)- and (Z)-endoxifen isomers showed a maximum fluorescence emission at 382 nm. Spectral coloring indicates a decrease in the length of the wavelength starting with red color for the longer wavelength (400 nm) and blue color for the shorter wavelength (335 nm).

APPENDIX B

BIODEGRADATION

B.1 pH monitoring during endoxifen degrader enrichment
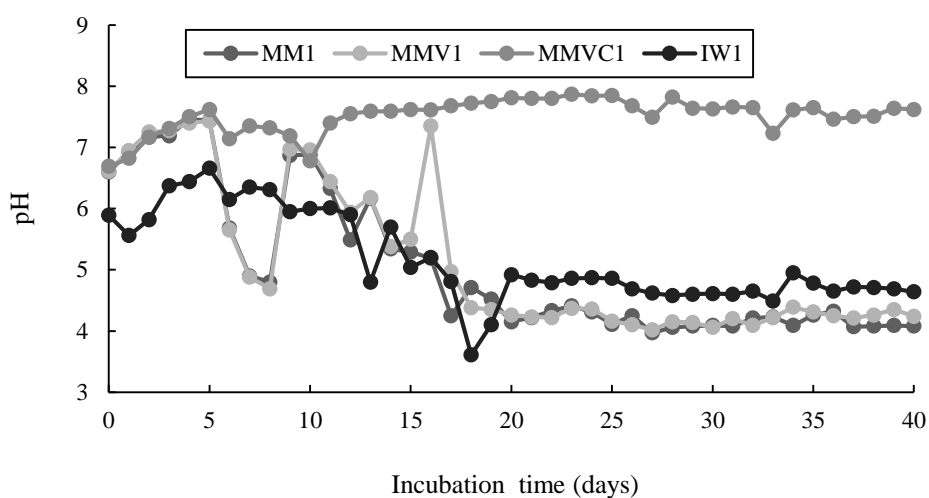
Figure B.1. Variation of pH in MM1, MMV1, MMVC1, and IW1 during endoxifen degrader enrichment for 40 days.
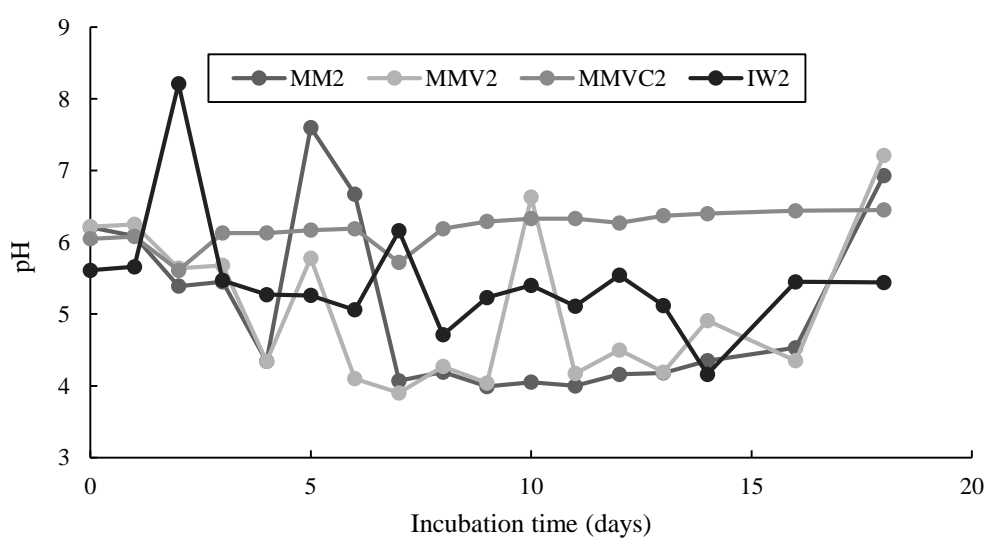
Figure B.2. Variation of pH in MM2, MMV2, MMVC2, and IW2 during endoxifen degrader enrichment for 18 days.
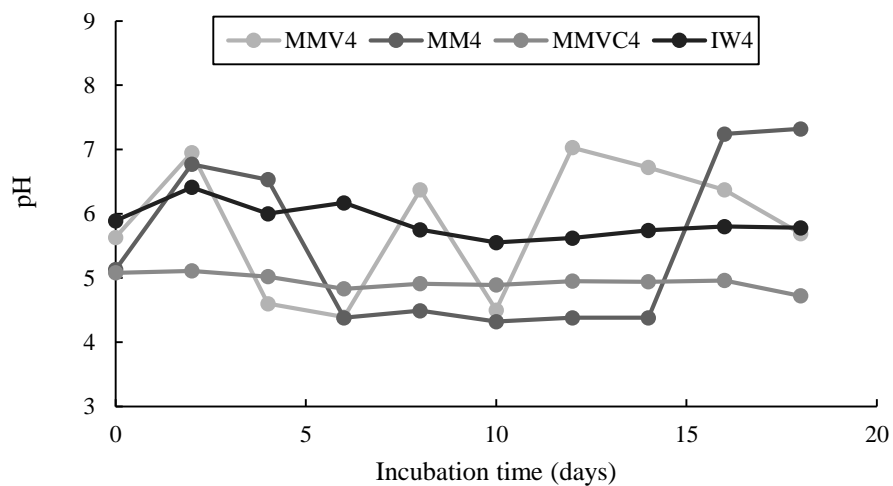
Figure B.3. Variation of pH in MM4, MMV4, MMVC4, and IW4 during endoxifen degrader enrichment for 18 days.

B.2 Temperature monitoring during endoxifen degrader enrichment
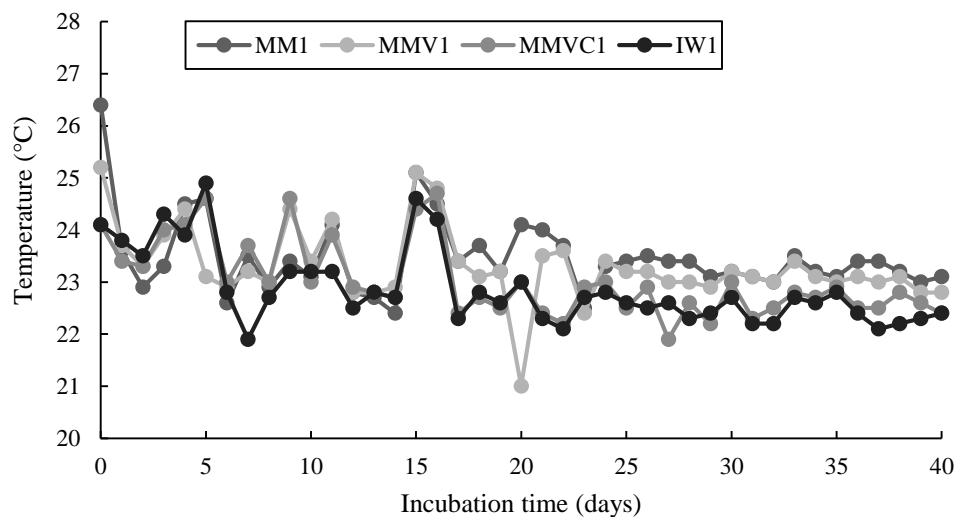
Figure B.4. Variation of temperature in MM1, MMV1, MMVC1, and IW1 during endoxifen degrader enrichment for 40 days.
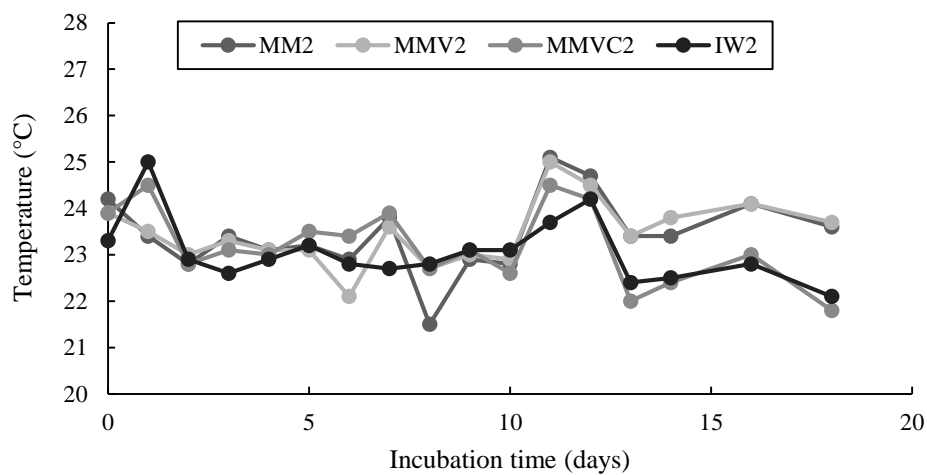
Figure B.5. Variation of temperature in MM2, MMV2, MMVC2, and IW2 during endoxifen degrader enrichment for 18 days.
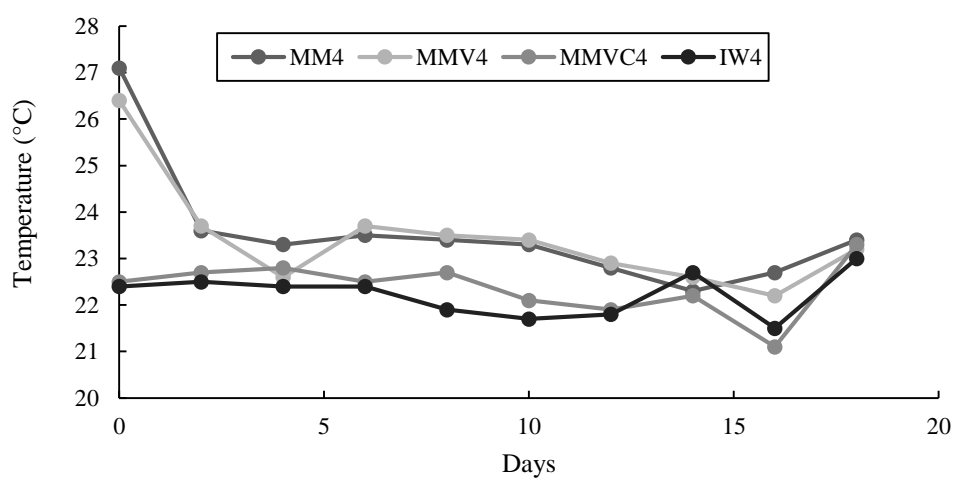
Figure B.6. Variation of temperature in MM4, MMV4, MMVC4, and IW4 during endoxifen degrader enrichment for 18 days.

B.3 Bacterial growth monitoring by VSS method during endoxifen degrader enichment
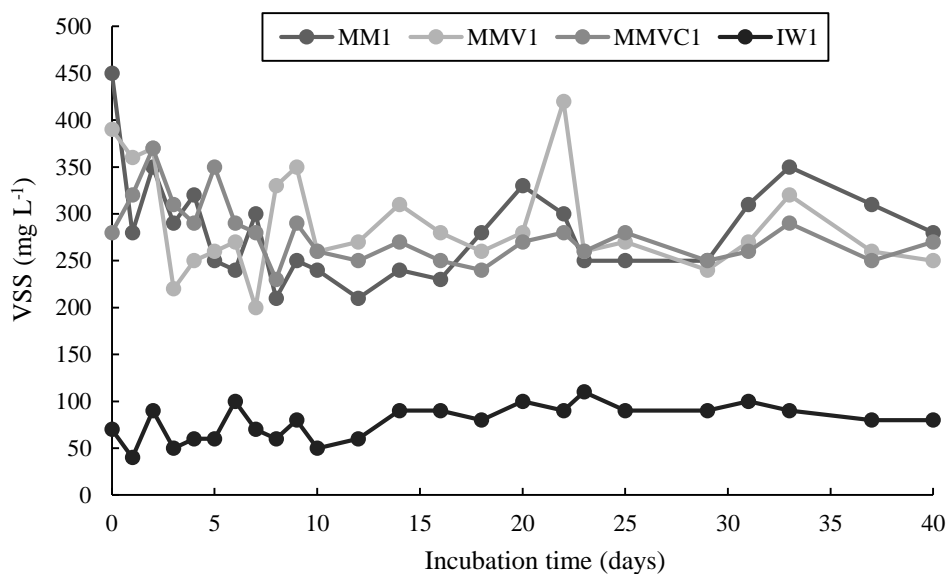
Figure B.7. VSS results for MM1, MMV1, MMVC1, and IW1 during endoxifen degrader enrichment for 40 days.
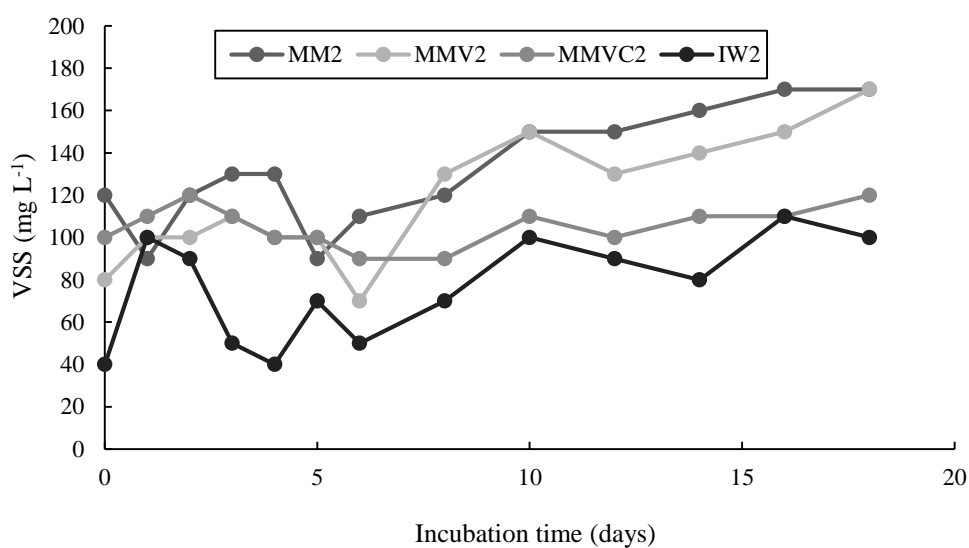
Figure B.8. VSS results for MM2, MMV2, MMVC2, and IW2 during endoxifen degrader enrichment for 18 days.
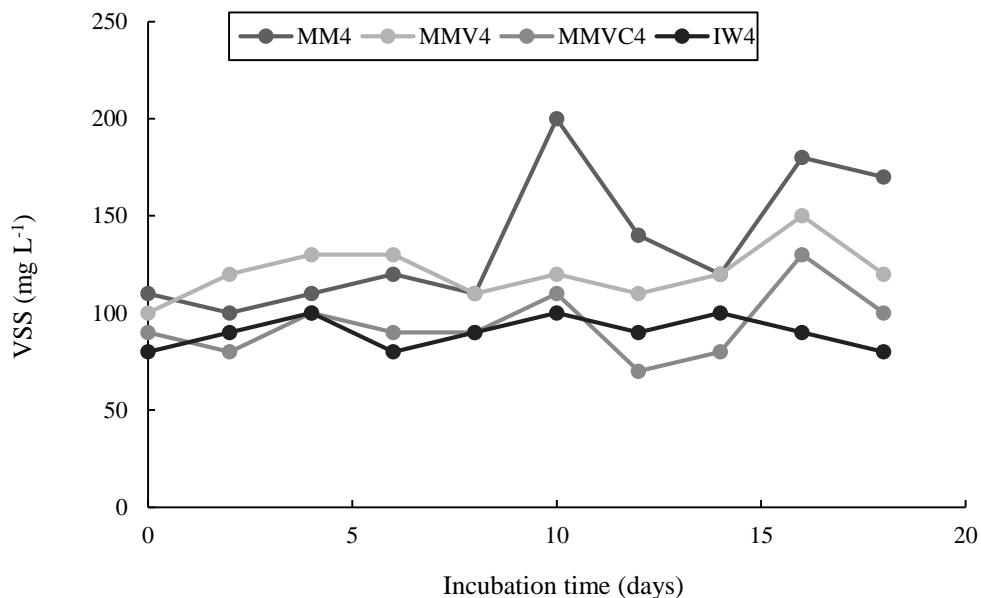
Figure B.9. VSS results for MM4, MMV4, MMVC4, and IW4 during endoxifen degrader enrichment for 18 days.

B.4 Bacterial growth monitoring by plate count method during endoxifen degrader enrichment
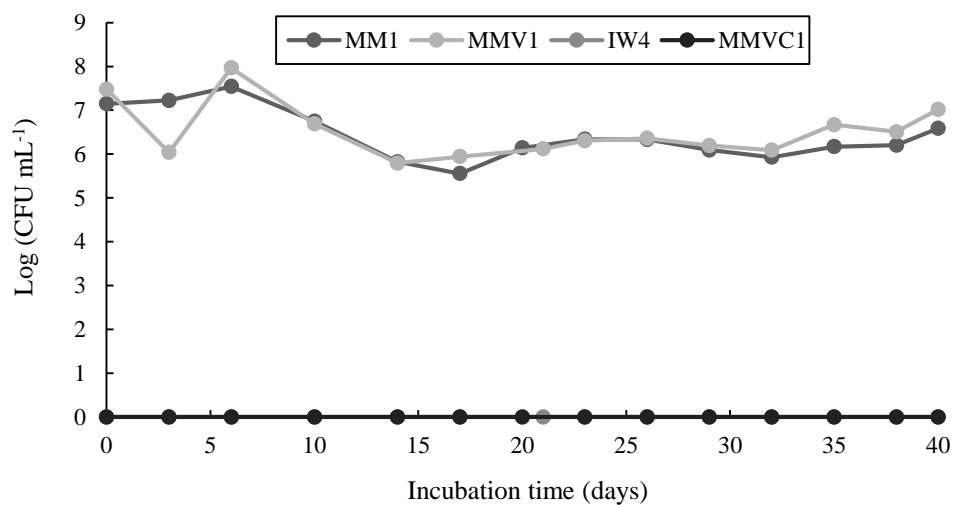
Figure B.10. Plate counting (Log (CFU mL^{-1})) results for MM1, MMV1, MMVC1, and IW1 during endoxifen degrader enrichment for 40 days.
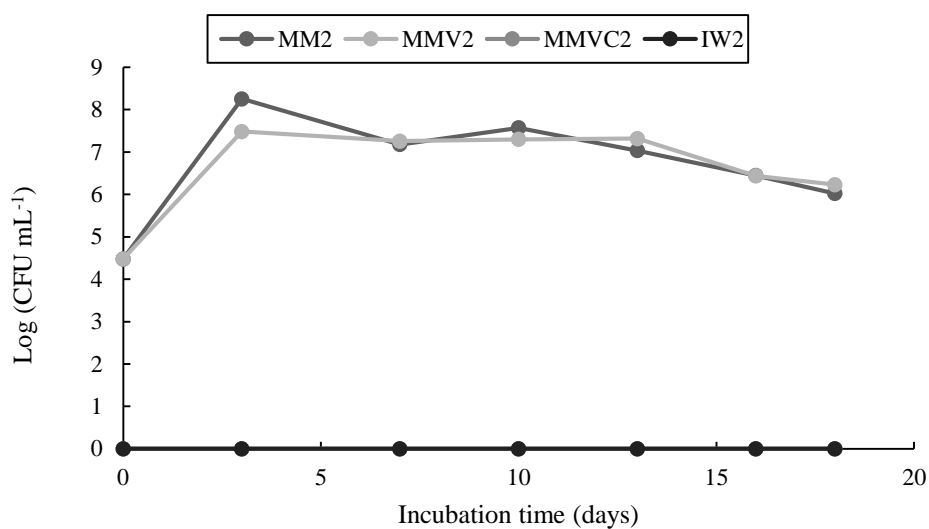
Figure B.11. Plate counting (Log (CFU mL^{-1})) results for MM2, MMV2, MMVC2, and IW2 during endoxifen degrader enrichment for 18 days.
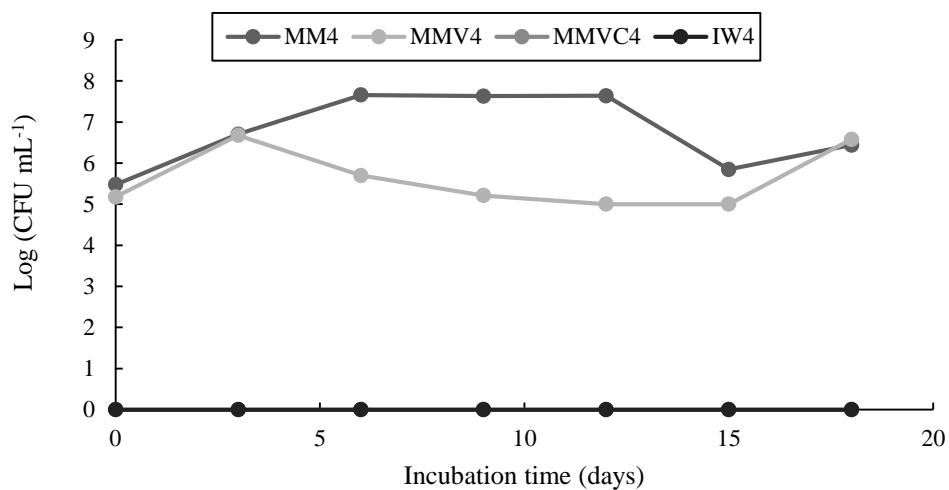
Figure B.12. Plate counting (Log (CFU mL^{-1})) results for MM4, MMV4, MMVC4, and IW4 during endoxifen degrader enrichment for 18 days.

APPENDIX C

PHOTODEGRADATION IN WATER

C.1 Photodegradation kinetic of (E)- and (Z)-endoxifen in water

Table C.1. Determination coefficient values (R^2), linear equations (first order), and rate constants (k) (first order) of (E)- and (Z)-endoxifen based on a first order kinetic model for five emission light intensities.

Analyte	UVLight Intensity (W s^{-1} cm^{-2})	Zero Order R^2	First Order R^2	Second Order R^2	Linear Equation (First Oder)	k (µM s^{-1}) (First Order)
(E)-endoxifen	28	0.918	0.996	0.968	y = -0.0177x - 0.056	17.7±1.0
	56	0.840	0.987	0.952	y = -0.0382x - 0.1364	38.2±1.7
	112	0.852	0.992	0.949	y = -0.0467x - 0.1287	46.7±2.5
	168	0.865	0.975	0.888	y = -0.0575x - 0.1114	57.5±3.7
	224	0.840	0.988	0.941	y = -0.0771x - 0.1153	77.1±5.4
(Z)-endoxifen	28	0.955	0.980	0.934	y = -0.0144x - 0.0454	14.5±1.0
	56	0.858	0.992	0.942	y = -0.0400x - 0.0943	40.0±2.8
	112	0.923	0.995	0.915	y = -0.0500x - 0.0039	50.0±2.9
	168	0.929	0.976	0.839	y = -0.0612x - 0.0083	61.2±4.9
	224	0.883	0.990	0.929	y = -0.0825x - 0.0295	82.5±5.6

C.2 Effects of UV light intensity, initial pH and initial concentration of (E)- and (Z)-endoxifen on photodegradation kinetics.

C.2.1 Effect of light intensity on photodegradation rate constant
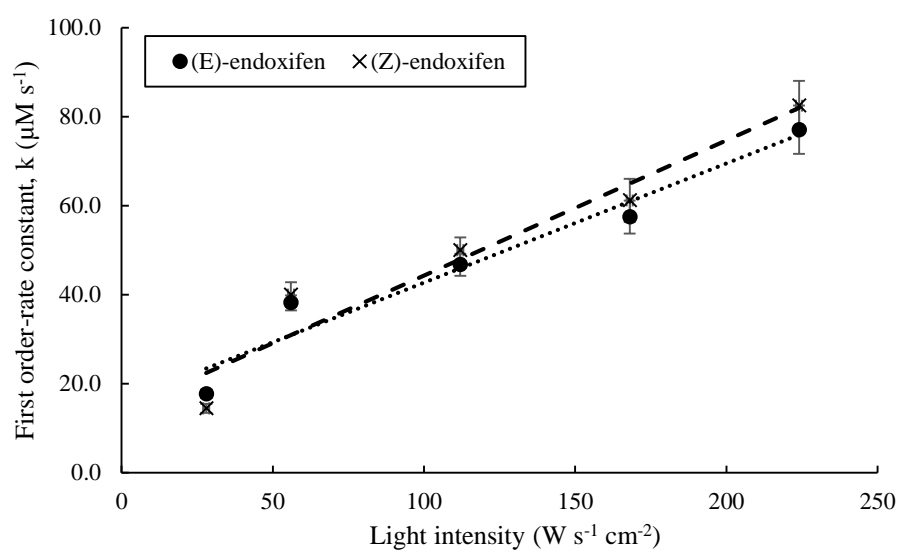
Figure C.1. Effect of light intensity (W s^{-1} cm^{-2}) on photodegradation rate constant (k) in aqueous solution spiked with (E)- and (Z)-endoxifen isomers (2 µg mL^{-1}, pH 7, and 22.4 °C)

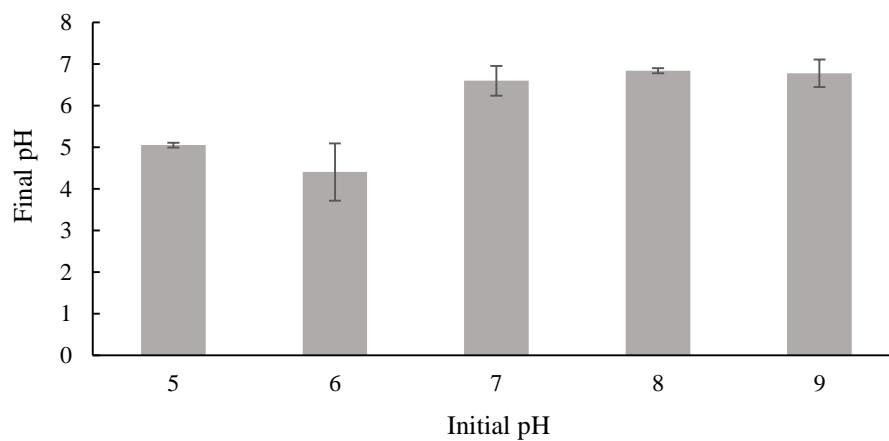*C.2.2 Change of pH before and after UV irradiation in water*

Figure C.2. pH variations after photodegradation reaction on aqueous solution spiked with (E)- and (Z)-endoxifen isomers (2 μg mL^{-1}) (22.4 °C) and irradiated with an emission light intensity of 28 W s^{-1} cm^{-2} for 80 seconds.

C.2.3 Effect of initial (E)- and (Z)-endoxifen concentration on photodegradation rate constant
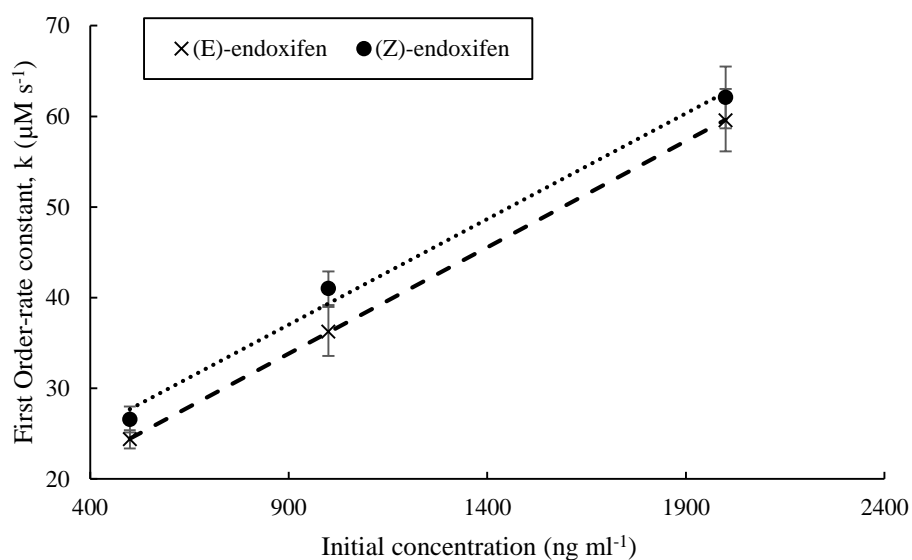
Figure C.3. Effect of initial concentration of (E)- and (Z)-endoxifen ($\mu g \, mL^{-1}$) on photodegradation rate constant (k) in aqueous solution spiked with (E)- and (Z)-endoxifen isomers (pH 7, and 22.4°C) and irradiated with an emission light intensity of 244 W s^{-1} cm^{-2}.

APPENDIX D

MOLAR EXTINCTION COEFFICIENT AND QUANTUM YIELD

D.1 Molar extinction coefficient of (E/Z)-endoxifen

y = 0.1097x - 0.0055
R² = 0.9994

Absorbance (253.7 nm)

Endoxifen Concentration (mM)
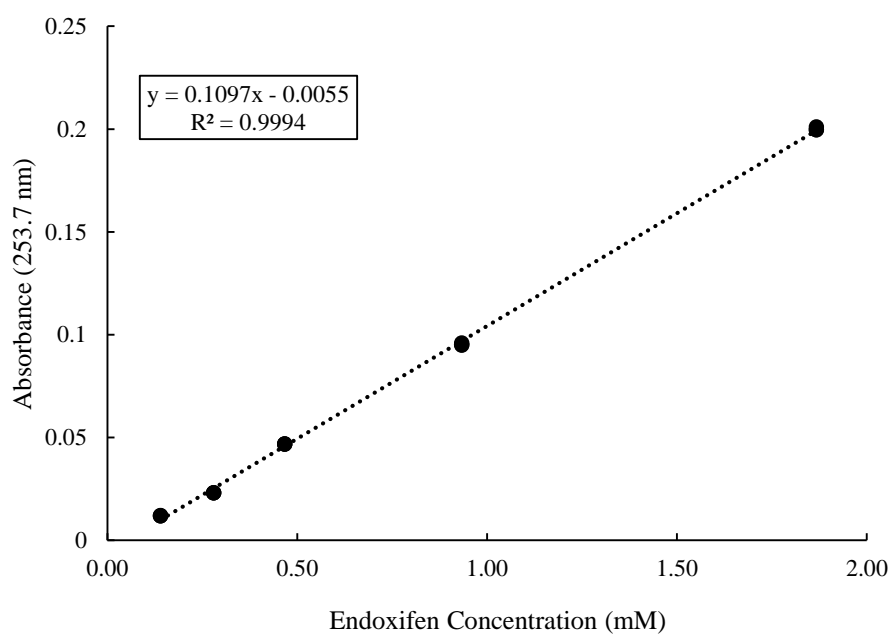
Figure D.1. Absorbance of (E/Z)-endoxifen (1:1, w/w) at 253.7 nm at five concentrations ranging from 0.375 to 5 mg L^{-1}. The slope (0.1097 mM^{-1} cm^{-1}) indicates the molar extintion coefficient of (E/Z)-endoxifen. (R^2>0.999).

D.2 Absorption spectra (510 nm) of Iron (III) solution after UV irradiation
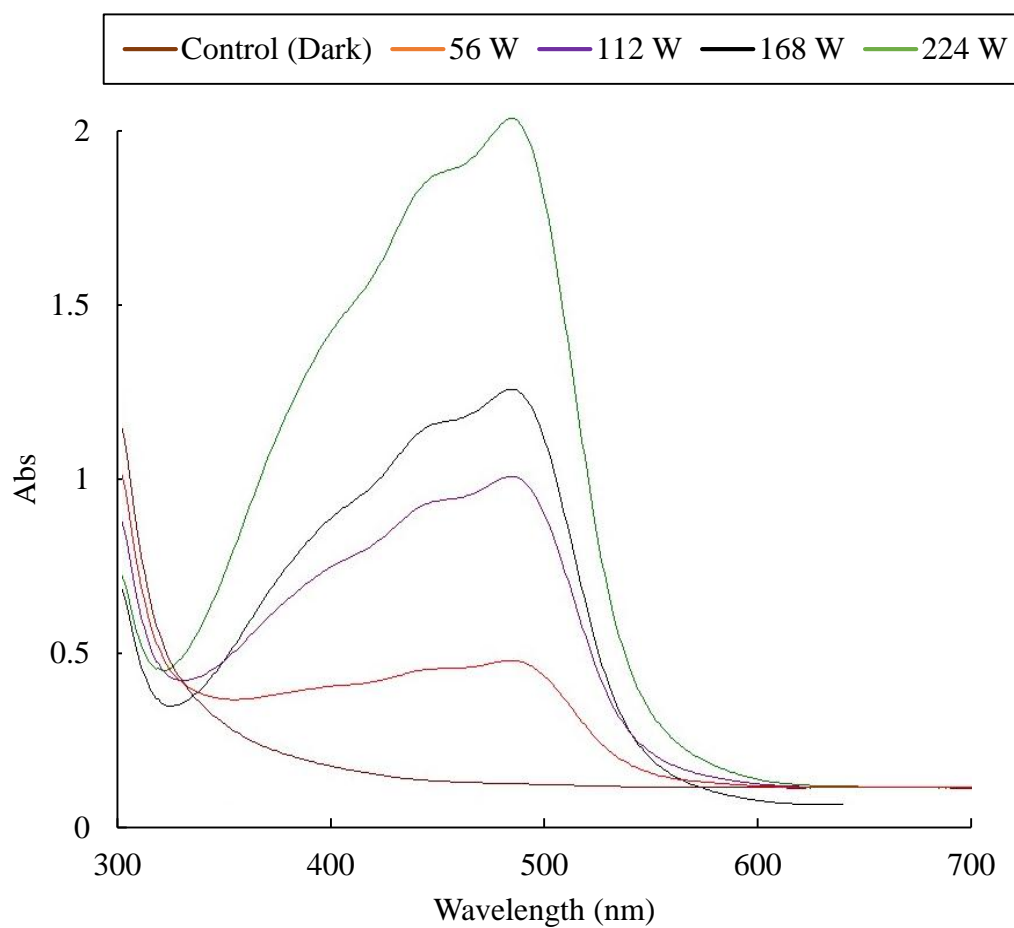
Figure D.2. Absorbance spectrum (300-700 nm) of Iron(III) sulfate solution after 1 minute irradiation with UV light at four emission light intensities (56, 112, 168, and 224 W s^{-1} cm^{-2}).

APPENDIX E

DETECTION AND IDENTIFICATION OF PBPs

E.1 HPLC-DAD chromatograms of (E)- and (Z)-endoxifen during UV irradiation
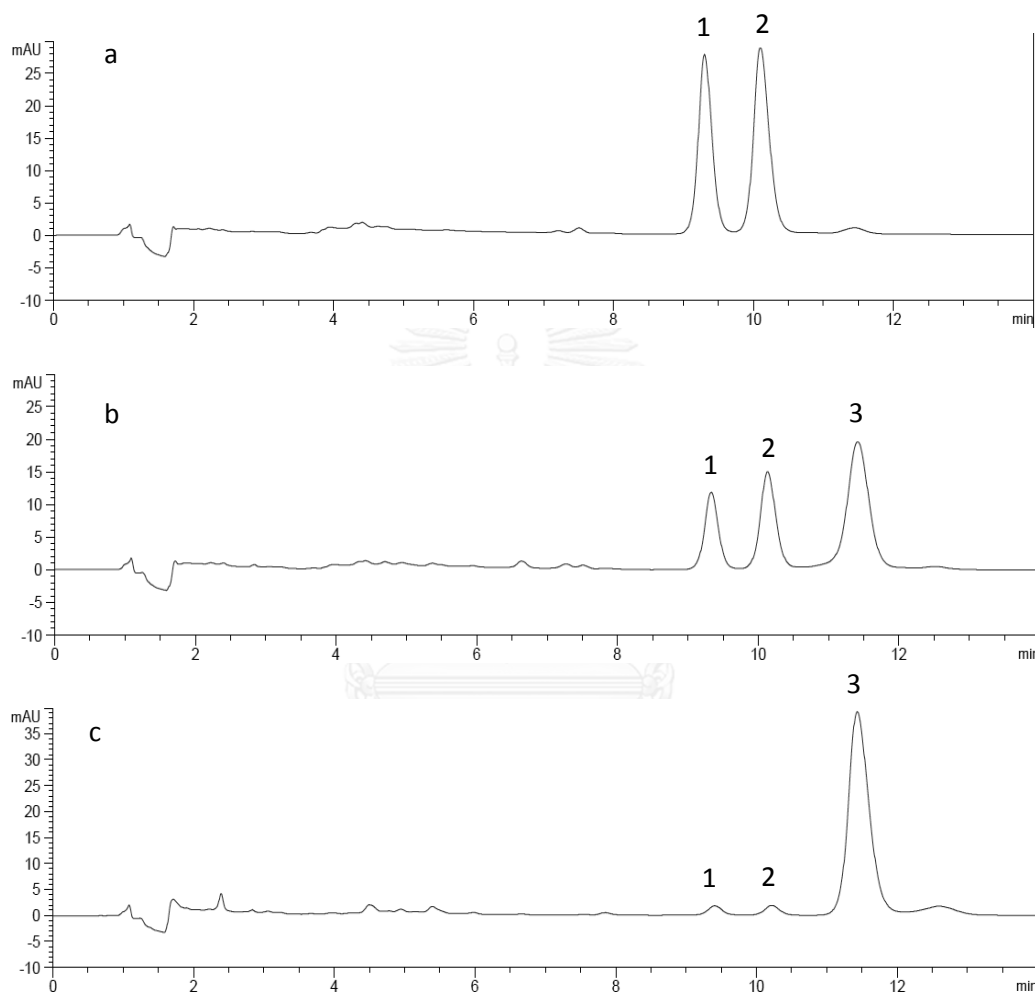
Figure E.1. HPLC-DAD chromatogram of (E)-endoxifen (1; Rt = 9.55 minutes) and (Z)-endoxifen (2; Rt = 10.12 minutes) (2 μg mL^{-1}, pH 7, 22.4°C, and emission light intensity of 224 W s^{-1} cm^{-2}) and the detection of a photodegradation by-product (3; Rt = 11.43 minutes): (a) before photodegradation reaction; (b) after 5 seconds of photodegradation reaction; (c) after 30 seconds of photodegradation reaction.

E.2 (E)- and (Z)-endoxifen detection by UPLC-MS/MS
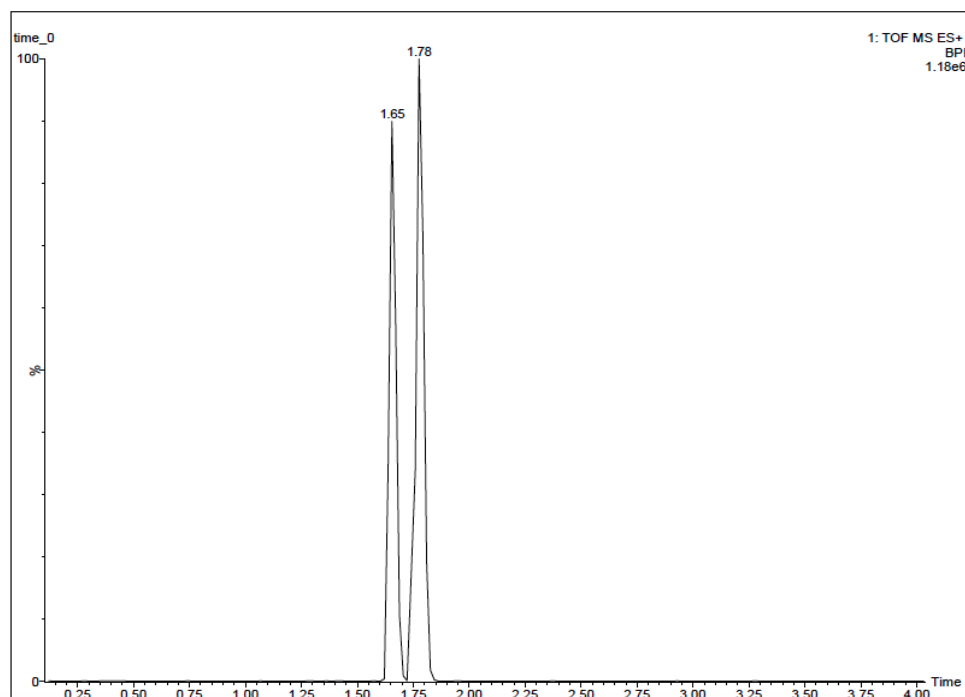
Figure E.2. Chromatograph of (E)-endoxifen (Rt = 1.65 minutes) and (Z)-endoxifen (Rt = 1.78 minutes) in aqueous solution at 1 μg mL^{-1} prior to photodegradation reaction.
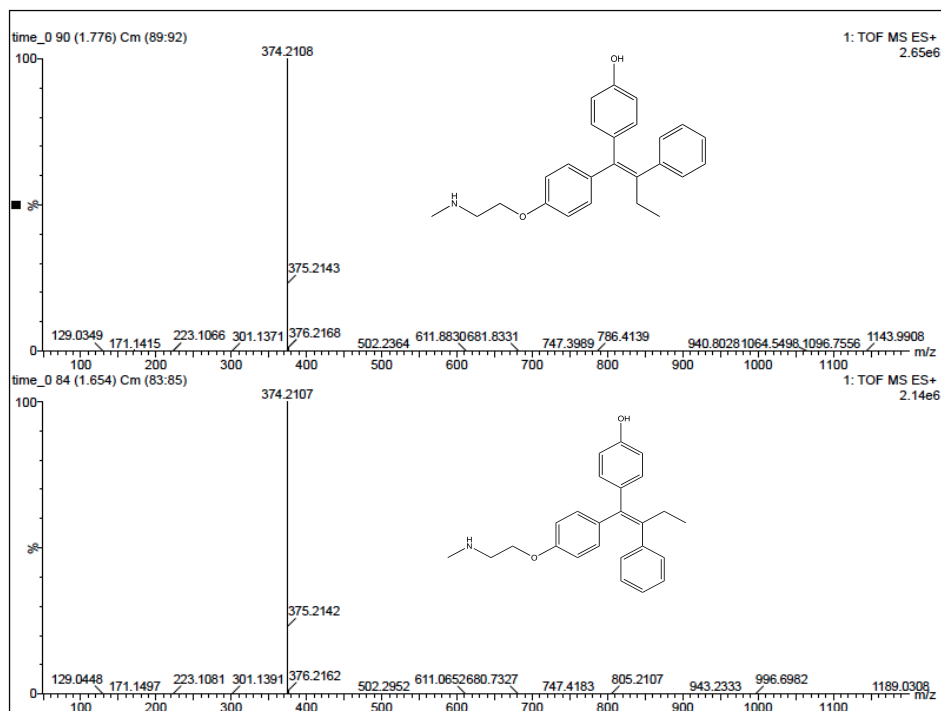
Figure E.3: Mass spectrometry of (E)- and (Z)-endoxifen isomers: (a) ion-*m/z* (374.2108) of (Z)-endoxifen isomer with a retention time of 1.78 minutes; (b) ion-*m/z* (374.2107) of (E)-endoxifen isomer with a retention time of 1.65 minutes.
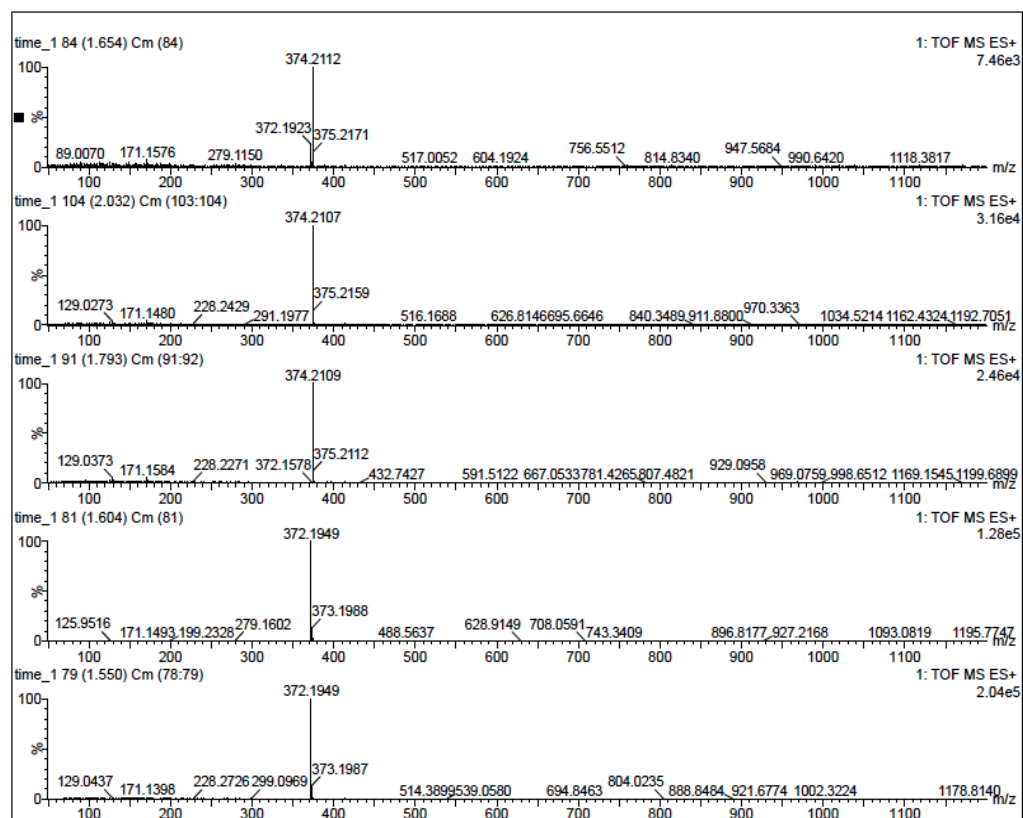
E.3 PBPs detection by UPLC-MS/MS

Figure E.4. Mass spectrometry of the five peaks observed at chromatogram after 35 seconds of irradiation emission light intensity: (a) ion-*m/z* of (E)-endoxifen isomer with retention time of 1.65 minutes; (b) ion-*m/z* of PB2 with retention time of 2.03 minutes; (c) ion-*m/z* of (Z)-endoxifen isomer with retention time of 1.79 minutes; (d) ion-*m/z* of PB1b with retention time of 1.60 minutes; and (e) ion-*m/z* of Pb1a with retention time of 1.55 minutes.
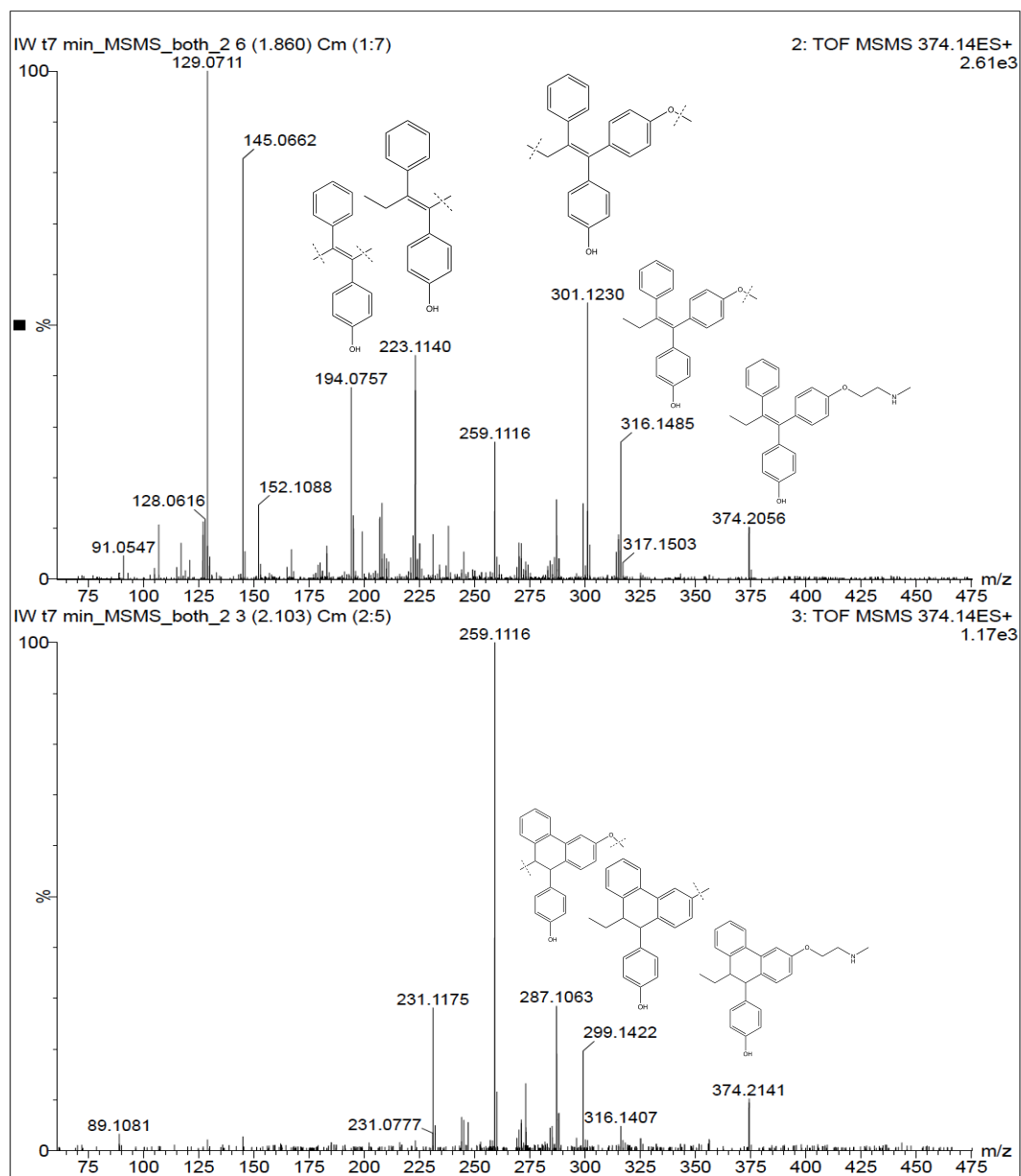
Figure E.5. MS/MS analyses of ion-*m/z* = 374.21 with the proposed molecular fragments: (a) fragmentation formed products ions of (E/Z)-endoxifen; (b) fragmentation formed products ions of PB2.
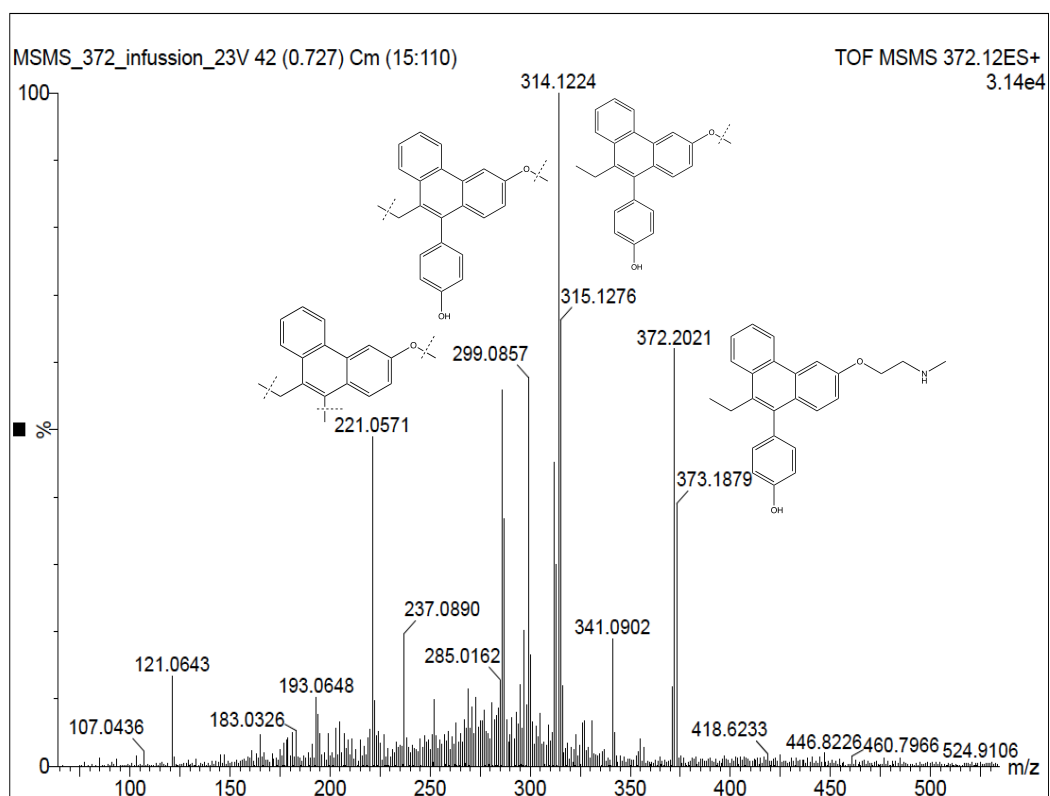
Figure E.6. MS/MS analyses of ion-*m/z* = 372.19 with the proposed molecular fragments for the fragmentation formed products ions of PB1(a, b).

APPENDIX F

PHOTODEGRADATION IN WASTEWATER

F.1 Correlation coefficients for zero, first and second order models

Table F.1 Correlation coefficients for zero, first, and second order fits on (E)- and (Z)-endoxifen photodegradation

Analyte	R^2		
	Zero Order	First Order	Second Order
(E)-endoxifen	0.854	0.972	0.996
(Z)-endoxifen	0.845	0.970	0.991

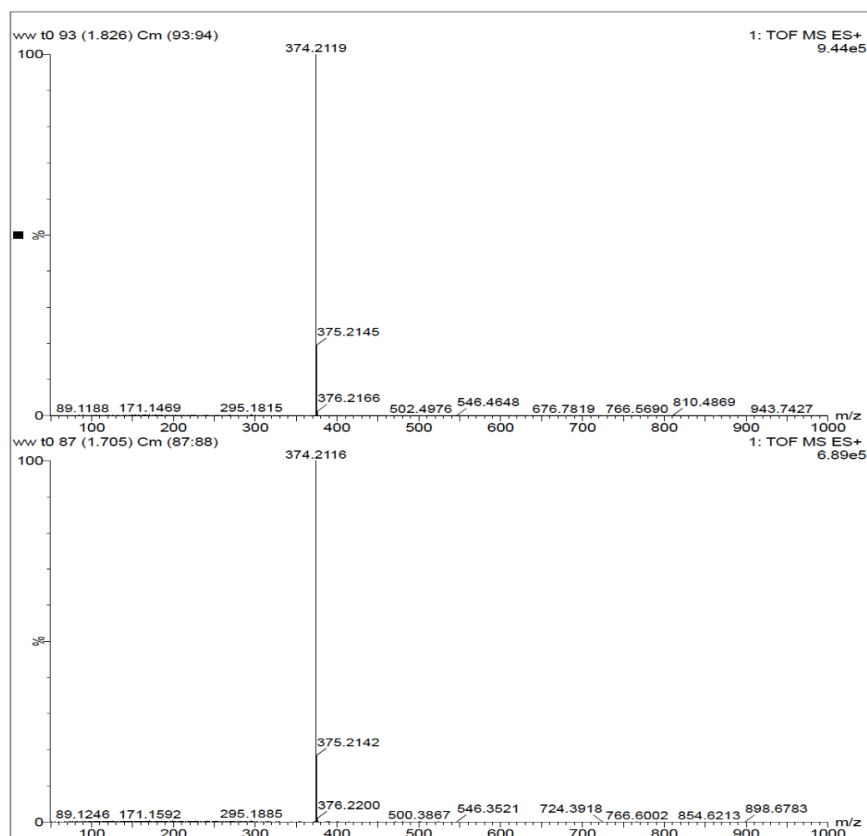**F.2 Mass spectrometry of (E)- and (Z)-endoxifen in wastewater by UPLC-MS/MS**

Figure F.1: MS of the wastewater sample spiked with (E)- and (Z)-endoxifen (1µg mL^{-1}) before irradiation with UV light (emission light intensity = 56 W s^{-1} cm^{-2}): (a) (Z)-endoxifen (Rt = 1.83 minutes, ion-m/z = 374.2119); (b) (E)-endoxifen (Rt = 1.71 minutes, ion-m/z = 374.2116)

F.3 Second-order fits for photodegradation of (E)- and (Z)-endoxifen in wastewater
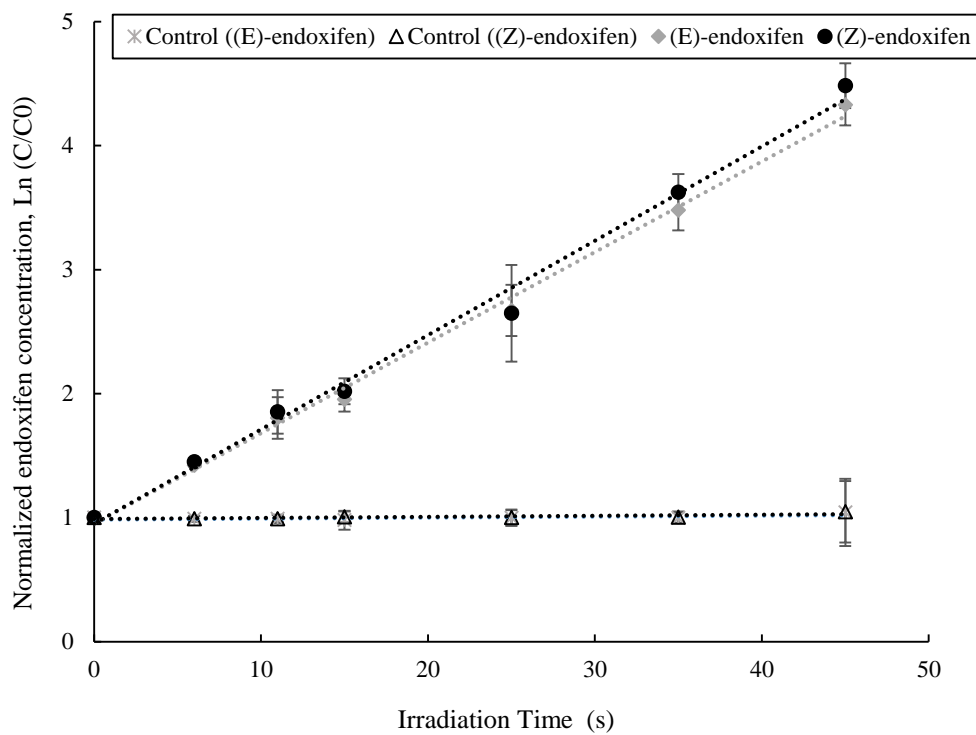

Figure F.2. Second order fits for (E)- and (Z)-endoxifen photodegradation in wastewater at 1 µg mL^{-1} (emission light intensity = 224 W s^{-1} cm^{-2}). Control samples ran in dark condition.

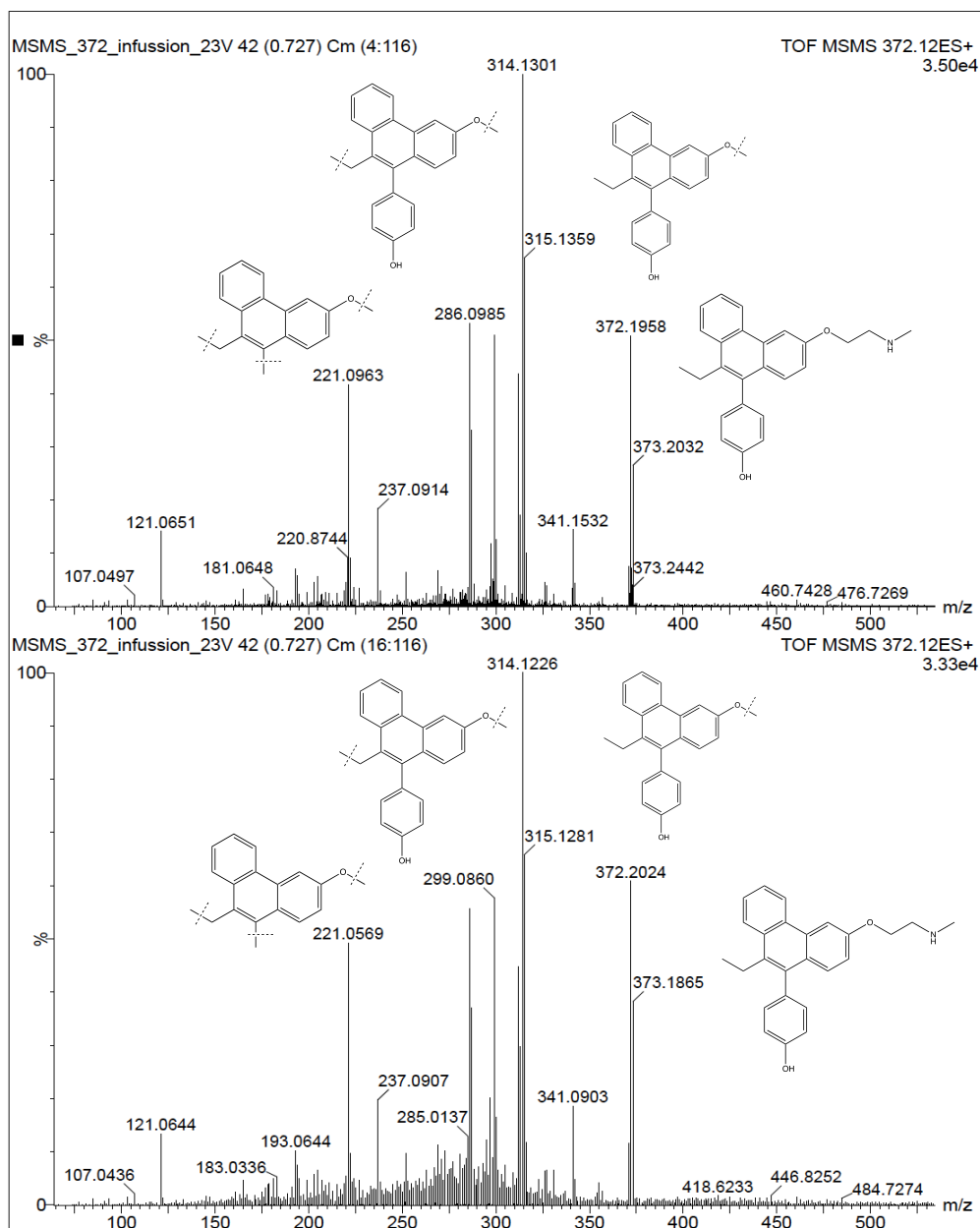**F.4 Tandem mass spectrometry of PB1 (a, b) in wastewater by UPLC-MS/MS**

Figure F.3. MS/MS analyses at ion-m/z = 372.19 with the proposed molecular fragments for wastewater sample after 45 seconds of irradiation with UV light (emission light intensity = 56 W s^{-1} cm^{-2}): (a) fragmentation formed products ions of PB1a; (b) fragmentation formed products ions of PB1b.

VITA

Miss Marina Ariño Martin was born on September 4, 1985 in Malaga, Spain. She obtained her Bachelor's degree in Biology from the Faculty of Sciences, Malaga University in 2012. She pursued her double Master's degree in: International Program in Hazardous Substance and Environmental Management, Graduate School, Chulalongkorn University in 2014; and, Environmental and Conservational Sciences, Graduate School, North Dakota State University in 2015. And finished both degrees in 2017.